

BIOACTIVITIES OF EXTRACTS AND PURE COMPOUND  
FROM MONOFLORAL BEE POLLEN OF WESTERN  
HONEYBEE *Apis mellifera*

Miss Phanthiwa Khongkarat



A Dissertation Submitted in Partial Fulfillment of the Requirements  
for the Degree of Doctor of Philosophy in Biotechnology  
FACULTY OF SCIENCE  
Chulalongkorn University  
Academic Year 2022  
Copyright of Chulalongkorn University

ฤทธิ์ทางชีวภาพของสารสกัดและสารประกอบบริสุทธิ์ของเกสรผึ้งที่มาจากดอกไม้ชนิดเดียวของผึ้ง  
พันธุ์ *Apis mellifera*



วิทยานิพนธ์นี้เป็นส่วนหนึ่งของการศึกษาตามหลักสูตรปริญญาวิทยาศาสตรดุษฎีบัณฑิต  
สาขาวิชาเทคโนโลยีชีวภาพ ไม่สังกัดภาควิชา/เทียบเท่า  
คณะวิทยาศาสตร์ จุฬาลงกรณ์มหาวิทยาลัย  
ปีการศึกษา 2565  
ลิขสิทธิ์ของจุฬาลงกรณ์มหาวิทยาลัย

Thesis Title	BIOACTIVITIES OF EXTRACTS AND PURE COMPOUND FROM MONOFLORAL BEE POLLEN OF WESTERN HONEYBEE <i>Apis mellifera</i>
By	Miss Phanthiwa Khongkarat
Field of Study	Biotechnology
Thesis Advisor	Professor Chanpen Chanchao, Ph.D.
Thesis Co Advisor	Professor PREECHA PHUWAPRAISIRISAN, Ph.D.

---

Accepted by the FACULTY OF SCIENCE, Chulalongkorn University in  
Partial Fulfillment of the Requirement for the Doctor of Philosophy

..... Dean of the FACULTY OF  
SCIENCE  
(Professor POLKIT SANGVANICH, Ph.D.)

#### DISSERTATION COMMITTEE

..... Chairman  
(Associate Professor Orawan Duangpakdee, Ph.D.)  
..... Thesis Advisor  
(Professor Chanpen Chanchao, Ph.D.)

..... Thesis Co-Advisor  
(Professor PREECHA PHUWAPRAISIRISAN, Ph.D.)

..... Examiner  
(Assistant Professor KRIENG KANCHANAWATEE,  
Ph.D.)

..... Examiner  
(Associate Professor APHICHART KARNCHANATAT,  
Ph.D.)

..... External Examiner  
(Assistant Professor Jintanart Wongchawalit, Ph.D.)

CHULALONGKORN UNIVERSITY

พันทิวา คงารัตน์ : ฤทธิ์ทางชีวภาพของสารสกัดและสารประกอบบริสุทธิ์ของเกสรผึ้งที่มาจากดอกไม้ชนิดเดียว  
ของผึ้งพันธุ์ *Apis mellifera*. ( BIOACTIVITIES OF EXTRACTS AND PURE  
COMPOUND FROM MONOFLORAL BEE POLLEN OF WESTERN  
HONEYBEE *Apis mellifera*) อ.ที่ปรึกษาหลัก : ศ. ดร.จันทรเพ็ญ จันทรเจ้า, อ.ที่ปรึกษาร่วม :  
ศ. ดร.ปรีชา ภูวไพโรศิรสา

เกสรผึ้งเป็นหนึ่งในผลิตภัณฑ์ผึ้งที่น่าสนใจซึ่งมีสารออกฤทธิ์ทางชีวภาพหลายชนิดเป็นองค์ประกอบ อย่างไรก็ตาม องค์ประกอบทางเคมีของเกสรผึ้งขึ้นอยู่กับแหล่งที่อยู่ของพืชและชนิดพืชที่ผึ้งใช้เป็นแหล่งอาหาร ส่งผลให้เกสรผึ้งมีฤทธิ์ทางชีวภาพที่หลากหลาย ในประเทศไทยมีเกสรผึ้งหลายชนิดแต่มีรายงานเกี่ยวกับฤทธิ์ทางชีวภาพน้อย งานวิจัยนี้จึงศึกษาเกสรผึ้งของผึ้งพันธุ์ *A. mellifera* โดยเก็บตัวอย่างและวิเคราะห์ชนิดของเกสรผึ้งที่มาจากดอกไม้ชนิดเดียวจำนวน 6 ชนิด พบว่าเป็นเกสรของดอกชา (*Camellia sinensis* L.), ทานตะวัน (*Helianthus annuus* L.), ไมยราบไร้หนาม (*Mimosa diplotricha*), บัวหลวง (*Nelumbo nucifera*), เหลืองทิพวรรณ (*Xyris complanata*), และ สาบแรังสาบกา (*Ageratum conyzoides*) จากนั้นสกัดเกสรผึ้งแต่ละชนิดด้วยเมทานอลแล้วสกัดแยกส่วนโดยใช้เฮกเซน ไคลลอร์โรมีเทนและเมทานอล นำสารสกัดที่ได้มาทดสอบหาปริมาณฟีนอลทั้งหมดและฟลาโวนอยด์รวมถึงตรวจวัดฤทธิ์ขจัดอนุมูลอิสระและฤทธิ์ยับยั้งการทำงานของเอนไซม์ จากปริมาณฟีนอลทั้งหมดและฟลาโวนอยด์พบว่าไคลลอร์โรมีเทนเป็นตัวอย่างที่ละลายที่เหมาะสมที่สุดในการสกัดแยกส่วน โดยเฉพาะสารสกัดชั้นไคลลอร์โรมีเทนของเกสรผึ้งดอกทานตะวันและไมยราบไร้หนามมีปริมาณฟีนอลทั้งหมดมากที่สุด และในขณะเดียวกันก็พบว่าสารสกัดชั้นไคลลอร์โรมีเทนของเกสรผึ้งดอกไมยราบไร้หนามมีปริมาณฟลาโวนอยด์มากที่สุด ซึ่งสอดคล้องกับฤทธิ์ขจัดอนุมูลอิสระดีที่สุดจากการตรวจสอบด้วยวิธี ABTS, DPPH, TEAC, และ FRAP สำหรับการศึกษากิจกรรมการทำงานของเอนไซม์ พบว่าสารสกัดจากดอกไม้ยราบไร้หนาม เหลืองทิพวรรณ ชา และทานตะวัน มีฤทธิ์ในการยับยั้งการทำงานของเอนไซม์ ไลโปอกซีจีเนส อะไมเลส ไลเปส และไทโรซิเนส ได้อย่างมีประสิทธิภาพตามลำดับ แต่ไม่มีสารสกัดใดที่แสดงฤทธิ์ยับยั้งการทำงานของเอนไซม์อะซิทีลโคลีนเอสเตอเรส เนื่องจากฤทธิ์ทางชีวภาพที่น่าสนใจในเชิงของความเข้มข้นของการยับยั้งที่ 50% (IC<sub>50</sub>) ของสารสกัดจากดอกทานตะวันและไมยราบไร้หนาม จึงนำสารสกัดทั้งสองมาทำให้บริสุทธิ์มากขึ้นด้วยเทคนิคโครมาโตกราฟีแบบต่าง ๆ เมื่อวิเคราะห์โครงสร้างทางเคมีของสารออกฤทธิ์พบว่า กรดปาล์มิก กรดไลโนเลอิก และกรดลิโนเลนิก ซึ่งอยู่ในกลุ่มกรดไขมันอิสระ เป็นสารออกฤทธิ์หลักในการยับยั้งเอนไซม์ไลเปส และพบว่า triferuloyl spermidines เป็นสารออกฤทธิ์หลักในการขจัดอนุมูลอิสระและยับยั้งเอนไซม์ไลโปอกซีจีเนสของเกสรผึ้งของดอกไม้ยราบไร้หนาม นอกจากนี้งานวิจัยนี้ยังทำการศึกษาฤทธิ์ยับยั้งการสร้างเมลานินในระดับเซลล์ของสาร safflospermidine A และ B ที่แยกได้จากเกสรผึ้งของดอกทานตะวัน พบว่า สารผสมกลุ่ม safflospermidine ลดระดับเมลานินภายในและภายนอกเซลล์เมลานโนไซท์ชนิด B16F10 ได้อย่างมีนัยสำคัญโดยไม่แสดงความเป็นพิษต่อเซลล์ การศึกษานี้ยังแสดงให้เห็นถึงฤทธิ์ทางชีวภาพมีความโดดเด่นแตกต่างกันในเกสรผึ้งแต่ละชนิด จึงกล่าวได้ว่าเกสรผึ้งมีศักยภาพในการใช้เป็นผลิตภัณฑ์เสริมอาหารที่มีสรรพคุณทางยา นอกจากนี้สารสกัดจากเกสรผึ้งจากดอกทานตะวันยังเป็นแหล่งของสารที่สามารถยับยั้งการสร้างเมลานิน และสามารถพัฒนาให้เป็นสารเติมแต่งในผลิตภัณฑ์เครื่องสำอางได้อีกด้วย

สาขาวิชา เทคโนโลยีชีวภาพ  
ปีการศึกษา 2565

ลายมือชื่อนิสิต .....  
ลายมือชื่อ อ.ที่ปรึกษาหลัก .....  
ลายมือชื่อ อ.ที่ปรึกษาร่วม .....

## 6172904023 : MAJOR BIOTECHNOLOGY

KEYWORD:

Phanthiwa Khongkarat : BIOACTIVITIES OF EXTRACTS AND PURE COMPOUND FROM MONOFLORAL BEE POLLEN OF WESTERN HONEYBEE *Apis mellifera*. Advisor: Prof. Chanpen Chanchao, Ph.D. Co-advisor: Prof. PREECHA PHUWAPRAISIRISAN, Ph.D.

Bee pollen is one of interesting bee products which contain many bioactive compounds. However, its constituents depend on habitats and species of food plants. That results in a variety of bioactivities. In Thailand, there are many types of bee pollen, but there are few reports on their biological activities. In this study, bee pollen of *A. mellifera* was focused. Six types of monofloral bee pollen were harvested and identified as floral pollen of tea (*Camellia sinensis* L.), sunflower (*Helianthus annuus* L.), giant sensitive plant (*Mimosa diplotricha*), lotus (*Nelumbo nucifera*), leuuang tipwan (*Xyris complanata*), and sap raeng sap ka (*Ageratum conyzoides*) flowers. The crude extracts were prepared sequentially with methanol, dichloromethane, and hexane. Total phenolic and flavonoid contents were determined. Then, antioxidant capacity and enzyme inhibitory properties were tested. For phenolic and flavonoid contents, it was found that dichloromethane is the most suitable partition solvent, especially partitioned extracts of *H. annuus* L. and *M. diplotricha* had the highest phenolic content. Meantimes, the extracts of *M. diplotricha* had the highest flavonoid content which coincided to the highest antioxidant properties in many assays (ABTS, DPPH, TEAC, and FRAP). For enzyme inhibitory activity, the extracts of *M. diplotricha*, *X. complanata*, *C. sinensis* L., and *H. annuus* L. were effective inhibitors for lipoxygenase,  $\alpha$ -amylase, lipase, and tyrosinase, respectively. In contrast, none of the extracts showed acetylcholinesterase inhibitory activity. According to the interesting activity in terms of the half-maximal inhibitory concentration (IC<sub>50</sub>) of the *H. annuus* L. and *M. diplotricha* extracts, they were purified by chromatographic techniques. By chemical structure analysis, it was found that palmitic acid, linoleic, and linolenic acids belonging to the group of free fatty acids were the major active compounds presenting porcine pancreatic lipase inhibitory activities. Also, triferuloyl spermidines isolated from *M. diplotricha* bee pollen exhibited as antioxidants and anti-lipoxygenase agents. In addition, the inhibitory effect of safflospermidine A and B isolated from *H. annuus* L. bee pollen on melanogenesis in B16F10 melanoma cells was studied. Safflospermidine mixture significantly reduced intracellular and extracellular melanin levels in B16F10 cells with no cytotoxicity. This study demonstrated that the predominant biological activity was depended on types of bee pollen. Therefore, bee pollens have the potential to be used as nutraceutical food. Also, anti-melanogenesis agents were rich in *H. annuus* L. bee pollen extract which can be developed to be an additive in cosmetic products.

Field of Study: Biotechnology  
Academic Year: 2022

Student's Signature .....  
Advisor's Signature .....  
Co-advisor's Signature .....

## ACKNOWLEDGEMENTS

I would like to express my deepest gratitude to my advisor, Professor Dr. Chanpen Chanchao, for her continuous kindness, invaluable counsel, priceless opportunities, and great patience throughout my Ph.D. studies. She consistently assists me in overcoming research-related obstacles. This thesis would not have been possible without her guidance and constant support.

My deep appreciation is expressed to Professor Dr. Preecha Phuwapraisirisan, my co-advisor, who has made this study successful through his fruitful information, advice on the experiment planning and arrangement, problem-solving, including laboratory facilities.

Furthermore, I sincerely appreciate Associate Professor Dr. Orawan Duangphakdee for serving as dissertation chairman, Associate Professor Dr. Aphichart Karnchanatat, Assistant Professor Dr. Krieng Kanchanawatee, and Assistant Professor Dr. Jintanart Wongchawalit, for serving as dissertation committee. Their comments and suggestions are always valuable.

I am grateful to Ms. Songchan Puthong for supplying me with cell culture facilities, offering valuable suggestions, and training me on cell culture techniques.

I would also like to extend my thanks to members of Central Molecular Laboratory, Department of Biology, members of Center of Excellence in Natural Product, Department of Chemistry, and all of my friends in Program in Biotechnology, Faculty of Science, Chulalongkorn University for their help, suggestions, and kind friendship. I really would like to thank the Science Achievement Scholarship of Thailand and the Ratchadaphiseksomphot Endowment Fund for financial support.

Lastly, I wish to convey my heartfelt thanks to my family members for their unending love, encouragement, and unconditional support throughout my entire life.

Phanthiwa Khongkarat

# TABLE OF CONTENTS

	<b>Page</b>
.....	iii
ABSTRACT (THAI) .....	iii
.....	iv
ABSTRACT (ENGLISH).....	iv
ACKNOWLEDGEMENTS.....	v
TABLE OF CONTENTS.....	vi
LIST OF TABLES.....	x
LIST OF FIGURES .....	xi
CHAPTER I.....	1
INTRODUCTION .....	1
1.1 Background.....	1
1.2 Objectives of the study .....	8
1.3 Scope of the study.....	8
1.4 Expected beneficial outcomes from the dissertation .....	8
References.....	9
CHAPTER II.....	12
First report of fatty acids in <i>Mimosa diplotricha</i> bee pollen with <i>in vitro</i> lipase inhibitory activity.....	12
2.1 Authors .....	12
2.1.1 First author .....	12
2.1.2 Corresponding author .....	12
2.2 Article status .....	12
2.3 Abstract.....	13
2.4 Introduction.....	14
2.5 Materials and Methods .....	16
2.5.1 Chemicals and reagents .....	16

2.5.2 Sample collection .....	17
2.5.3 Identification of the bee pollen.....	17
2.5.4 Crude extraction and partition.....	18
2.5.5 <i>In vitro</i> $\alpha$ -amylase inhibitory activity.....	19
2.5.6 <i>In vitro</i> AChEI inhibitory activity .....	20
2.5.7 <i>In vitro</i> porcine pancreatic lipase inhibitory (PPLI) activity.....	20
2.5.8 Enrichment of active fractions .....	21
2.5.9 Chemical structure analysis by NMR.....	22
2.5.10 Preparation of FAMES.....	23
2.5.11 GC-FID analysis.....	23
2.5.12 Data analysis.....	24
2.6 Results.....	26
2.6.1 Palynological analysis of the six BP samples .....	26
2.6.2 Identification of the pollen species in each BP sample by molecular analysis .....	28
2.6.3 The partitioned extracts of BP.....	28
2.6.4 <i>In vitro</i> $\alpha$ -amylase inhibitory activity.....	29
2.6.5 <i>In vitro</i> AChEI activity.....	30
2.6.6 <i>In vitro</i> PPLI activity.....	30
2.6.7 <i>In vitro</i> PPLI activity of active compounds from DCMMBP .....	33
2.6.8 Principal chemical composition analysis (TLC and NMR) of fractions DCMMBP2-1 and DCMMBP2-2 .....	34
2.6.9 Analysis of the fatty acids of fraction DCMMBP2-1.....	36
2.7 Discussion.....	37
2.8 Conclusions.....	40
2.9 List of abbreviations .....	41
References.....	42
Supplements.....	48
CHAPTER III .....	54



Phytochemical content, especially spermidine derivatives, presenting antioxidant and antilipoxygenase activities in Thai bee pollens .....	54
3.1 Authors .....	54
3.1.1 First author .....	54
3.1.2 Corresponding author .....	54
3.2 Article status .....	54
3.3 Abstract.....	55
3.4 Introduction.....	56
3.5 Materials & Methods .....	58
3.5.1 Sample collection .....	58
3.5.2 Crude extraction and partition.....	58
3.5.3 Determination of the TPC .....	59
3.5.4 Determination of the FC.....	59
3.5.5 Determination of the antioxidant capacity .....	60
3.5.6 <i>In vitro</i> TYRI activity .....	61
3.5.7 <i>In vitro</i> LOXI activity.....	62
3.5.8 Enrichment of active fractions .....	62
3.5.9 Chemical structure analysis by <sup>1</sup> H-NMR and MS.....	63
3.5.10 Data analysis.....	64
3.6 Results.....	66
3.6.1 The partitioned extracts of BPs .....	66
3.6.2 Determination of the TPC and FC.....	66
3.6.3 Antioxidant activity of the partitioned extracts.....	67
3.6.4 Enzyme inhibitory activity .....	69
3.6.5 Antioxidant and LOXI activities of compounds from DCMMBP.....	70
3.6.6 Structural identification of compounds 1 and 2 .....	73
3.7 Discussion.....	75
3.8 Conclusions.....	78
References.....	79

Supplements.....	84
CHAPTER IV .....	90
Inhibitory effect of safflospemidines from the bee pollen of <i>Helianthus annuus</i> L. on melanogenesis of B16F10 melanoma cells.....	90
4.1 Abstract.....	90
4.2 Introduction.....	91
4.3 Materials and methods .....	92
4.3.1 Compound preparation .....	92
4.3.2 Cell culture .....	93
4.3.3 Cell viability assay .....	94
4.3.4 Melanin content assay .....	94
4.3.5 Data analysis.....	95
4.4 Results.....	95
4.4.1 Effect of safflospemidine A and B on cell viability.....	95
4.4.2 Effect of safflospemidine A and B on cellular melanin content .....	97
4.5 Discussion.....	102
4.6 Conclusion .....	103
References.....	104
CHAPTER V .....	108
CONCLUSION.....	108
REFERENCES .....	110
VITA.....	112

## LIST OF TABLES

	<b>Page</b>
<b>Table 2.1</b> The weight, yield, and character of the partitioned extracts. ....	29
<b>Table 2.2</b> The percentage of enzyme inhibition (mean $\pm$ S.D.) and IC50 value ( $\mu$ g/mL) of the partitioned extracts.....	31
<b>Table 2.3</b> Characteristics and PLLI activity (IC50 value) of all pooled fractions after the first (500-mL column) and second (250-mL colume) SiG60-CC fractionation. ...	34
<b>Table 2.4</b> Fatty acid composition of the DCMMBP2-1 (as FAMES). ....	36
<b>Table 3.1</b> Detail of sample collection. ....	58
<b>Table 3.2</b> The TPC and FC of the partitioned BP extracts.....	67
<b>Table 3.3</b> Antioxidant activity of the partitioned extracts.....	68
<b>Table 3.4</b> The TYRI and LOXI activities (%/IC50) of the partitioned extracts. ....	69
<b>Table 3.5</b> Antioxidant and LOXI activities of the respective fractions after SiG60 and HPLC chromatography. ....	72
<b>Table 4.1</b> Chemical structures and descriptions of pure compounds.....	93

## LIST OF FIGURES

	Page
<b>Figure 1.1</b> The sequence alignment of the partial ITS-2 region of <i>Camellia sinensis</i> L. species with sequences from the GenBank database .....	3
<b>Figure 1.2</b> The sequence alignment of the partial ITS-2 region of <i>Helianthus annuus</i> L. species with sequences from the GenBank database .....	4
<b>Figure 1.3</b> The sequence alignment of the partial ITS-2 region of <i>Mimosa diplotricha</i> species with sequences from the GenBank database .....	4
<b>Figure 1.4</b> The sequence alignment of the partial ITS-2 region of <i>Nelumbo nucifera</i> species with sequences from the GenBank database .....	5
<b>Figure 1.5</b> The sequence alignment of the partial ITS-2 region of <i>Xyris complanata</i> species with sequences from the GenBank database .....	5
<b>Figure 1.6</b> The sequence alignment of the partial ITS-2 region of <i>Ageratum conyzoides</i> species with sequences from the GenBank database .....	6
<b>Figure 2.1</b> Summary for extraction, screening and enrichment procedures for the selected BP .....	25
<b>Figure 2.2</b> Representative LM images (400 x magnification) of (A–F) BP1–6, respectively, identified as (A) <i>C. sinensis</i> L., (B) <i>H. annuus</i> L., (C) <i>M. diplotricha</i> , (D) <i>N. nucifera</i> , (E) <i>X. complanata</i> , and (F) <i>A. conyzoides</i> flower pollen. ....	27
<b>Figure 2.3</b> Representative SEM images (1,500–5,000 x magnification) of (A–F) BP1–6 respectively, identified as (A) <i>C. sinensis</i> L., (B) <i>H. annuus</i> L., (C) <i>M. diplotricha</i> , (D) <i>N. nucifera</i> , (E) <i>X. complanata</i> , and (F) <i>A. conyzoides</i> flower pollen. ....	27
<b>Figure 2.4</b> The (A) $\alpha$ -amylase inhibition activity (%) of DCMXBP, (B) PPLI activity (%) of DCM partitioned extracts, and (C) PPLI activity (%) of DCMMBP2 and DCMMBP2-1. Data are shown as the mean $\pm$ SD .....	32
<b>Figure 2.5</b> The (A) $\alpha$ -amylase inhibition (%) of acarbose, (B) AChEI activity (%) of physostigmine, and (C) PPLI activity (%) of orlistat. Data are shown as the mean $\pm$ SD. ....	33
<b>Figure 2.6</b> TLC images showing the profile of DCMMBP2 (lane 1), DCMMBP2-1 (lane 2), DCMMBP2-2 (lane 3), DCMMBP2-3 (lane 4), and naringenin (lane 5) under (A) UV light and (B) after 3% (v/v) anisaldehyde in MeOH. ....	35

- Figure 2.7** Structural formula of naringenin (A) and the chemical structures of palmitic acid, C16:0 (B), linoleic acid, C18:2n6c (C), and  $\alpha$ -linolenic acid, C18:3n3 (D).....37
- Figure 3.1** Summary of the extraction, screening, and enrichment procedures for the selected BP.....65
- Figure 3.2** The HPLC chromatogram of DCMMBP3 showing the elution of DCMMBP3-1 and DCMMBP3-2 at a retention time of 15.352 and 20.182 min, respectively. ....73
- Figure 3.3** <sup>1</sup>H-NMR (500 MHz, MeOD-D4) in the range of 7.6–5.7 ppm of (A) compound 1 and (B) compound 2. The chemical structures of (C–F) spermidine derivatives. <sup>1</sup>H-NMR (500 MHz, MeOD-D4) in the range of 7.6–5.7 ppm of (A) compound 1 and (B) compound 2. The chemical structures of (C) *N*<sup>1</sup>,*N*<sup>5</sup>,*N*<sup>10</sup>-tri-(*Z,E,E*)-feruloyl spermidine, (D) *N*<sup>1</sup>,*N*<sup>5</sup>,*N*<sup>10</sup>-tri-(*E,Z,E*)-feruloyl spermidine, (E) *N*<sup>1</sup>,*N*<sup>5</sup>,*N*<sup>10</sup>-tri-(*E,E,Z*)-feruloyl spermidine, and (F) *N*<sup>1</sup>, *N*<sup>5</sup>, *N*<sup>10</sup>-tri-(*E,E,E*)-feruloyl spermidine.....75
- Figure 4.1** Effect of safflospersmidine A and B and kojic acid on cell viability of B16F10 melanoma cells in the absence of  $\alpha$ -MSH using MTT assay. The percentage value of treated B16F10 cells was reported by being relative to that of the control group. The values were the mean  $\pm$  S.D. from three independent experiments. \* indicates a value significantly different from the control group [ $p < 0.05$ ; one-way ANOVA and Post Hoc (Tukey) test]. ....96
- Figure 4.2** Effect of safflospersmidine A and B and kojic acid on cell viability of B16F10 melanoma cells in the presence of  $\alpha$ -MSH using MTT assay. The percentage value of treated B16F10 cells was reported by being relative to that of the control group. The values were the mean  $\pm$  S.D. from three independent experiments. \* indicates a value significantly different from the control group [ $p < 0.05$ ; one-way ANOVA and Post Hoc (Tukey) test]. ....97
- Figure 4.3** Effect of a sample (safflospersmidine A and B) on intracellular melanin content in B16F10 melanoma cells. Baseline melanin content in control wells exposed to only  $\alpha$ -MSH was set at 100%. Data were expressed as a percentage of control. Each column represents the mean  $\pm$  SD from three independent experiments. \* indicates a value significantly different from control group [ $p < 0.05$ ; one-way ANOVA and Post

Hoc (Tukey) test]. The bottom panel represents the color intensity of dissolving melanin after cell lysis. ....98

**Figure 4.4** Effect of a sample(safflospersmidine A and B) on extracellular melanin content in B16F10 melanoma cells. Baseline melanin content in control wells exposed to only  $\alpha$ -MSH was set at 100%. Data were expressed as a percentage of control. Each column represents the mean  $\pm$  SD from three independent experiments. \* indicates value significantly different from control group [ $p < 0.05$ ; one-way ANOVA and Post Hoc (Dunnett T3) test]. The bottom panel represents the color intensity of melanin production in media. ....99

**Figure 4.5** Morphology of B16F10 cells after exposed to safflospersmidine A and B for 72 h under light microscope (200X); (A) negative control, (B) control, (C) B16F10 cells with 62.5  $\mu\text{g}/\text{mL}$  of compound, (D) B16F10 cells with 125  $\mu\text{g}/\text{mL}$  of compound, (E) B16F10 cells with 250  $\mu\text{g}/\text{mL}$  of compound, (F) B16F10 cells with 500  $\mu\text{g}/\text{mL}$  of compound, (G) B16F10 cells with 1,000  $\mu\text{g}/\text{mL}$  of sample, and (H) B16F10 cells with 250  $\mu\text{g}/\text{mL}$  of kojic acid. Each picture is a representative of three independent experiments. Scale bar = 50  $\mu\text{m}$  ..... 101

# CHAPTER I

## INTRODUCTION

### 1.1 Background

In recent years, consumers' nutritional patterns have changed. Natural and functional foods have become more popular as people realize they can prevent and treat ailments. Consequently, natural products, particularly bee products, are gaining popularity (Gercek et al., 2021). Valuable bee products such as honey, royal jelly, bee wax, bee pollen, propolis, and even bee venom were mostly produced by western honeybee *A. mellifera* (Giampieri et al., 2022), native to Europe, the Middle East, and Africa. However, it has been spread extensively beyond its natural zone due to economic benefits (Tihelka et al., 2020). *A. mellifera* was brought to be cultured in the beekeeping industry because it can be managed in a hive box. Also, it has harmless behavior. Therefore, it is convenient to harvest bee products, and plays an important role as pollinators of native plants and agricultural crops (Hung et al., 2018). Bee pollen is one of the economic bee products produced by honeybees. When workers collect nectar from flowers as food sources, they also collect floral pollen. The collected floral pollen is mixed with nectar, enzyme, wax, and bee secretion. Then, a small pellet is formed and kept in a pollen basket at hind legs. Bee pollen has highly complexing and nutritionally chemical compositions, but its constituents are variable depending on biogeographic (regional) origin, ecological habitat, floral origin, or even the season. The major components include proteins, essential amino acids, reducing sugars, lipids, and crude fiber. The minor components are minerals (such as Ca, Mg, Fe, Zn, Cu), vitamins [such as provitamin A ( $\beta$ -carotene), vitamin E (tocopherol), niacin, thiamine, biotin, folic acid], and enzymes or co-enzymes. Bioactive substances are flavonoids, polyphenols, unsaturated/saturated fatty acids (linoleic,  $\gamma$ -linoleic, arachidic, phospholipids, phytosterols, including  $\beta$ -sitosterol, P-sitosterol), and terpenes. In addition, bee pollen is found to be variously dominant in bioactivities such as anti-inflammatory, anticarcinogenic, antibacterial, antifungicidal, and hepatoprotective activities (Denisow & Denisow-Pietrzyk, 2016).

Bee pollen is reported as a good source of polyphenol and flavonoid compounds, which can scavenge free radicals. The mixed pollen loads from Bayburt contain flavonoids such as rutin, kaempferol, and quercetin that have antioxidant activity (Gercek et al., 2021). In addition, rutin, *p*-hydroxybenzoic acid, benzoic acid, resveratrol, quercetin, cinnamic acid, vanillin, kaempferol, protocatechuic acid, and *p*-coumaric acid in methanol extract of rape bee pollen from China had the better antioxidant properties than ascorbic acid (positive control) (Sun et al., 2017). Therefore, rape bee pollen extracts could be used as an antioxidant agent. As known, the antioxidant is also needed to prevent people from diseases and skin disorders that can occur by free radical-induced processes. Moreover, bee pollen is found to be the source of many enzyme inhibitors that can be used to treat many diseases and can substitute the use of artificial enzyme inhibitors, which have some adverse side effects. The multifloral bee pollen, dominant in the floral pollen of *Myrcia* spp., showed good lipoxygenase inhibition while the bee pollen, dominant in the floral pollen of *Spondias* spp., showed lipase inhibitory activity. Therefore, bee pollen in this work could be used as an anti-asthma and anti-obesity agent (Araújo et al., 2017). Also, luteolin from n-butanol partition extract of *Fagopyrum esculentum* bee pollen showed a strong acetylcholinesterase inhibitory activity, therefore, luteolin might be applied to use in Alzheimer's disease treatment (Li et al., 2019). According to Daudu (2019), the  $\alpha$ -amylase inhibitory activity from bee pollen in Nigeria was more significantly potent than acarbose. Furthermore, it showed that bee pollen contained phenol and flavonoid compounds which were effective inhibitors of  $\alpha$ -amylase, indicating the therapeutic potential of bee pollen in managing diabetes. The polyphenol in apricot and sunflower bee pollen is the active component for tyrosinase inhibitory activity (Zhang et al., 2015). In addition, the key component in tyrosinase inhibition is trisubstituted hydroxycinnamic acid with the substituents of *p*-coumaroyl, caffeoyl, and feruloyl spermidines isolated from camellia bee pollen extract (Su et al., 2021). Moreover, rape bee pollen extract can suppress intracellular tyrosinase (TYR) activity, reduce mRNA expression of TYR and TRP-1, and significantly decrease melanin content in B16 mouse melanoma cells and promote glutathione synthesis. These results revealed that rape bee pollen extract could be used as a skin whitening agent in cosmetic products (Sun et al., 2017).



From previous reports on bioactivity, bee pollen has been proven to be used in nutritional supplements and pharmaceutical benefits. According to the large number of diverse monocrops cultivated in Thailand, many types of monofloral bee pollen exist. Bee pollen is considered monofloral when it comes from a single botanical source or when at least 80% of the sample is composed of pollen from a single species (Campos et al., 2008). However, due to little attention to the bioactivity of bee pollen, people are unaware of the benefits of bee pollen. Therefore, to increase value and promote the consumption of bee pollen, in this work, many types of monofloral bee pollens from the floral pollen of *Camellia sinensis* L., *Helianthus annuus* L., *Mimosa diplotricha*, *Nelumbo nucifera*, *Xyris complanata*, and *Ageratum conyzoides* will be collected. Floral origin will be identified to confirm the types of bee pollen. All the partial ITS-2 DNA sequences obtained in this study were aligned with identified sequences from the GenBank database (Figures 1.1-1.6).

**Camellia sinensis cultivar Bannockburn-777 5.8S ribosomal RNA gene, partial sequence; internal transcribed spacer 2, complete sequence; and large subunit ribosomal RNA gene, partial sequence**  
 Sequence ID: [MN242039.1](#) Length: 440 Number of Matches: 1

Range 1: 13 to 440		<a href="#">GenBank</a>	<a href="#">Graphics</a>	<a href="#">Next Match</a>	<a href="#">Previous Match</a>
Score	Expect	Identities	Gaps	Strand	
791 bits(428)	0.0	428/428(100%)	0/428(0%)	Plus/Minus	
Query	31	CGGTTGCTCGCCGTTACTAGGGGAATCCTTGAAGTTCTTTTCCTCGCTTATTGATA	90		
Sbjct	440	CGGTTGCTCGCCGTTACTAGGGGAATCCTTGAAGTTCTTTTCCTCGCTTATTGATA	381		
Query	91	TGCTTAAACTCAGCGGGTAATCCCGCTGACTGGGGTCGCGATCGGAGCGCTTGCCGG	150		
Sbjct	380	TGCTTAAACTCAGCGGGTAATCCCGCTGACTGGGGTCGCGATCGGAGCGCTTGCCGG	321		
Query	151	CGGCGGATAGGGTCACGACAGGCTCCCGCGACGGACCGGACGCGCGAGGGCGACGCA	210		
Sbjct	320	CGGCGGATAGGGTCACGACAGGCTCCCGCGACGGACCGGACGCGCGAGGGCGACGCA	261		
Query	211	ACGGTTTGTCAACCACCACTCGTCGCGACGCGTCTGTCGGTCCGGGGGACTCGCTTTGG	270		
Sbjct	260	ACGGTTTGTCAACCACCACTCGTCGCGACGCGTCTGTCGGTCCGGGGGACTCGCTTTGG	201		
Query	271	GCCGACCGCGCGCGCGCGCGGGGGCCAAATCCGCCCGCAGCCCTTCTTCCCCC	330		
Sbjct	200	GCCGACCGCGCGCGCGCGCGGGGGCCAAATCCGCCCGCAGCCCTTCTTCCCCC	141		
Query	331	TTGCGCGGGGAGGGGGCGCGGGCGACGCAACGTGAGACGCCAGGCAGGCGTCCCTCA	390		
Sbjct	140	TTGCGGGGGAGGGGGCGCGGGCGACGCAACGTGAGACGCCAGGCAGGCGTCCCTCA	81		
Query	391	ACCTAATGGCTTCGGGCGCAACTTGC GTTCAAAGACTCGATGGTTCCGGGGATTCTGCAA	450		
Sbjct	80	ACCTAATGGCTTCGGGCGCAACTTGC GTTCAAAGACTCGATGGTTCCGGGGATTCTGCAA	21		
Query	451	TTCACACC	458		
Sbjct	20	TTCACACC	13		

**Figure 1.1** The sequence alignment of the partial ITS-2 region of *Camellia sinensis* L. species with sequences from the GenBank database

**Helianthus annuus external transcribed spacer, 18S ribosomal RNA gene, internal transcribed spacer 1, 5.8S ribosomal RNA gene, internal transcribed spacer 2, and 26S ribosomal RNA gene, complete sequence**

Sequence ID: [KF767534.1](#) Length: 9814 Number of Matches: 1

Range 1: 3850 to 4213 [GenBank](#) [Graphics](#) [Next Match](#) [Previous Match](#)

Score	Expect	Identities	Gaps	Strand
577 bits(312)	5e-160	347/364(95%)	1/364(0%)	Plus/Minus
Query 1	GGGAATCCTTGTAAGTTCTTTTCTCCGCTTATTGATATGCTTAAACTCAGCGGGTAGT	60		
Sbjct 4213	GGGAATCCTTAGTAAGTTCTTTTCTCCGCTTATTGATATGCTTAAACTCAGCGGGTAGT	4154		
Query 61	CCCGCCTGACCTGGGGTCGCGATCGAAGCATCGTCATAAGACAACACATCAGTGGACTTT	120		
Sbjct 4153	CCCGCCTGACCTGGGGTCGCGATCGAAGCATCGTCATAAGACAACACATCAGGGTACTTT	4094		
Query 121	AAAAGGATCTACTCTCAAGAAAGTAAACGCACGACGATACGACAGTCTTATCAACCAC	180		
Sbjct 4093	AAGAGCATCTACTCTCAAGAAAGTAAACGCACGACGACGAGACGACTGCTTATCAACCAC	4034		
Query 181	CACTAGTCGTGCGTCACTCATGAGGGGACTTCTATTTAGGCCAACCGTGCCATGG-CACA	239		
Sbjct 4033	CACTAGCCGTGCGTCCCTCGCGAGGAGACTCTATTTAGGCCAACCGCCATGGGCACG	3974		
Query 240	GGAGACCAATCTCCGCCCAACACAAGACAGCCCTATAGGGGATGCTGGTGGGGGCGAC	299		
Sbjct 3973	GGAGACCAATCTCCGCCCAACACAAGACAGCCCTATAGGGGATGCTGGTGGGGGCGAC	3914		
Query 300	GTGATGCGTGACGCCAGGCAGACGTGCCCTCAACCGAATGGCTTCGGGCACAACTTGG	359		
Sbjct 3913	GTGATGCGTGACGCCAGGCAGACGTGCCCTCAACCGAATGGCTTCGGGCACAACTTGG	3854		
Query 360	TTCA 363			
Sbjct 3853	TTCA 3850			

**Figure 1.2** The sequence alignment of the partial ITS-2 region of *Helianthus annuus* L. species with sequences from the GenBank database

**Mimosa diplotricha voucher LSC115 18S ribosomal RNA gene, partial sequence; internal transcribed spacer 1, 5.8S ribosomal RNA gene, and internal transcribed spacer 2, complete sequence; and 26S ribosomal RNA gene, partial sequence**

Sequence ID: [MH768249.1](#) Length: 633 Number of Matches: 1

[See 1 more title\(s\)](#) [See all Identical Proteins \(IPG\)](#)

Range 1: 275 to 633 [GenBank](#) [Graphics](#) [Next Match](#) [Previous Match](#)

Score	Expect	Identities	Gaps	Strand
664 bits(359)	0.0	359/359(100%)	0/359(0%)	Plus/Minus
Query 65	TTATTGATATGCTTAAACTCAGCGGGTGGCCCCGCTGACCTGGGGTGCACGCGATTTCG	124		
Sbjct 633	TTATTGATATGCTTAAACTCAGCGGGTGGCCCCGCTGACCTGGGGTGCACGCGATTTCG	574		
Query 125	GGGGATCCGCCCGCGGGAACCCATCCCTTGGCGCCCATGCCGGCGGCTCGCGCACG	184		
Sbjct 573	GGGGATCCGCCCGCGGGAACCCATCCCTTGGCGCCCATGCCGGCGGCTCGCGCACG	514		
Query 185	TCAGGTCTCGAGCGCTCGTGGACACTCAACCACCGTGGACCTGGCGGCCGTCGCGTCTG	244		
Sbjct 513	TCAGGTCTCGAGCGCTCGTGGACACTCAACCACCGTGGACCTGGCGGCCGTCGCGTCTG	454		
Query 245	GCCCCTTTTTCGGCCGGCCGGGGGGCTTGGCCCCGGGAGGCCATCATCCGCCGTGCCCC	304		
Sbjct 453	GCCCCTTTTTCGGCCGGCCGGGGGGCTTGGCCCCGGGAGGCCATCATCCGCCGTGCCCC	394		
Query 305	GGGACGGGGGGTTGGCGACGTTTGGCTGACACCCAGGCAGACGTGCCCTCGGCCTAACGGC	364		
Sbjct 393	GGGACGGGGGGTTGGCGACGTTTGGCTGACACCCAGGCAGACGTGCCCTCGGCCTAACGGC	334		
Query 365	TTCCGGCGCAACTTGGCTTCAAAGACTCGATGGTTACGGGATTCTGCAATTACACCA	423		
Sbjct 333	TTCCGGCGCAACTTGGCTTCAAAGACTCGATGGTTACGGGATTCTGCAATTACACCA	275		

**Figure 1.3** The sequence alignment of the partial ITS-2 region of *Mimosa diplotricha* species with sequences from the GenBank database

**Nelumbo nucifera voucher cdK139 18S ribosomal RNA gene, partial sequence; internal transcribed spacer 1, 5.8S ribosomal RNA gene, and internal transcribed spacer 2, complete sequence; and 26S ribosomal RNA gene, partial sequence**

Sequence ID: [FJ599761.1](#) Length: 737 Number of Matches: 1

Range 1: 344 to 737 [GenBank](#) [Graphics](#) [Next Match](#) [Previous Match](#)

Score	Expect	Identities	Gaps	Strand
728 bits(394)	0.0	394/394(100%)	0/394(0%)	Plus/Minus
Query 74	CTTTTCCTCCGCTTATTGATATGCTTAAATTCAGCGGGTGGCCCCGCCGTGACCTGGGGTC			133
Sbjct 737	CTTTTCCTCCGCTTATTGATATGCTTAAATTCAGCGGGTGGCCCCGCCGTGACCTGGGGTC			678
Query 134	GCAAGGCAGGCTCCGTCACAACGGATCCCTAATCGGGTCACACACTCGACACCCCAATG			193
Sbjct 677	GCAAGGCAGGCTCCGTCACAACGGATCCCTAATCGGGTCACACACTCGACACCCCAATG			618
Query 194	ACAACACAACTGGCACAACGTCCAGCATTCCACACCTAAGATTGAACCAACCCGTCG			253
Sbjct 617	ACAACACAACTGGCACAACGTCCAGCATTCCACACCTAAGATTGAACCAACCCGTCG			558
Query 254	TGGCACTTTGTTGTCGGGGCCATCATTGGGCCAACCGCACAAAACGGAACGAGAGGC			313
Sbjct 557	TGGCACTTTGTTGTCGGGGCCATCATTGGGCCAACCGCACAAAACGGAACGAGAGGC			498
Query 314	CAACATCTGCACCAACTCTCCAACACCTAATGGGAAAGGGAAAGGGCAACGATGCG			373
Sbjct 497	CAACATCTGCACCAACTCTCCAACACCTAATGGGAAAGGGAAAGGGCAACGATGCG			438
Query 374	TGACGCCAGGCAGGCATGCCCTTGGCCAAAGGCCTCGGGCGCAACTTGCCTCAAAGA			433
Sbjct 437	TGACGCCAGGCAGGCATGCCCTTGGCCAAAGGCCTCGGGCGCAACTTGCCTCAAAGA			378
Query 434	CTCGATGGTTACGGGATTCTGCAATTCACACCA 467			
Sbjct 377	CTCGATGGTTACGGGATTCTGCAATTCACACCA 344			

**Figure 1.4** The sequence alignment of the partial ITS-2 region of *Nelumbo nucifera* species with sequences from the GenBank database

**Xyris complanata voucher XCS 5.8S ribosomal RNA gene, partial sequence; internal transcribed spacer 2, complete sequence; and large subunit ribosomal RNA gene, partial sequence**

Sequence ID: [MW113223.1](#) Length: 498 Number of Matches: 1

Range 1: 27 to 491 [GenBank](#) [Graphics](#) [Next Match](#) [Previous Match](#)

Score	Expect	Identities	Gaps	Strand
859 bits(465)	0.0	465/465(100%)	0/465(0%)	Plus/Minus
Query 1	GGATTCTCAGCTGGGCTGCTCCCGGTTTCGCTCGCCGTTACTAGGGGAATCCTCGTAAGTT			60
Sbjct 491	GGATTCTCAGCTGGGCTGCTCCCGGTTTCGCTCGCCGTTACTAGGGGAATCCTCGTAAGTT			432
Query 61	TCTCTCCTCCGCTTATTATATGCTTAAATTCGGCGGGTGGTCCCGCTGACCTGGGGT			120
Sbjct 431	TCTCTCCTCCGCTTATTATATGCTTAAATTCGGCGGGTGGTCCCGCTGACCTGGGGT			372
Query 121	CGCGGTCCGGGGGGCGCGCAATGGCTCCCGACCCGGCCGGGTTCCCGTGGGCCGCTCG			180
Sbjct 371	CGCGGTCCGGGGGGCGCGCAATGGCTCCCGACCCGGCCGGGTTCCCGTGGGCCGCTCG			312
Query 181	CCGGCGTGGCGGGCGGGCGGGCGCCGAGCAATCGGGTTCCACAGAGCTCGCCGCGACC			240
Sbjct 311	CCGGCGTGGCGGGCGGGCGGGCGCCGAGCAATCGGGTTCCACAGAGCTCGCCGCGACC			252
Query 241	GCCCGTGCCTCCGGCGACCCGCTCTTCGGCCACCGCGCGCGCGCGAGGGGCCAG			300
Sbjct 251	GCCCGTGCCTCCGGCGACCCGCTCTTCGGCCACCGCGCGCGCGCGAGGGGCCAG			192
Query 301	CGTCCGCGTCCGCAATGACACACCCGTGGGCGCCCGCGCTACGGGGCAGGCGTCGCGCG			360
Sbjct 191	CGTCCGCGTCCGCAATGACACACCCGTGGGCGCCCGCGCTACGGGGCAGGCGTCGCGCG			132
Query 361	GGGCGCGGAGCGTGTGCAGTCTGTGACGCCAGGCGAGGCGTCCCTCGGCCGATGGCCT			420
Sbjct 131	GGGCGCGGAGCGTGTGCAGTCTGTGACGCCAGGCGAGGCGTCCCTCGGCCGATGGCCT			72
Query 421	CGGGCGCAACTTGCCTTCAAAGACTCGATGGTTCCGAGGATTCTG 465			
Sbjct 71	CGGGCGCAACTTGCCTTCAAAGACTCGATGGTTCCGAGGATTCTG 27			

**Figure 1.5** The sequence alignment of the partial ITS-2 region of *Xyris complanata* species with sequences from the GenBank database

**Ageratum conyzoides isolate AGCO\_RR\_2of3 5.8S ribosomal RNA gene, partial sequence; internal transcribed spacer 2, complete sequence; and large subunit ribosomal RNA gene, partial sequence**

Sequence ID: [KY700213.1](#) Length: 499 Number of Matches: 1

Range 1: 16 to 437 [GenBank](#) [Graphics](#) [Next Match](#) [Previous Match](#)

Score	Expect	Identities	Gaps	Strand
719 bits(389)	0.0	411/422(97%)	0/422(0%)	Plus/Minus
Query 1		CCCGGTCGCTCGCCGTTACTAAGGGAATCCTTGTAAAGTTCTTTTCTCCGCTTATTGA		60
Sbjct 437		CCCGGTCGCTCGCCGTTACTAAGGGAATCCTTGTAAAGTTCTTTTCTCCGCTTATTGA		378
Query 61		TATGCTTAAACTCAGCGGTGGTCTTGCCCTGACCTGGGGTCGCGATCGAAAGGCCGTAC		120
Sbjct 377		TATGCTTAAACTCAGCGGTGGTCTTGCCCTGACCTGGGGTCGCGATCGAAAGGCCGTAC		318
Query 121		AAGAACACACATCATGGCAATTTTAAAGTCATTCGCTTAAAGAGTCAGAGCACACGACC		180
Sbjct 317		AAGAACACACATCATGGTACTTTCAAGTCATTCGCTTAAAGAGTCAGAGCACACGCC		258
Query 181		AAGACGACTGTGAAATCAAACCACACCAAGTCGTCCTTTCTTTAGCGGACTCGTGT		240
Sbjct 257		GAGACGACTGTGAAATCAAACCACACCAAGTCGTCCTTTCTTTAGCGGACTCGTGT		198
Query 241		TGGGCCAACACACCATGGGCACGGGAGACCAGTATCCGCCACGTAATACAGATCCAA		300
Sbjct 197		TGGGCCAACACACCATGGGCACGGGAGACCAGTATCCGCCACGTAATACACAAATCCAA		138
Query 301		GAAAGGATGTGTGACGTGGGCACGTGATGCGTGACGCCAGGCAGACATGCCCTCAACC		360
Sbjct 137		GAAAGGATGTGTGACGGGCGACGTGATGCGTGACGCCAGGCAGACATGCCCTCAACC		78
Query 361		GGGTGGCTCAGGCGCAACTTGGGTTCAAAAACCTGATGGTTCACGGGATTCGCAATTC		420
Sbjct 77		GGGTGGCTCAGGCGCAACTTGGGTTCAAAAACCTGATGGTTCACGGGATTCGCAATTC		18
Query 421		AC 422		
Sbjct 17		AC 16		

**Figure 1.6** The sequence alignment of the partial ITS-2 region of *Ageratum conyzoides* species with sequences from the GenBank database

Then, crude extraction and partition will be performed. First, total phenolic and flavonoid content will be assayed. After that, all crude extracts will be investigated on the antioxidant activity using different assays, e.g. free radical scavenging assay (ABTS, TEAC, and DPPH), ferric reducing power (FRP), and enzyme inhibitory activities such as  $\alpha$ -amylase, acetylcholinesterase, tyrosinase, lipoxigenase, and lipase. After that, chromatographic techniques will be used to purify a compound with the highest target bioactivity. Chemical compositions of the active compound will be analyzed. Moreover, pure compounds isolated from bee pollen with the most active in anti-tyrosinase activity at the *in vitro* level will be further performed for the anti-melanogenesis at the cellular levels. The data obtained from this work can be applied to the field of nutritional supplements, cosmetics, and alternative drugs.

In this study, bee pollen was utilized from six plant species: *Camellia sinensis* L., *Helianthus annuus* L., *Mimosa diplotricha*, *Nelumbo nucifera*, *Xyris complanata*, and *Ageratum conyzoides*. Each flowering plant has distinctive flower component traits that attract pollinating insects. *Camellia sinensis* flowers have five to seven white petals with yellow disc in the center, up to 4 cm in diameter, and sweet fragrance. Numerous stamens with yellow anthers are found on the flowers and produce brownish-red capsules (Tariq et al., 2010). *Helianthus annuus* L. flowers consist of two types of flowers. The outer flowers, known as ray flowers, have 16 to 30 yellow to gold-colored petals surrounding a large central disc. The densely clustered flowers in the middle of the head are known as disk flowers which are formed of several dark brown to purple tiny tubular flowers (Fernández-Luqueño et al., 2014). The pinkish-violet flowers of *Mimosa diplotricha* resemble a clustered and fluffy ball. They are approximately 12 mm in diameter and developed from the leaf joints of young leaves on short stalks. The corolla is fused and contains two stamens for every petal (Uko et al., 2020). The flowers of *Nelumbo nucifera* are solitary and large (10–42 cm in diameter). Twenty or more pink or white oblong-elliptic to obovate tepals are arranged spirally. There are 100–200 stamens with thin filaments and linear anthers. Individual pistils are embedded in a flattened yellow carpellary turbinate receptacle (5–10 cm in diameter) (Gowthami et al., 2021). The flowers of *Xyris complanata* are yellow with three 5–9 mm long petals and 3 stamens inserted on the petals. Flower buds are within a brownish head-tight oval, 5–25 mm long, and 3–10 mm in diameter (Phonsena et al., 2013). *Ageratum conyzoides* flowers consist of the branched and terminal inflorescence and bear about 4–18 flower heads, with 60–75 tubular flowers. Individual flower heads are light blue, white, or violet, carry 50–150 mm in length peduncles, and are 5 mm in diameter. The flower head is surrounded by two or three rows of rectangular and green bracts (Chahal et al., 2021).

## **1.2 Objectives of the study**

1.2.1 To determine bioactivities of bee pollen extracts from many types of monofloral pollens

1.2.2 To find out main active compounds in active bee pollen extracts

1.2.3 To investigate the antimelanogenesis of an active compound from a targeted bee pollen at the cellular level.

## **1.3 Scope of the study**

The process begins with collecting several types of monofloral bee pollen in Thailand and identifying flower origin. Then, bee pollen extracts were prepared, and their phenolic and flavonoid content was assessed. Afterward, the antioxidant and enzyme inhibitory activities were evaluated, and the structure of the active components was identified using various chromatographic techniques. In addition, anti-tyrosinase activity of the active compound was also assessed at the cellular level.

## **1.4 Expected beneficial outcomes from the dissertation**

Bee pollen extracts with a targeted bioactivity will be obtained. Also, a pure compound with revealed potential on the antityrosinase activity will be obtained. At last, they can be applied for the field of nutritional supplements, cosmetics, and alterative drugs.

## References

- Araújo JS, Chambó ED, Costa MAPDC, Cavalcante da Silva SMP, Lopes de Carvalho CA, M Estevinho L. 2017. Chemical composition and biological activities of mono- and heterofloral bee pollen of different geographical origins. *International Journal of Molecular Sciences* **18**: 921 DOI 10.3390/ijms18050921
- Campos MG, Bogdanov S, de Almeida-Muradian LB, Szczesna T, Mancebo Y, Frigerio C, Ferreira F. 2008. Pollen composition and standardisation of analytical methods. *Journal of Apicultural Research* **47**: 154-161 DOI 10.1080/00218839.2008.11101443
- Chahal R, Nanda A, Akkol EK, Sobarzo-Sánchez E, Arya A, Kaushik D, Mittal V. 2021. *Ageratum conyzoides* L. and its secondary metabolites in the management of different fungal pathogens. *Molecules* **26**: 2933 DOI 10.3390/molecules26102933
- Daudu OM. 2019. Bee pollen extracts as potential antioxidants and inhibitors of  $\alpha$ -amylase and  $\alpha$ -glucosidase enzymes *in vitro* assessment. *Journal of Apicultural Science* **63**: 315-325 DOI 10.2478/jas-2019-0020
- Denisow B, Denisow-Pietrzyk M. 2016. Biological and therapeutic properties of bee pollen: a review. *Journal of the Science of Food and Agriculture* **96**: 4303-4309 DOI 10.1002/jsfa.7729
- Fernández-Luqueño F, López-Valdez F, Miranda-Arámbula M, Rosas-Morales M, Pariona N, Espinoza-Zapata R. 2014. An introduction to the sunflower crop. *Sunflowers: Growth and Development, Environmental Influences and Pests/Diseases. Valladolid, Spain: Nova Science Publishers* **1**: 1-18
- Gercek YC, Celik S, Bayram S. 2021. Screening of plant pollen sources, polyphenolic compounds, fatty acids, and antioxidant/antimicrobial activity from bee pollen. *Molecules* **27**: 117 DOI 10.3390/molecules27010117
- Giampieri F, Quiles JL, Cianciosi D, Forbes-Hernández TY, Orantes-Bermejo FJ, Alvarez-Suarez JM, Battino M. 2022. Bee products: an emblematic example of underutilized sources of bioactive compounds. *Journal of Agricultural and Food Chemistry* **70**: 6833-6848 DOI 10.1021/acs.jafc.1c05822

- Gowthami R, Sharma N, Pandey R, Agrawal A. 2021. A model for integrated approach to germplasm conservation of Asian lotus (*Nelumbo nucifera* Gaertn.). *Genetic Resources and Crop Evolution* **68**: 1269-1282 DOI 10.1007/s10722-021-01111-w
- Hung KLJ, Kingston JM, Albrecht M, Holway DA, Kohn JR. 2018. The worldwide importance of honeybees as pollinators in natural habitats. *Proceedings of the Royal Society B: Biological Sciences* **285**: 20172140 DOI 10.1098/rspb.2017.2140
- Li F, Guo S, Zhang S, Peng S, Cao W, Ho CT, Bai N. 2019. Bioactive constituents of *F. esculentum* bee pollen and quantitative analysis of samples collected from seven areas by HPLC. *Molecules* **24**: 2705 DOI 10.3390/molecules24152705
- Phonsena P, Chantaranothai P, Meesawat A. 2013. Revision of *Xyris* L. (Xyridaceae) in Thailand. *Thai Forest Bulletin (Botany)* **41**: 102-139
- Su J, Yang X, Lu Q, Liu R. 2021. Antioxidant and anti-tyrosinase activities of bee pollen and identification of active components. *Journal of Apicultural Research* **60**: 297-307 DOI 10.1080/00218839.2020.1722356
- Sun L, Guo Y, Zhang Y, Zhuang Y. 2017. Antioxidant and anti-tyrosinase activities of phenolic extracts from rape bee pollen and inhibitory melanogenesis by cAMP/MITF/TYR pathway in B16 mouse melanoma cells. *Frontiers in Pharmacology* **8**: 104 DOI 10.3389/fphar.2017.00104
- Tariq M, Naveed A, Barkat AK. 2010. The morphology, characteristics, and medicinal properties of *Camellia sinensis*' tea. *Journal of Medicinal Plants Research* **4**: 2028-2033 DOI 10.5897/JMPR10.010
- Tihelka E, Cai C, Pisani D, Donoghue PC. 2020. Mitochondrial genomes illuminate the evolutionary history of the western honey bee (*Apis mellifera*). *Scientific Reports* **10**: 1-10 DOI 10.1038/s41598-020-71393-0
- Uko I, Amadioha AC, Okolie H, Okonkwo NJ. 2020. Problems and prospects of giant sensitive plant (*Mimosa invisa* Mart.) in agroecosystems in Nigeria: a review. *International Journal of Agriculture and Biosciences* **9**: 95-102



Zhang H, Wang X, Wang K, Li C. 2015. Antioxidant and tyrosinase inhibitory properties of aqueous ethanol extracts from monofloral bee pollen. *Journal of Apicultural Science* **59**: 119-128 DOI 10.1515/JAS-2015-0013 DOI 10.1515/JAS-2015-001



## CHAPTER II

### First report of fatty acids in *Mimosa diplotricha* bee pollen with *in vitro* lipase inhibitory activity

#### 2.1 Authors

##### 2.1.1 First author

- **Phanthiwa Khongkarat**

Affiliation: Program in Biotechnology, Faculty of Science, Chulalongkorn University, 254 Phayathai Road, Bangkok 10330, Thailand,  
[parephanthiwa@gmail.com](mailto:parephanthiwa@gmail.com), +66824976525

##### 2.1.2 Corresponding author

- **Professor Chanpen Chanchao, Ph.D (Advisor)**

Affiliation: Department of Biology, Faculty of Science, Chulalongkorn University, 254 Phayathai Road, Bangkok 10330, Thailand,  
[chanpen.c@chula.ac.th](mailto:chanpen.c@chula.ac.th), +66859130412

#### 2.2 Article status

This article was published on 3<sup>rd</sup> January 2022 in Peer J, volume 10 on pages of 12722-12747.

### 2.3 Abstract

Bee pollen (BP) is full of nutrients and phytochemicals, and so it is widely used as a health food and alternative medicine. Its composition and bioactivity mainly depend on the floral pollens. In this work, different BPs collected by *Apis mellifera* from different monoculture flowering crops (BP1-6) were used. The types of floral pollen in each BP were initially identified by morphology, and subsequently confirmed using molecular phylogenetic analysis. Data from both approaches were consistent and revealed each BP to be monofloral and derived from the flowers of *Camellia sinensis* L., *Helianthus annuus* L., *Mimosa diplotricha*, *Nelumbo nucifera*, *Xyris complanata*, and *Ageratum conyzoides* for BP1 to BP6, respectively. The crude extracts of all six BPs were prepared by sequential partition with methanol, dichloromethane (DCM), and hexane. The crude extracts were then tested for the *in vitro* (i)  $\alpha$ -amylase inhibitory, (ii) acetylcholinesterase inhibitory (AChEI), and (iii) porcine pancreatic lipase inhibitory (PPLI) activities in terms of the percentage enzyme inhibition and half maximum inhibitory concentration ( $IC_{50}$ ). The DCM partitioned extract of *X. complanata* BP (DCMXBP) had the highest active  $\alpha$ -amylase inhibitory activity with an  $IC_{50}$  value of  $1,792.48 \pm 50.56$   $\mu\text{g/mL}$ . The DCM partitioned extracts of *C. sinensis* L. BP (DCMCBP) and *M. diplotricha* BP (DCMMBP) had the highest PPLI activities with an  $IC_{50}$  value of  $458.5 \pm 13.4$  and  $500.8 \pm 24.8$   $\mu\text{g/mL}$ , respectively), while no crude extract showed any marked AChEI activity. Here, the *in vitro* PPLI activity was focused on. Unlike *C. sinensis* L. BP, there has been no previous report of *M. diplotricha* BP having PPLI activity. Hence, DCMMBP was further fractionated by silica gel 60 column chromatography, pooling fractions with the same thin layer chromatography profile. The pooled fraction of DCMMBP2-1 was found to be the most active ( $IC_{50}$  of  $52.6 \pm 3.5$   $\mu\text{g/mL}$ ), while nuclear magnetic resonance analysis revealed the presence of unsaturated free fatty acids. Gas chromatography with flame-ionization detection analysis revealed the major fatty acids included one saturated acid (palmitic acid) and two polyunsaturated acids (linoleic and linolenic acids). In contrast, the pooled fraction of DCMMBP2-2 was inactive but pure, and was identified as naringenin, which has previously been reported to be present in *M. pigra* L. Thus, it can be concluded that naringenin was

compound marker for *Mimosa* BP. The fatty acids in BP are nutritional and pose potent PPLI activity.

Keywords: bee pollen, anti-lipase activity, fatty acids, phytochemicals, floral pollen

## 2.4 Introduction

Bee pollen (BP) is one of the economic bee products. It is derived from the flower's male gametophyte produced within anther sacs in the flowers of angiosperms, and is collected by foragers of bees and mixed with the plant's nectar, wax, and bee's saliva to compact the powder into pollen grains. The BP is then loaded into a pollen basket (corbicula), which is part of the tibia on the hind legs (Costa et al., 2019), and later stored in the hive as an essential food for the larva and adults in addition to honey, bee bread, and royal jelly. Nutritionally, BP is known as a functional food for humans and due to its high content of protein and carbohydrates, along with crude fiber, amino acids, vitamins, minerals, and fatty acids (Yang et al., 2013). However, floral identification of BP should be done prior to the consumption as a few people display allergic and anaphylactic reactions after consumption of certain floral pollens (Shahali, 2015; Jagdis and Sussman, 2012). In particular, bee pollen composed of ash (Oleaceae), oak (Fagaceae), willow and poplar (Salicaceae), or corn (*Zea mays*) as the dominant floral pollen requires caution (Vieths et al., 2012).

In addition, BP is also composed of secondary metabolites (polyphenols and flavonoids) of plants (Rzepecka-Stojko et al., 2015). In folk medicine, BP has long been used as a tonic and a multipurpose remedy, and it is widely known that various phytochemicals in BP are bioactive. Chilean BP has been reported to have an antioxidative activity in both the 2,2'-azino-bis(3-ethylbenzothiazoline-6-sulfonate (ABTS) radical and 2,2-diphenyl-1-picryl-hydrazyl-hydrate (DPPH) scavenging capacity assays. Both activities were related to their polyphenols content, especially caffeic acid, coumaric acid, luteolin, and pinocembrin (Munoz et al., 2020).

In addition, BP harvested by the stingless bee, *Scaptotrigona affinis postica*, in Brazil showed an anti-inflammatory activity by inhibiting cyclooxygenase (COX-1 and COX-2) and reducing the edema in male *Mus musculus* mice (Swiss strain) when using the carrageenan- and dextran-induced paw edema tests (Lopes et al., 2020).

However, the composition and phytochemicals in BP mainly depend on the bee species, and its botanical and geographical origins. For example, alkaloids in the BP of *Catharanthus roseus*, saponins in the BP of *Momordica charantia*, sterols and flavinoids in *Butea monosperma*, and tannins in *Syzygium cuminii* all showed a potent antidiabetic activity (Ghoshal and Saoji, 2013). In addition, in Slovakia, *Apis mellifera* BP dominant in rape *Brassica napus* floral pollen had a higher antioxidative activity than BP dominant in poppy *Papaver somniferum* L. and sunflower *Helianthus annuus* L. floral pollen, respectively, (Fatrcova-Sramkova et al., 2013).

The BP collected by the stingless bee, *Melipona fasciculata*, was harvested from three cities in Brazil and revealed different anti-inflammatory and antinociceptive activities, with the highest activities in the BP from Chapadinha City, while the BP collected by *M. fasciculata* showed higher anti-inflammatory and antinociceptive activities than that collected by *A. mellifera* (Lopes et al., 2019).

The BPs collected from different geographical regions in Brazil had different chemical compositions and bioactivities (Araújo et al., 2017). Monofloral BPs of *Eucalyptus* spp. and multifloral BP exhibited potent inhibitory activities against  $\alpha$ -amylase, acetylcholinesterase (AChE), tyrosinase, lipoxygenase, lipase, and hyaluronidase, but with different half maximal inhibitory concentration (IC<sub>50</sub>) values. Monofloral BP of *Cocos nucifera* and *Miconia* spp. also exhibited antioxidant properties.

From 18 samples of mono- and poly-floral BPs harvested from 16 different localities in South Korea, all were found to have anti-oxidant, anti-human  $\beta$ -amyloid precursor cleavage enzyme, AChE inhibitory (AChEI), anti-human intestinal bacteria, and anticancer activities, but with different IC<sub>50</sub> values (Zou et al., 2020).

In terms of their nutrient compositions, polyfloral BPs gave more benefits than mono-floral ones, in terms of having more diverse secondary metabolite-like compounds. Metabolomics analysis revealed that beehive pollen from diverse species of plants contained key ingredients for health (lactate, a pentose sugar, myo-inositol, phosphate, and a furanose), but not in BP dominated by canola floral pollen (Arathi et al., 2018). In addition, *A. mellifera* fed with polyfloral BP were more tolerant to the microsporidian *Nosema ceranae* (Di Pasquale et al., 2013). However, in terms of the quality control standards for BP consumption by humans and its industrial production,

monofloral BP is more fruitful because known bioactive molecules and their precise concentration can be more easily and economically ascertained (Kostic et al., 2021).

The BPs from several countries, including Argentina, Brazil, China, and Spain, have been commercialized after their chemical compositions and bioactivities were reported (Sindhi et al., 2013). However, little is known about the BP in Thailand, which is high in both bee and plant diversities (Chantarudee et al., 2012; Rattanawanee and Chanchao, 2011).

In order to identify the bioactive molecules in BP that originated from native plants in Thailand, monofloral BP harvested by *A. mellifera* from six types of floral pollen was examined. The type of floral pollen in each of the BPs (BP1 to BP6) were first identified by palynological analysis using light microscopy (LM) and scanning electron microscopy (SEM), and then by molecular analysis examining the partial sequence of the second internal transcribed sequence (ITS-2) of the ribosomal RNA genes. Then, each of the six BPs was sequentially extracted with methanol, dichloromethane (DCM), and hexane, and the partitioned extracts were screened for  $\alpha$ -amylase, AChE, and lipase inhibitory activities. Among these bioactivities, the lipase inhibitory activity was targeted due to there being a few previous reports on this activity in BP. The most active sample was subjected to further fractionation by chromatography, and the obtained fractions were analyzed for purity/composition by thin layer chromatography (TLC) and, for fatty acids, by gas chromatography with a flame ionization detector (GC-FID) after conversion to fatty acid methyl esters (FAMES). Seemingly pure active compounds were analysed by nuclear magnetic resonance (NMR). A chemical compound marker was revealed in the typical bee pollen. The obtained data support the safety and benefit of BP consumption.

## 2.5 Materials and Methods

### 2.5.1 Chemicals and reagents

The chemicals ( $\alpha$ -amylase, acarbose, AChE from electric eel, acetylthiocholine iodide, 5,5'-dithiobis (2-nitrobenzoic acid), physostigmine, crude porcine pancreatic lipase type II, p-nitrophenyl palmitate, and orlistate) used in this study were from Sigma-Aldrich, Darmstadt, Germany.

### 2.5.2 Sample collection

Six *A. mellifera* BPs (BP1 to BP6), one from each of six localities in Thailand, were collected in 2018, that were suspected, based on the available flowers near the hives, of being monofloral and derived from *Camellia sinensis* L. and *Mimosa diplotricha* in Chiangmai province (BP 1 and BP3, respectively), *Helianthus annuus* L. in Lopburi province (BP2), *Nelumbo nucifera* in Nakhon Sawan province (BP4), *Xyris complanata* in Udon Thani province (BP5), and *Ageratum conyzoides* in Lamphun province (BP6), respectively. The BP samples used were dried using a specific process and stored at room temperature (25 °C) until used.

### 2.5.3 Identification of the bee pollen

#### *By palynological analysis*

The morphology of each BP was initially observed under LM at 400X magnification. Briefly, the respective BP was dispersed in distilled water (d-H<sub>2</sub>O) on a glass slide, and pictures and characteristics of the BPs were recorded and compared to the reported publications.

Next, the morphology was observed under SEM at 1,500–5,000X magnification. Briefly, BPs were washed three times with ethanol (5 min each), and then three times with acetone (5 min each). The samples were then sent for SEM and energy dispersive X-ray spectrometry (6610LV; Tokyo, Japan) imaging at the Scientific and Technological Research Equipment Center of Chulalongkorn University. The morphology and characteristics of the BPs were recorded and compared to the reported publications.

#### *By molecular analysis*

Each BP was further identified by comparison of the partial ITS-2 DNA sequences (Richardson et al., 2015) to the species-annotated sequences in the GenBank database. For this, the genomic DNA was extracted from approximately 100 mg of BP using a DNeasy Plant Mini Kit (catalog no. 69104, Qiagen, Germany). The quality of the extracted DNA was determined by 1.2% (w/v) agarose gel electrophoresis and the ratio of absorbance at 260 and 280 nm. After DNA isolation, the ITS-2 region was amplified using the polymerase chain reaction (PCR) with the

forward (5'-ATGCGATACTTGGTGTGAAT-3') and reverse (5'-GACGCTTCTCCA GACTAC AAT-3') primers. Each PCR amplification was performed in a 25  $\mu$ L final reaction volume comprised of 12.5  $\mu$ L of 2X EmeraldAmp® PCR master mix (catalog # RR300A, Takara), 1  $\mu$ L of each of primer (10  $\mu$ M), at least 30 ng of genomic DNA template, and nuclease-free d-H<sub>2</sub>O. The PCR thermal cycling was performed as 98 °C for 30 s, followed by 30 cycles of 98 °C for 10 s, 59 °C for 30 s, and 72 °C for 30 s; and then a final 72 °C for 10 min. The PCR product (500 bp) was checked by 1.2% (w/v) agarose gel electrophoresis in 1X Tris-borate-EDTA buffer at 80 V for 45 min after Ecodye staining. The PCR product was extracted using QIAquick PCR Purification Kit (catalog no. 28106, Qiagen, Germany) and sent for commercial direct sequencing. The obtained sequences were used to search for homologous sequences in the GenBank database of the National Center for Biotechnology Information using the Basic Local Alignment Search Tool for nucleotide (BLASTn) algorithm.

#### 2.5.4 Crude extraction and partition

The extraction and partition was modified from Chantarudee et al. (2012). Each BP (140 g) was mixed with 800 mL of methanol (MeOH), shaken at 100 rpm, 15 °C for 18 h, and then centrifuged at 6,000 rpm, 4 °C, for 15 min. The supernatant was collected, while the solid residue (pellet) was re-extracted three more times in the same manner with 800 mL of MeOH each time. The supernatants were pooled and evaporated under reduced pressure at a maximum temperature of 40–45 °C to obtain the crude MeOH extracts, which were kept at -20 °C in the dark until used.

The MeOH crude extracts were sequentially partitioned by hexane (low polarity), to eliminate the lipid and non-polar compounds; DCM (medium polarity), and finally MeOH (high polarity). To this end, the six MeOH crude extracts (one for each of BP1–6) were separately dissolved in MeOH until it was not sticky and then mixed with an equal volume of hexane in a separating funnel and left to phase separate, whereupon the upper hexane phase was collected. The lower MeOH phase was then further extracted with hexane in the same manner twice more, and the hexane extracts were pooled and evaporated under reduced pressure at a maximum temperature of 40–45 °C to yield the hexane partitioned (HX) extracts of BP1–6 (bee



pollen from *C. sinensis* L., *H. annuus* L., *M. diplotricha*, *N. nucifera*, *X. complanata*, and *A. conyzoides*, respectively, and designated as HXCBP, HXHBP, HXMBP, HXNBP, HXXBP, and HXABP, respectively). Meanwhile, the residual MeOH phase was then extracted with an equal volume of DCM three times in the same manner as above (except the DCM phase was the lower layer), with the pooled DCM extracts evaporated as above. The sample from this step was named the DCM partitioned extracts of *C. sinensis* L., *H. annuus* L., *M. diplotricha*, *N. nucifera*, *X. complanata* and *A. conyzoides* flower BP (BP1–6, respectively), and designated as DCMCBP, DCMHBP, DCMMBP, DCMNBP, DCMXBP, and DCMABP, respectively.

Finally, the residual MeOH phase was evaporated as above to yield the MeOH-partitioned (MT) extract of *C. sinensis* L., *H. annuus* L., *M. diplotricha*, *N. nucifera*, *X. complanata* and *A. conyzoides* flower BPs (BP1–6, respectively, and designated as MTCBP, MTHBP, MTMBP, MTNBP, MTXBP, and MTABP, respectively). All partitioned extracts were kept at -20 °C in the dark until used to test the biological activities.

### 2.5.5 *In vitro* $\alpha$ -amylase inhibitory activity

The  $\alpha$ -amylase inhibition assay was modified from Akoro et al. (2017). The partitioned extract of BP was dissolved in dimethyl sulfoxide (DMSO) and subsequently diluted in MeOH at different concentrations (125, 250, 500, 1,000, and 2,000  $\mu\text{g}/\text{mL}$ ). Two hundred and fifty  $\mu\text{L}$  of  $\alpha$ -amylase solution [0.5 units (U)/mL] dissolved in buffer [ $\text{Na}_2\text{HPO}_4/\text{NaH}_2\text{PO}_4$  (0.02 M) and NaCl (0.006 M)] at pH 6.9 was mixed with 250  $\mu\text{L}$  of the extract and incubated at 37 °C for 10 min. After that, 250  $\mu\text{L}$  of the starch solution [0.5% (w/v) in d- $\text{H}_2\text{O}$ ] was added and incubated at 37 °C for 10 min. The reaction was terminated by the addition of 500  $\mu\text{L}$  DNSA reagent (12 g of sodium potassium tartrate tetrahydrate in 8.0 mL of 2 M NaOH, and 20 mL of 96 mM of 3,5-dinitrosalicylic acid solution) and was heated at 85–90 °C for 5 min in a water bath. The mixture was cooled to room temperature and was diluted with 5 mL of d- $\text{H}_2\text{O}$ , and the absorbance was measured at 540 nm ( $A_{540}$ ) using a UV-Visible spectrophotometer (Sunrise, Tecan, Austria). Acarbose was used as the positive inhibitor. Each sample was performed and measured in triplicate. The inhibitory percentage of  $\alpha$ -amylase was calculated using the equation given below.

$$\text{Percentage of } \alpha\text{-amylase inhibition} = \frac{[(A-B) - (C-D)]}{(A-B)} \times 100$$

where A is the  $A_{540}$  after incubation without an extract, B is the  $A_{540}$  after incubation without an extract and  $\alpha$ -amylase, C is the  $A_{540}$  after incubation with an extract and  $\alpha$ -amylase, and D is the  $A_{540}$  after incubation with an extract, but without  $\alpha$ -amylase.

The %  $\alpha$ -amylase inhibition (Y axis) was plotted against the extract concentrations (X axis) and the  $IC_{50}$  value was obtained using regression analysis.

#### 2.5.6 *In vitro* AChEI inhibitory activity

Evaluation of the AChEI activity was modified from Li et al. (2019) based on Ellman's method. Firstly, 160  $\mu$ L of TTB [50 mM Tris-HCl buffer pH 8 with 1% (v/v) Triton X-100], 20  $\mu$ L of the extract dissolved in DMSO (500  $\mu$ g/mL), and 10  $\mu$ L of 0.2 U/mL AChE from electric eel dissolved in 0.1% (w/v) bovine serum albumen in TTB were mixed and incubated at 4  $^{\circ}$ C for 20 min. Then, 5  $\mu$ L of 15 mM acetylthiocholine iodide in d- $H_2O$  and 5  $\mu$ L of 2 mM 5,5'-dithiobis (2-nitrobenzoic acid) (DTNB) in TTB containing 0.1 M NaCl and 0.02 M  $MgCl_2$  were added per well and incubated at 37  $^{\circ}$ C for 20 min. The absorbance at a wavelength of 412 nm ( $A_{412}$ ) was measured using a microplate reader (Sunrise, Tecan, Austria). Physostigmine was used as the positive control. All the reactions were performed in triplicate. The percentage inhibition was calculated as follows.

$$\text{Percentage of AChE inhibition} = \frac{[(A-B) - (C-D)]}{(A-B)} \times 100$$

where A is the  $A_{412}$  after incubation without an extract, B is the  $A_{412}$  after incubation without an extract and AChE, C is the  $A_{412}$  after incubation with an extract and AChE, and D is the  $A_{412}$  after incubation with an extract, but without AChE.

The % AChEI (Y axis) was plotted against the extract concentrations and the  $IC_{50}$  values were obtained using linear or non-linear regression analysis.

#### 2.5.7 *In vitro* porcine pancreatic lipase inhibitory (PPLI) activity

The enzyme solution was prepared immediately before use as previously described (Jamous et al., 2018) with some modifications. Crude PPL type II was suspended in 50 mM Tris-HCl buffer pH 8 to a concentration of 2 mg/mL. The suspension was mixed and centrifuged at 16,000x g for 10 min. The clear supernatant was recovered and kept. The PPLI assay was adapted from Maqsood et al. (2017).

Briefly, 100  $\mu\text{L}$  of the extract at different concentrations (200, 400, 600, 800, and 1,000  $\mu\text{g}/\text{mL}$  for DCMCBP, DCMMBP, DCMNBP, DCMXBP, and DCMABP; and 12.5, 25, 50, 100, and 200  $\mu\text{g}/\text{mL}$  for DCMMBP2 and DCMMBP2-1) dissolved in DMSO and 600  $\mu\text{L}$  of 50 mM Tris-HCl buffer (pH 8.0) were pre-incubated with 200  $\mu\text{L}$  of 2 mg/mL of PPL solution at 37  $^{\circ}\text{C}$  for 30 min. Afterwards, 100  $\mu\text{L}$  of 1.5 mM of p-nitrophenyl palmitate (p-NPP) in isopropanol was added and incubated at 37  $^{\circ}\text{C}$  for 2 h. Lipase activity was determined by measuring the hydrolysis of p-NPP to p-nitrophenol product via measuring the absorbance at 410 nm ( $A_{410}$ ) using a microplate reader. Orlistat was used as the positive standard. Each sample was performed and measured in triplicate. The percentage of lipase inhibition was calculated according the following formula.

$$\text{Percentage of lipase inhibition} = \left[ \frac{(A-B) - (C-D)}{(A-B)} \right] \times 100$$

where A is the  $A_{410}$  after incubation without an extract, B is the  $A_{410}$  after incubation without an extract and lipase, C is the  $A_{410}$  after incubation with an extract and lipase, and D is the  $A_{410}$  after incubation with an extract, but without lipase.

The % lipase inhibition (Y axis) was plotted against the extract concentrations (X axis) and the  $\text{IC}_{50}$  values were obtained from the graph.

#### 2.5.8 Enrichment of active fractions

Among the mentioned bioactivities, the extract with the most potent *in vitro* PPLI activity was used for further fractionation (enrichment) by silica gel 60 column chromatography (SiG60-CC).

##### (A) Large scale SiG60-CC (500-mL column)

A 500-mL column was packed with fine SiG60 (Merck). The partitioned extract (6.0 g) was dissolved in 20 mL of MeOH and combined with 20 g of rough SiG60 and allowed to dry, whereupon it was poured over the surface of the packed SiG60 column. The column was first eluted with 6.5 L of DCM, followed by 8.5 L of 7% (v/v) MeOH in DCM and then 3.5 L of MeOH, respectively. Eluted fractions (250 mL each) were collected, and the solvent was removed by evaporation under reduced pressure at a maximum temperature of 40–45  $^{\circ}\text{C}$ . The pattern of chemical compounds in each fraction was profiled by TLC (see below). Fractions with the same TLC

pattern were pooled together and tested for *in vitro* PPLI activity using the assay as above.

*(B) Small scale SiG60-CC (250-mL column)*

A 250-mL column was packed with fine SiG60. The active fraction (300 mg) was dissolved in 5 mL of MeOH and combined with 5 g of rough SiG60 and allowed to dry, whereupon it was poured over the surface of the packed SiG60 column. The column was eluted with 1,000 mL of 2% (v/v) MeOH in DCM and then 500 mL of MeOH, respectively. Eluted fractions (7 mL each) were collected, and the solvent was removed by evaporation under reduced pressure at a maximum temperature of 40–45°C. The pattern of chemical compounds in each fraction was profiled by TLC (see below). Fractions with the same TLC pattern were assumed to be chemically similar and were pooled. After that, each fraction was tested for its *in vitro* PPLI activity using the assay as above.

*One-dimensional TLC*

A 5 x 5 cm<sup>2</sup> TLC plate with silica as the immobile phase was prepared. The sample was spotted onto the solvent front line of the plate by a capillary tube, allowed to dry at room temperature, and then resolved in one direction using the appropriate mobile phase solvent of 7% (v/v) MeOH: DCM. The resolved compounds on the TLC plate were visualized under UV light at 254 nm or by dipping in 3% (v/v) anisaldehyde in MeOH and heating over a hot plate.

2.5.9 Chemical structure analysis by NMR

Among the fractions obtained from the SiG60-CC (250-mL size), the most active fraction for PPLI activity was evaporated and analysed. Briefly, the evaporated sample was dissolved in an appropriate deuterated solvent (Chloroform-d or MeOH-d<sub>4</sub>, Merck) at a ratio of 5–20 mg of compound to 600 µL of deuterated solvent. It was then transferred to an NMR tube and shaken until completely dissolved. The NMR spectrum was recorded on a Jeol JNM-ECZ (JNM-ECZ500R, Tokyo, Japan) 500MHz operated at 500 MHz for <sup>1</sup>H-NMR nuclei in order to detect the functional groups using tetramethylsilane as the internal standard. The chemical shift in δ (ppm) was assigned with reference to the signal from the residual protons in the deuterated

solvents, while the chemical shift and J coupling value were determined using the MestReNova version 12.0.3 software.

#### 2.5.10 Preparation of FAMES

A portion (26.7 mg) of the fraction with the highest PPLI activity obtained from SiG60-CC (250-mL size), was added to absolute MeOH (2 mL), followed by 0.5 mL of concentrated H<sub>2</sub>SO<sub>4</sub>. The reaction mixture was stirred and heated at 60 °C for 3.5 h. The reaction mixture was then evaporated to dryness, diluted with DCM (6 mL) and extracted with saturated NaHCO<sub>3</sub>. The DCM layer was collected and washed several times with d-H<sub>2</sub>O until pH of the solution was 7. The combined DCM layer was dried over anhydrous Na<sub>2</sub>SO<sub>4</sub> and evaporated to dryness. Prior to analysis of the prepared FAMES by GC-FID analysis (6890N GC, California, USA), the formation of FAMES was confirmed by <sup>1</sup>H-NMR analysis (JNM-ECZ500R, Tokyo, Japan), where the singlet signal of the methoxy group at δ<sub>H</sub> 3.65 ppm was observed (Supplement 3).

#### 2.5.11 GC-FID analysis

The prepared FAMES of the fraction with the highest PPLI activity from the SiG60-CC (250-mL size) fractionation was submitted to the Food Research and Laboratory (Faculty of Science, Chulalongkorn University) for analysis of its fatty acid components by GC-FID following the AOAC method 996.06. Briefly, chromatographic analysis was performed using a GC-FID system (Agilent 6890 N) equipped with an autosampler and split-splitless injector. A SPTM 2560 FULED SILICA capillary column with an internal diameter of 0.25 mm and 0.2 μm film thickness was used for the chromatographic separation. Helium was used as the carrier gas at 1.1 mL/min. The injector and detector temperatures were set at 260 and 250 °C, respectively. The initial GC oven temperature was 140 °C, held for 5 min, increased to 240 °C at 20 °C/min, and held at 250 °C for 0.5 min. A volume of 1.0 μL of sample was injected using the split injection mode (100:1). The peaks were identified by comparison of their relative retention times with a standard FAME mixture. The results were expressed as mg/g fatty acid.

### 2.5.12 Data analysis

Experiments were performed in triplicate. Numerical data are reported as the mean  $\pm$  one standard deviation ( $\pm$  SD), determined in the Microsoft Excel 2019 software. One-way ANOVA and T-test were used to test for significant differences in IC<sub>50</sub> values. Tukey's test ( $p < 0.05$ ) was applied for the pairwise multiple comparisons. The statistical analyses were performed using IBM SPSS statistics version 22 for windows.

The overall procedure of BP screening and enrichment for the PPLI active component in the most active extract is summarized schematically in Figure 2.1.



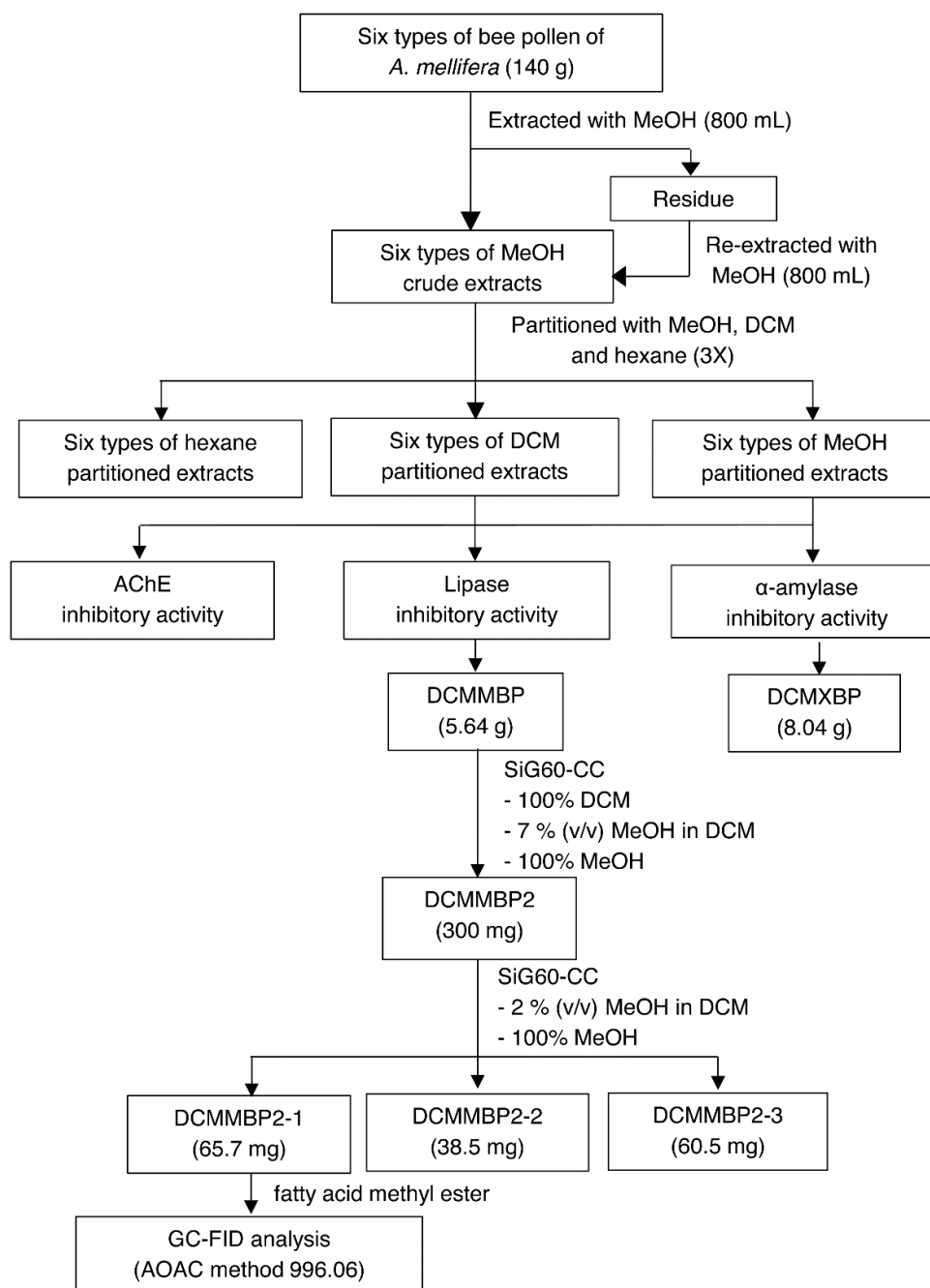


**Figure 2.1** Summary for extraction, screening and enrichment procedures for the selected BP.

## 2.6 Results

### 2.6.1 Palynological analysis of the six BP samples

The major floral pollen types present in BP must be identified in order to report the type of floral pollen present in the BP. The simplest way is by morphology using LM and SEM analyses. Under LM and SEM, the morphology of bee pollen was observed. The pollen grains in BP1 were convex triangular with tricolporate, and the exine ornamentation was verrucate (Figures 2.2, A and 2.3, A). This is consistent with the pollen grains of *C. sinensis* (L.) Kuntze (Ariyaratna et al., 2011; Fan et al., 2019). The pollen grains of BP2 were close to spherical with triaperturate, and the exine ornamentation was echinate (Figures 2.2, B and 2.3, B), supported it to be the pollen grains of *H. annuus* L. (Ali et al., 2021). The pollen grains of BP3 were spherical or prolate spheroidal in shape with four (tetrad) pollen subunits, and the exine ornamentation was tuberculate (Figures 2.2, C and 2.3, C), supporting it to be the pollen grains of *M. diplotricha* (Lima et al., 2008; Peukpiboon et al., 2017). The pollen grains of BP4 were spherical in shape with tricolpate, and the exine ornamentation was uniformly dense reticulate (Figures 2.2, D and 2.3, D), supporting that they were the pollen grains of *N. nucifera* (Sangsuk et al., 2021; Zhang et al., 2019). The pollen grains of BP5 were ellipsoidal in polar view, flattened/convex in equatorial view with monosulcate and operculate, and the exine ornamentation was reticulate (Figures 2.2, E and 2.3, E), they consistent with the pollen grains of *X. complanata* (da Luz et al., 2015). Finally, the pollen grains of BP6 were spherical in shape with tricolporate, and the exine ornamentation was echinate (Figures 2.2, F and 2.3, F) confirming they were the pollen grains of *A. conyzoides* (Zafar et al., 2017; Garg, 1996).



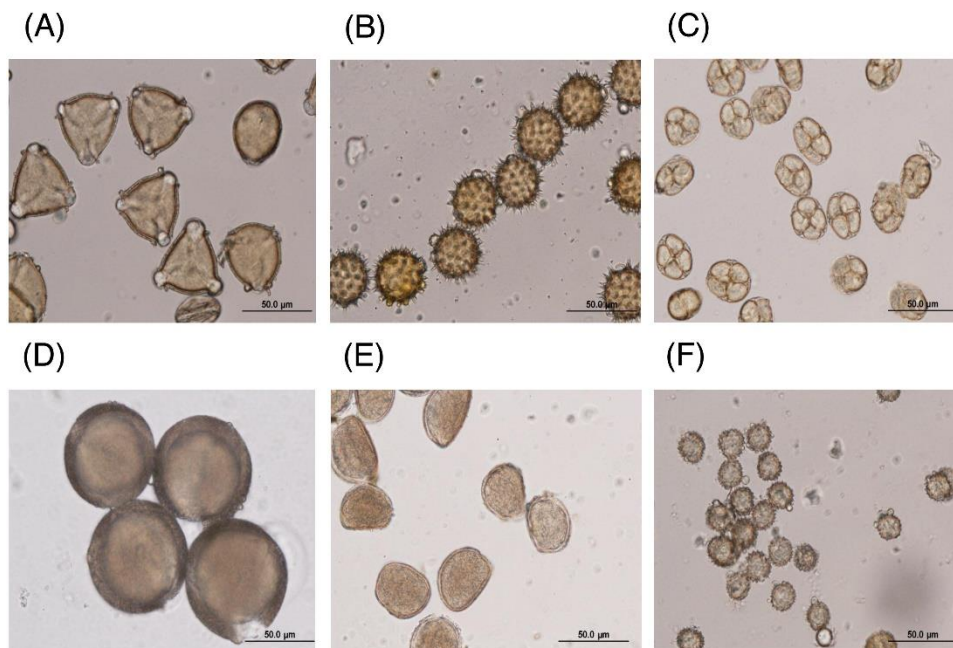


**Figure 2.2** Representative LM images (400 x magnification) of (A–F) BP1–6, respectively, identified as (A) *C. sinensis* L., (B) *H. annuus* L., (C) *M. diplotricha*, (D) *N. nucifera*, (E) *X. complanata*, and (F) *A. conyzoides* flower pollen.

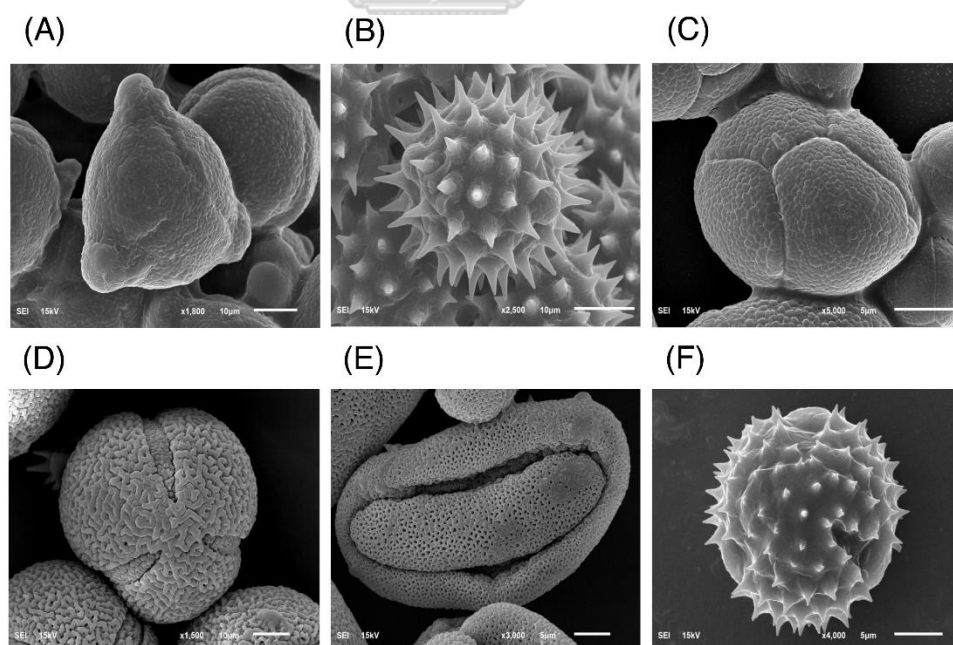


**Figure 2.3** Representative SEM images (1,500–5,000 x magnification) of (A–F) BP1–6 respectively, identified as (A) *C. sinensis* L., (B) *H. annuus* L., (C) *M. diplotricha*, (D) *N. nucifera*, (E) *X. complanata*, and (F) *A. conyzoides* flower pollen.

### 2.6.2 Identification of the pollen species in each BP sample by molecular analysis

The six BP samples (BP1–6) were also identified by sequence analysis of the ITS-2 region of the rRNA genes. In each case, PCR amplification of the ITS-2 region gave an amplicon of the expected size (500 bp). After sequencing the amplicons and using them as the query sequence to BLASTn search the GenBank reference sequences, the same plant pollen species identifications were obtained as by the LM and SEM morphological analyses. Sample BP1 showed 100% nucleotide identity to the sequence of *C. sinensis* L. (accession # MN242039.1), BP2 at 95.33% nucleotide identity to the sequence of *H. annuus* L. (accession # KF767534.1), BP3–6 at 100% nucleotide identity to the sequence of *M. diplotricha* (accession # MH768249.1), *N. nucifera* (accession # FJ599761.1), *X. complanata* (accession # MW113223), and *A. conyzoides* (accession # KY700213.1), respectively.

Thus, the six BPs were confirmed to be essentially monofloral, matching the principal flowers around the hives, and with the morphological and molecular analyses congruent with each other. Thus, floral origin of each BP was clarified in this work.

### 2.6.3 The partitioned extracts of BP

For the six BPs, they were separately sequentially partitioned by MeOH, DCM, and hexane, three organic solvents with different polarities. The yield and character of all 18 obtained extracts (three solvents for each of BP1-6) are summarized in Table 2.1. The highest yield was obtained from the MeOH-partitioned extracts in all six samples (above 40%). Only a sticky solid form was obtained for the DCM-partitioned extracts, while an oil form was obtained in both the MeOH- and hexane-partitioned extracts.

However, only the MeOH and DCM partitioned extracts of all six types of BP were tested for the three enzyme inhibitory activities because the hexane-partitioned extracts were insoluble in each of the respective enzyme assay buffer solutions.

**Table 2.1** The weight, yield, and character of the partitioned extracts.

Sample	Weight (g)	Yield (%)	Character
MTCBP	64.93	46.38	Pale brown oil
DCMCBP	7.41	5.29	Sticky dark brown solid
HXCBP	7.73	5.52	Dark brown oil
MTHBP	79.97	57.12	Dark brown oil
DCMHBP	12.55	8.96	Sticky dark brown solid
HXHBP	8.98	6.41	Dark brown oil
MTMBP	57.90	41.36	Dark brown oil
DCMMBP	9.89	7.06	Sticky dark brown solid
HXMBP	7.43	5.31	Dark brown oil
MTNBP	79.49	56.8	Pale brown oil
DCMNBP	4.68	3.34	Sticky brown solid
HXNBP	5.31	3.79	Pale brown oil
MTXBP	96.81	69.15	Dark brown oil
DCMXBP	8.04	56.8	Sticky dark brown solid
HXXBP	11.7	8.36	Dark brown oil
MTABP	79.28	56.63	Dark brown oil
DCMABP	5.75	4.11	Sticky dark brown solid
HXABP	8.47	6.05	Dark brown oil

#### 2.6.4 *In vitro* $\alpha$ -amylase inhibitory activity

The partitioned extracts were initially used at a final concentration of 2 mg/mL, and the  $\alpha$ -amylase inhibitory activity (%) is presented as the mean  $\pm$  SD in Table 2.2. At this concentration, DCMXBP provided the highest *in vitro*  $\alpha$ -amylase inhibitory activity ( $54.8 \pm 2.8\%$ ). The subsequent dose response assay revealed the anti  $\alpha$ -amylase activity of DCMXBP was concentration dependent (Figure 2.4, A, supplement 1) with an  $IC_{50}$  value of  $1,792.5 \pm 51.0$   $\mu$ g/mL (Table 2.2), which was markedly less effective than that of acarbose, the positive control (Figure 2.5, A, supplement 2) with a 63-fold lower  $IC_{50}$  value of  $28.1 \pm 2.7$   $\mu$ g/mL. In contrast,

DCMMBP and MTXBP had no real anti- $\alpha$ -amylase activity at this concentration of 2 mg/mL ( $1.19 \pm 2.06\%$  and  $0.00 \pm 0.00\%$ , respectively).

#### 2.6.5 *In vitro* AChEI activity

The partitioned extracts were initially screened for AChEI activity at a final concentration of 500  $\mu\text{g/mL}$ . The *in vitro* AChEI activity (%) is presented as the mean  $\pm$  SD in Table 2.2. At this concentration, DCMCBP provided the highest AChEI activity at  $19.3 \pm 1.5\%$ . However, the AChEI activity of all the partitioned extracts were negligible compared to that of physostigmine, the positive control, with an over 230-fold lower  $\text{IC}_{50}$  value of  $0.082 \pm 0.002 \mu\text{g/mL}$  (Figure 2.5, B and Table 2.2, supplement 2).

#### 2.6.6 *In vitro* PPLI activity

The partitioned extracts were initially screened for PPLI activity at a final concentration of 400  $\mu\text{g/mL}$  with the results (as the % PPLI activity) presented as the mean  $\pm$  SD in Table 2.2. This concentration was selected because it was the highest concentration that could be totally dissolved in DMSO. At this concentration, some DCM partitioned extracts showed a PPLI activity close to 50%, and so they were further evaluated at different concentrations. The PPLI activity was found to be dose-dependent (Figure 2.4, B, supplement 1) and broadly similar between DCMCBP and DCMMBP, with  $\text{IC}_{50}$  values of  $458.5 \pm 13.4$  and  $500.8 \pm 24.8 \mu\text{g/mL}$ , respectively. However, they were markedly less effective than orlistat, the positive control, with an over 21,800-fold lower  $\text{IC}_{50}$  value of  $0.021 \pm 0.000 \mu\text{g/mL}$  (Figure 2.5, C, supplement 2).

**Table 2.2** The percentage of enzyme inhibition (mean  $\pm$ S.D.) and IC<sub>50</sub> value ( $\mu$ g/mL) of the partitioned extracts.

Sample	$\alpha$ -amylase / IC <sub>50</sub>	AChE/IC <sub>50</sub>	PPLI/IC <sub>50</sub>
MTCBP	16.12 $\pm$ 1.81 / -	7.74 $\pm$ 0.23 / -	7.74 $\pm$ 0.56 / -
DCMCBP	38.58 $\pm$ 3.87 / -	19.25 $\pm$ 1.50 / -	49.47 $\pm$ 1.31 / 458.48 $\pm$ 13.38 <sup>b</sup>
MTHBP	14.31 $\pm$ 0.99 / -	11.34 $\pm$ 0.92 / -	29.86 $\pm$ 1.15 / -
DCMHBP	42.70 $\pm$ 2.49 / -	8.23 $\pm$ 1.97 / -	3.65 $\pm$ 1.72 / -
MTMBP	11.68 $\pm$ 1.05 / -	13.95 $\pm$ 1.51 / -	14.38 $\pm$ 1.38 / -
DCMMBP	1.19 $\pm$ 2.06 / -	10.22 $\pm$ 3.72 / -	42.89 $\pm$ 2.23 / 500.80 $\pm$ 24.76 <sup>b</sup>
MTNBP	7.92 $\pm$ 1.12 / -	4.13 $\pm$ 0.47 / -	31.58 $\pm$ 0.64 / -
DCMNBP	4.50 $\pm$ 2.88 / -	5.91 $\pm$ 1.74 / -	39.49 $\pm$ 1.48 / 876.09 $\pm$ 24.15 <sup>d</sup>
MTXBP	0.00 $\pm$ 0.00 / -	7.37 $\pm$ 1.71 / -	38.51 $\pm$ 0.13 / -
DCMXBP	54.82 $\pm$ 2.76 / 1,792.48 $\pm$ 50.96 <sup>b</sup>	7.76 $\pm$ 3.67 / -	35.09 $\pm$ 1.04 / 960.49 $\pm$ 38.19 <sup>e</sup>
MTABP	13.72 $\pm$ 1.44 / -	6.81 $\pm$ 0.85 / -	14.53 $\pm$ 0.94 / -
DCMABP	41.45 $\pm$ 4.23 / -	9.95 $\pm$ 3.59 / -	37.38 $\pm$ 2.39 / 646.09 $\pm$ 19.41 <sup>c</sup>
Acarbose	- / 28.08 $\pm$ 2.65 <sup>a</sup>	-	-
Physostigmin	- /	- /	-
e		0.082 $\pm$ 0.002	
Orlistat	-	-	- / 0.021 $\pm$ 0.000 <sup>a</sup>

**Notes:**

The IC<sub>50</sub> values were calculated using nonlinear regression except for DCMNBP and orlistat that were calculated using linear regression. Data are shown as the mean. Within a column, means with a different superscript letter are significantly different [ $p < 0.05$ ; One-way ANOVA for anti-amylase activity ( $p = 0.000$ ) and Post Hoc (Tukey) test for anti-lipase activity ( $p = 0.000$  except  $p$  between DCMNBP and DCMXBP = 0.008)].

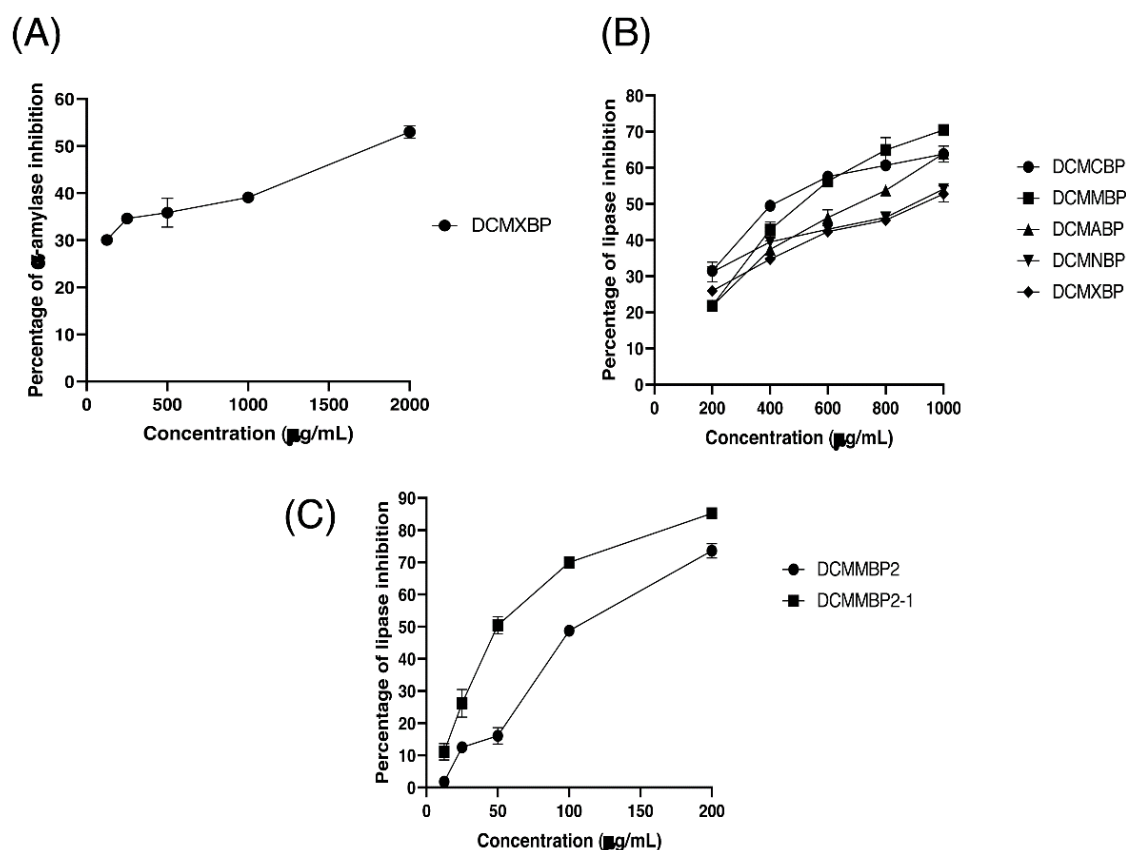


**Figure 2.4** The (A)  $\alpha$ -amylase inhibition activity (%) of DCMXBP, (B) PPLI activity (%) of DCM partitioned extracts, and (C) PPLI activity (%) of DCMMBP2 and DCMMBP2-1. Data are shown as the mean  $\pm$  SD.

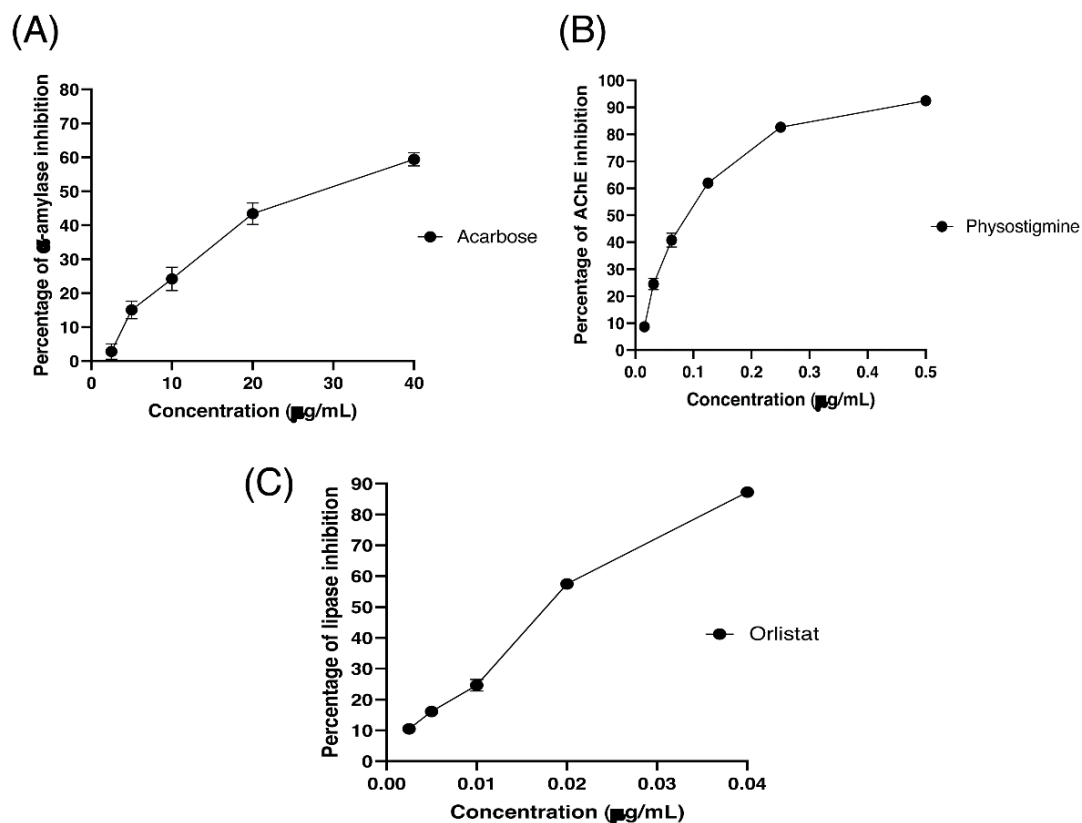


**Figure 2.5** The (A)  $\alpha$ -amylase inhibition (%) of acarbose, (B) AChEI activity (%) of physostigmine, and (C) PPLI activity (%) of orlistat. Data are shown as the mean  $\pm$  SD.

### 2.6.7 *In vitro* PPLI activity of active compounds from DCMMBP

#### *Fractionation of DCMMBP by SiG60-CC*

From Table 2.2, although the DCMCBP and DCMMBP had no marked difference in their PPLI activity ( $\text{IC}_{50}$  of  $458.5 \pm 13.4$  and  $500.8 \pm 24.8$   $\mu\text{g/mL}$ , respectively), DCMMBP was selected for further fractionation by SiG60-CC because there have been numerous previous studies on the lipase inhibitory activity of *Camellia sinensis* L (Chen et al., 2020), but the lipase inhibitory activity of *M. diplotricha* flower BP has not been reported yet.

From 5.64 g of DCMMBP, a total of 74 fractions were collected. After comparison of their TLC profiles and pooling fractions with a similar pattern, five different fractions (DCMMBP1-5) were obtained. Their weight, yield, and appearance are summarized in Table 2.3. All five pooled fractions were a sticky solid. Fraction DCMMBP5 provided the highest yield (42.20%). These five pooled fractions were

then tested for their PPLI activity, with the results shown in Figure 2.4, C and the derived  $IC_{50}$  values reported in Table 2.3 (supplement 1). Fraction DCMMBP2 gave the highest PPLI activity ( $IC_{50}$  of  $128.5 \pm 3.0 \mu\text{g/mL}$ ).

Since the DCMMBP2 fraction had the highest PPLI activity, it was further enriched by SiG60-CC (250-mL size) to yield a total of 150 fractions. After a pooling of fractions with similar TLC profiles, three different fractions (DCMMBP2-1, DCMMBP2-2, and DCMMBP2-3) were obtained. Their weight, yield, and appearance are summarized in Table 2.3. With respect to their PPLI activity (Figure 2.4, C), fraction DCMMBP2-1 had the highest PPLI activity ( $IC_{50}$  of  $52.6 \pm 3.5 \mu\text{g/mL}$ ), while DCMMBP2-2 and DCMMBP2-3 had essentially no PPLI activity.

**Table 2.3** Characteristics and PPLI activity ( $IC_{50}$  value) of all pooled fractions after the first (500-mL column) and second (250-mL column) SiG60-CC fractionation.

Sample	Weight (mg)	Yield (%)	Appearance	$IC_{50}$ ( $\mu\text{g/mL}$ )
<b>After 1stSiG60-CC:</b>				
DCMMBP1	210	3.72	Sticky brown solid	–
DCMMBP2	300	5.32	Sticky brown solid	$128.48 \pm 3.01^c$
DCMMBP3	2,060	36.52	Sticky pale-yellow solid	–
DCMMBP4	410	7.27	Sticky brown solid	–
DCMMBP5	2,380	42.20	Sticky dark brown solid	–
Orlistat	–	–	–	$0.021 \pm 0.00^a$
<b>After 2ndSiG60-CC:</b>				
DCMMBP2-1	65.7	21.9	Sticky brown solid	$52.63 \pm 3.50^b$
DCMMBP2-2	38.5	12.83	Yellow solid	–
DCMMBP2-3	60.5	20.17	Brown solid	–
Orlistat	–	–	–	$0.021 \pm 0.00^a$

#### 2.6.8 Principal chemical composition analysis (TLC and NMR) of fractions DCMMBP2-1 and DCMMBP2-2

After SiG60-CC, the chemical composition of the three obtained fractions was tested by TLC (Figure 2.6). For DCMMBP2-1, no band was observed under UV light



at 254 nm (Figure 2.6, A), but a dark blue spot was found after dipping in 3% (v/v) anisaldehyde in MeOH and heating over a hot plate (Figure 2.6, B). The structure of fraction DCMMBP 2-1 was first analyzed by  $^1\text{H-NMR}$ , where the signal at  $\delta$  0.85 to 2.85 ppm and the signal at  $\delta$  5.35 ppm showed the characteristics of unsaturated free fatty acids (UFFAs; Supplement 4). Therefore, fraction DCMMBP2-1 was prepared as FAMES for the GC-FID analysis.

In contrast, only a sharp band was observed on the TLC plate for fraction DCMMBP2-2, which indicated it was enriched to apparent homogeneity (potentially pure) compound. Therefore, the chemical structure of the compound, named compound 1, in fraction DCMMBP2-2 was analyzed by  $^1\text{H-NMR}$ . Compared to naringenin isolated from the *M. pigra* L. flower BP (Khongkarat et al., 2021), the obtained NMR peaks in the chemical shift pattern were  $^1\text{H-NMR}$  (500 MHz, MeOH- $d_4$ )  $\delta$ : 7.30 (d,  $J=8.5$  Hz, 2H), 6.80 (d, 8.5 Hz, 2H), 5.86 (q,  $J=2.2$  Hz, 2H), 5.33 (dd,  $J=13.0, 3.0$  Hz, 1H), 3.09 (dd,  $J=17.1, 13.0$  Hz, 1H), and 2.67 (dd,  $J=17.1, 3.0$  Hz, 1H) (Supplement 5). Thus compound 1 was identified as naringenin (Figure 2.7, A). However, the structure of DCMMBP2-3 was not identified from the NMR results because it did not have any marked PPLI activity.

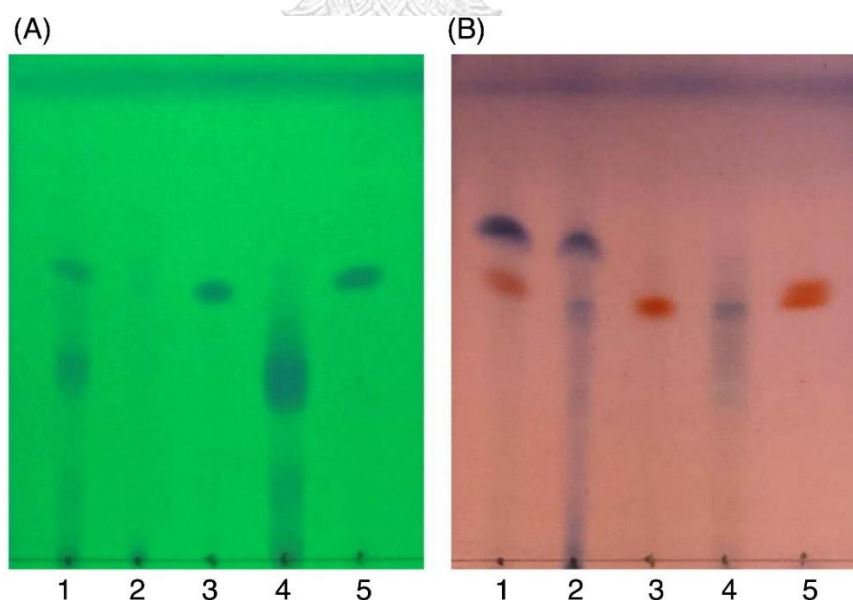


**Figure 2.6** TLC images showing the profile of DCMMBP2 (lane 1), DCMMBP2-1 (lane 2), DCMMBP2-2 (lane 3), DCMMBP2-3 (lane 4), and naringenin (lane 5) under (A) UV light and (B) after 3% (v/v) anisaldehyde in MeOH.

### 2.6.9 Analysis of the fatty acids of fraction DCMMBP2-1

The fatty acids were identified and divided into saturated fatty acids (SFAs) without C=C double bonds, monounsaturated fatty acids (MUFAs) with one such bond, and polyunsaturated fatty acids (PUFAs) with two or more double bonds between two connected carbon atoms. The fatty acid content in DCMMBP2-1 is summarized in Table 2.4. The major fatty acids included one SFA (palmitic acid) and two PUFAS (linoleic and linolenic) (Figure 2.7, B-D), together with small amounts of stearic acid, oleic acid, myristic acid, pentadecanoic acid, lignoceric acid, margaric acid, ecosadienoic acid, eicosenoic acids,  $\gamma$ -linolenic acid, behenic acid, palmitoleic acid, heptadecenoic acid, and eicosanoic acid (Supplement 6).

**Table 2.4** Fatty acid composition of the DCMMBP2-1 (as FAMES).

Peak #	Fatty acid	Type	Abbreviation	Retention time (min)	Fatty acid (mg/g)
1	Myristic acid	SFAs	C14: 0	20.187	4.4292
2	Pentadecanoic acid	SFAs	C15: 0	21.877	3.1227
3	Palmitic acid	SFAs	C16: 0	23.586	247.7186
4	Palmitoleic acid	MUFAs	C16: 1	24.766	1.6687
5	Margaric acid	SFAs	C17: 0	25.196	2.9375
6	Heptadecenoic acid	MUFAs	C17: 1	26.224	1.3405
7	Stearic acid	SFAs	C18: 0	26.773	18.9883
8	Oleic acid	MUFAs	C18: 1n9c	27.768	16.5952
9	Linoleic acid	PUFAs	C18: 2n6c	29.316	497.5391
10	Eicosanoic acid	SFAs	C20: 0	29.799	1.0764
11	$\gamma$ -linolenic acid	PUFAs	C18: 3n6	30.379	2.2933
12	Eicosenoic acids	MUFAs	C20: 1	30.717	2.5925
13	$\alpha$ -linolenic acid	PUFAs	C18: 3n3	30.930	184.2923
14	Ecosadienoic acid	PUFAs	C20: 2	32.155	2.6826
15	Behenic acid	SFAs	C22: 0	32.663	1.8952
16	Lignoceric acid	SFAs	C24: 0	35.655	3.0019

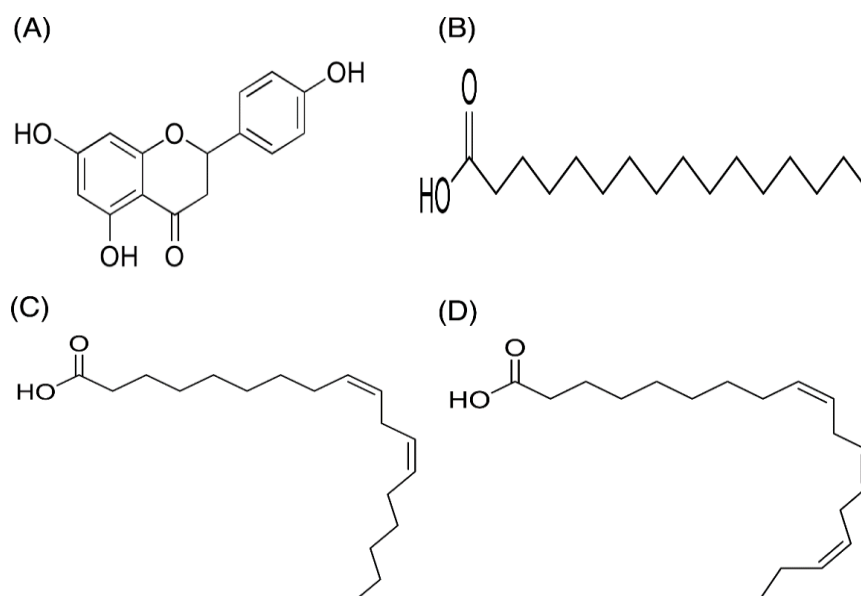


**Figure 2.7** Structural formula of naringenin (A) and the chemical structures of palmitic acid, C16:0 (B), linoleic acid, C18:2n6c (C), and  $\alpha$ -linolenic acid, C18:3n3 (D).

## 2.7 Discussion

Aging societies are found in most developed and many developing countries due to the leap in progress in medicine and standard of living (nutrition, shelter, etc.) leading to people living longer. However, these new life styles, especially in the increased access to goods and processed food exposes the population to face many diseases, such as diabetics, Alzheimer's, and obesity. The drugs to treat these diseases are expensive, especially when imported, as is the case in Thailand. These include acarbose and orlistat as expensive anti-diabetic as anti-obesity drugs, respectively. In addition, those drugs can cause adverse side effects. Orlistat can cause several mild-to-moderate gastrointestinal adverse effects, serious adverse hepatic effects, and rare cases of acute kidney injury. In addition, it interferes with the absorption of many drugs, resulting in their decreased bioavailability and effectiveness (Filippatos et al., 2008).

Hence, finding alternative treatments from local, sustainable, and natural products is necessary. Many types of fruit, vegetables, and mushrooms (fungi) have been shown to inhibit  $\alpha$ -amylase activity (Papoutsis et al., 2021), while a mixture of flavonoids and phenolics acids from *Aristolelia chilensis* leaves and coumarins have

potential AChEI activity (Cespedes et al., 2017; de Souza et al., 2016). In addition, lipase inhibitors have been reported from both synthetic compounds (phosphonates, boronic acids, fats analogues) and natural compounds from many spices and plants, such as hydroxybenzoic acids, hydroxycinnamic acid, flavonol, isoflavonoid, flavanone, and hydroxycoumarin from *Momordica charantia* fruits (Bialecka-Florjanczyk et al., 2018; Chanda et al., 2019; Sellami et al., 2017).

In this work, BP harvested by *A. mellifera*, the most well managed honeybee, was our target. Due to the rapid growth of industries in Thailand, many agricultural areas have become fragmented and the agroecosystem has been changed into monocrop cultures, which results in a higher proportion of bee hives having monofloral BP. As known, the bioactivity of BP is mainly dependent on its botanical origin (Rebiai and Lanez, 2012). Thus, the monofloral BP from various botanical and geographical origins in Thailand was the focus of this study. With the standard methods used in pollen identification (Bell et al., 2016), the six BP samples in this work were ascribed to have originated from *C. sinensis* L., *H. annuus* L., *M. diplotricha*, *N. nucifera*, *X. complanata*, and *A. conyzoides* for BP1–6, respectively. Three bioactivities (anti-amylase, AChEI, and PPLI activities) were focused on because there have been rare reports on these activities in BP, especially in Thailand.

Although *in vitro* assays were used, the obtained data was reliable. The anti-amylase activity was performed using  $\alpha$ -amylase from porcine pancreas, which shows a close relationship to human  $\alpha$ -amylase (Butterworth et al., 2011). For the AChEI activity, AChE from electric eel, which has the same active site as human AChE, was selected (Orhan et al., 2011), while PPL has a similar active site to human pancreatic lipase was used in the anti-lipase assay (Winkler et al., 1990). Therefore, these *in vitro* assays were used as a screening method to search for potential human enzyme inhibitors.

Bioactivity could be found in either the crude/partition extracts, partially purified extracts or pure form (Feas et al., 2012; Khongkarat et al., 2020). In the crude partition extracts of this study, only DCMXBP showed anti-amylase activity. With respect to the AChEI activity, only one of the partition extracts showed a weak AChEI activity. For the anti-lipase (as PPLI) activity, all the DCM partition extracts showed PPLI activity, but with only a weak PPLI activity shown by DCMHBP. In

contrast, DCMMBP and DCMCBP showed a moderate PPLI activity. Thus, DCM is the best partition solvent for our extraction method. However, these three activities were reported previously in the methanolic extracts of mono- and hetero-floral BP in Brazil (Araújo et al., 2017) and the anti-amylase activity was found in the aqueous-ethanolic extract of BP in Nigeria (Daudu et al., 2019). Thus, the solvent and extraction method used could not be ignored.

Among the three bioactivities examined in this study, the PPLI activity of *M. diplotricha* BP became the main interest in this study due to the scarcity of reports on this activity in BP. Thus, DCMMBP from *M. diplotricha* BP was further fractionated by SG60 CC two times. After enrichment, two interesting fractions were derived and the chemical structure of the components in these two fractions was analyzed by <sup>1</sup>H-NMR. One was found to be a mixture of FFAs and showed the highest PPLI activity, while the other fraction was naringenin, a flavanone compound that has been reported in *Mimosa pigra* L. bee pollen (Khongkarat et al., 2021). Therefore, it can be used as a marker of *Mimosa* spp. bee pollen.

To study the FFA composition, the fatty acid fraction was esterified to FAME and analyzed by GC-FID following the AOAC method 996.06. The result showed that this fraction consisted of two major PUFAs (linoleic acid at 49.75% and  $\alpha$ -linolenic at 18.43%) and one major SFA (palmitic acid at 24.77%). The major fatty acid composition of *M. diplotricha* BP is consistent with the fatty acid compositions that have been reported previously (Araújo et al., 2017), except that linoleic acid was found at the highest proportion in our study and not  $\alpha$ -linolenic acid. It is possible that linoleic acid provided the observed PPLI activity in *M. diplotricha* BP, consistent with the previously reported anti-lipase activity of a fatty acid mixture from *Nigella sativa* extracts with linoleic acid as the dominant fatty acid. This showed a mixed inhibition type (the inhibitor can bind to enzyme whether or not the enzyme has already bound the substrate) (Shamsiya et al., 2016). The lipase enzyme active site at Ser152 is within a hydrophobic hexapeptide sequence (Val-Gly-His-Ser-Gln-Gly) (Duan, 2000), and the long HC chain of linoleic acid can bind with lipase via hydrophobic interactions.

Overall, the results indicate that *M. diplotricha* BP has an anti-lipase property due to its FFA composition, which is safe to consume and has the potential to be developed for use as a pharmaceutical supplement.

## 2.8 Conclusions

Active biomolecule analysis of BP with PPLI activity contributed to a deeper characterisation of BP. The highest PPLI activity was revealed in *A. mellifera* monofloral MP dominant in *M. diplotricha* floral pollen. Floral identification ensured both the safety for consumption and the standard of quality control. Although naringenin was found not to have a PPLI activity in this work and was also without any antioxidant activity in a previous study, it could be used as a marker for monofloral BP dominant in *Mimosa* spp. The FFAs found in this bee product are here reported to present an *in vitro* lipase inhibitory activity. Thus, this work promotes the use of bee products as a natural nutrient supplement and indicates the benefit of *Mimosa* spp., which are generally regarded as only weeds. However, *in vivo* assessment is still required.

## 2.9 List of abbreviations

BP1: bee pollen of *Camellia sinensis* L., BP2: bee pollen of *Helianthus annuus* L., BP3: bee pollen of *Mimosa diplotricha*, BP4: bee pollen of *Nelumbo nucifera*, BP5: bee pollen of *Xyris complanata*, and BP6: bee pollen of *Ageratum conyzoides*

DCMCBP: DCM partitioned extract of *C. sinensis* L. bee pollen, DCMBP: DCM partitioned extract of *H. annuus* L. bee pollen, DCMMBP: DCM partitioned extract of *M. diplotricha* bee pollen, DCMNBP: DCM partitioned extract of *N. nucifera* bee pollen, DCMXBP: DCM partitioned extract of *X. complanata* bee pollen, DCMABP: DCM partitioned extract of *A. conyzoides* bee pollen

HXCBP: hexane partitioned extract of *C. sinensis* L. bee pollen, HXHBP: hexane partitioned extract of *H. annuus* L. bee pollen, HXMBP: hexane partitioned extract of *M. diplotricha* bee pollen, HXNBP: hexane partitioned extract of *N. nucifera* bee pollen, HXXBP: hexane partitioned extract of *X. complanata* bee pollen, HXABP: hexane partitioned extract of *A. conyzoides* bee pollen

MTCBP: MeOH partitioned extract of *C. sinensis* L. bee pollen, MTHBP: MeOH partitioned extract of *H. annuus* L. bee pollen, MTMBP: MeOH partitioned extract of *M. diplotricha* bee pollen, MTNBP: MeOH partitioned extract of *N. nucifera* bee pollen, MTXBP: MeOH partitioned extract of *X. complanata* bee pollen, MTABP: MeOH partitioned extract of *A. conyzoides* bee pollen

DCMMBP1-5: pooled fraction 1-5 after SiG60-CC (500-mL size) of DCMMBP

DCMMBP2-1, 2-2, and 2-3: pooled fraction 1, 2, and 3 after SiG60-CC (250-mL size) of DCMMBP2

## References

- Akoro SM, Ogundare CO, Oladipupo OR. 2017. Phytochemical study and alpha-amylase inhibitory properties of leaf extracts of *Croton zambesicus* (Müll. Arg.). *Biotechnology Journal International* **18**:1-8 DOI: 10.9734/BJI/2017/32441.
- Ali N, Akhtar N, Khan SA, Ul Uza N. 2021. Palynological investigation of selected species of family Asteraceae using light and scanning electron microscopic techniques. *Microscopy Research and Technique* **84**:261-270 DOI: 10.1002/jemt. 23583.
- Arathi HS, Bjostad L, Bernklau E. 2018. Metabolomic analysis of pollen from honey bee hives and from canola flowers. *Metabolomics* **14**:86 DOI: 10.1007/s11306-018-1381-5.
- Araujo JS, Chambo ED, de Carvalho Costa MAP, da Silva SMPC, de Carvalho CAL, Estevinho LM. 2017. Chemical composition and biological activities of mono- and heterofloral bee pollen of different geographical origins. *International Journal of Molecular Sciences* **18**:921 DOI: 10.3390/ijms18050921.
- Ariyaratna HACK, Gunasekare MTK, Kottawa-Arachchige JD, Paskarathevan R, Ranaweera KK, Ratnayake M, Kumara JBDAP. 2011. Morpho-physiological and phenological attributes of reproductive biology of tea (*Camellia sinensis* (L.) O. Kuntze) in Sri Lanka. *Euphytica* **181**:203–215 DOI: 10.1007/s10681-011-0399-9.
- Bell KL, de Vere N, Keller A, Richardson RT, Gous A, Burgess KS, Brosi BJ. 2016. Pollen DNA barcoding: current applications and future prospects. *Genome* **59**:629-640 DOI: 10.1139/gen-2015-0200.
- Bialecka-Florjanczyk E, Fabiszewska AU, Krzyczkowska J, Kurylowicz A. 2018. Synthetic and natural lipase inhibitors. *Mini-Reviews in Medicinal Chemistry* **18**:672-683 DOI: 10.2174/1389557516666160630123356.
- Butterworth PJ, Warren FJ, Ellis PR. 2011. Human  $\alpha$ -amylase and starch digestion: an interesting marriage. *Starch-Stärke* **63**:395-405 DOI: doi.org/10.1002/star.201000150.



- Cespedes CL, Balbontin C, Avila JG, Dominguez M, Alarcon J, Paz C, Burgos V, Ortiz L, Penaloza-Castro I, Seigler DS, Kubo I. 2017. Inhibition on cholinesterase and tyrosinase by alkaloids and phenolics from *Aristotelia chilensis* leaves. *Food and Chemical Toxicology* **109(Pt 2)**:984-995 DOI: 10.1016/j.fct.2017.05.009.
- Chanda J, Mukherjee PK, Biswas R, Malakar D, Pillai M. 2019. Study of pancreatic lipase inhibition kinetics and LC-QTOF-MS-based identification of bioactive constituents of *Momordica charantia* fruits. *Biomedical Chromatography* **33**:e4463 DOI: 10.1002/bmc.4463.
- Chantarudee A, Phuwapraisirisan P, Kimura K, Okuyama M, Mori H, Kimura A, Chanchao C. 2012. Chemical constituents and free radical scavenging activity of corn pollen collected from *Apis mellifera* hives compared to floral corn pollen at Nan, Thailand. *BMC Complementary and Alternative Medicine* **12**:45 DOI: 10.1186/1472-6882-12-45.
- Chen D, Chen G, Sun Y, Zeng X, Ye H. 2020. Physiological genetics, chemical composition, health benefits and toxicology of tea (*Camellia sinensis* L.) flower: a review. *Food Research International* **137**:109584 DOI: 10.1016/j.foodres.2020.109584.
- Costa MCA, Morgano MA, Ferreira MMC, Milani RF. 2019. Quantification of mineral composition of Brazilian bee pollen by near infrared spectroscopy and PLS regression. *Food Chemistry* **273**:85–90 DOI: 10.1016/j.foodchem.2018.02.017.
- Da Luz CFP, dos Santos VL, Guedes JS, de Oliveira Silva-Cobra G, Wanderley MGL. 2015. Pollen morphology of some Brazilian *Xyris* Gronov. ex L. (*Xyridaceae*) species. *Brazilian Journal of Botany* **38**:937-950 DOI: 10.1007/s40415-015-0192-4.
- Daudu OM. 2019. Bee pollen extracts as potential antioxidants and inhibitors of  $\alpha$ -amylase and  $\alpha$ -glucosidase enzymes *in vitro* assessment. *Journal of Apicultural Science* **63**:315-325 DOI: 10.2478/jas-2019-0020.
- De Souza LG, Renna MN, Figueroa-Villar JD. 2016. Coumarins as cholinesterase inhibitors: a review. *Chemico-Biological Interactions* **254**:11-23 DOI: 10.1016/j.cbi.2016.05.001.

- Di Pasquale G, Salignon M, Le Conte Y, Belzunces LP, Decourtye A, Kretzschmar A, Suchail S, Brunet JL, Alaux C. 2013. Influence of pollen nutrition on honey bee health: do pollen quality and diversity matter? *PLoS One* **8**:e72016 DOI: 10.1371/journal.pone.0072016.
- Duan RD. 2000. *Fat Digestion and Absorption*. AOCS Press, Champaign III Coden 69ACBA Conference.
- Fan TF, Potroz MG, Tan EL, Ibrahim MS, Miyako E, Cho NJ. 2019. Species-specific biodegradation of sporopollenin-based microcapsules. *Scientific Reports* **9**:1-13 DOI: 10.1038/s41598-019-46131-w.
- Fatrcova-Sramkova K, Nozkova J, Kacaniova M, Mariassyova M, Rovna K, Stricik M. 2013. Antioxidant and antimicrobial properties of monofloral bee pollen. *Journal of Environmental Science and Health, Part B* **48**:133-138 DOI: 10.1080/03601234.2013.727664.
- Feas X, Vazquez-Tato MP, Estevinho L, Seijas JA, Iglesias A. 2012. Organic bee pollen: botanical origin, nutritional value, bioactive compounds, antioxidant activity and microbiological quality. *Molecules* **17**:8359-8377 DOI: 10.3390/molecules17078359.
- Filippatos TD, Derdemezis CS, Gazi IF, Nakou ES, Mikhailidis DP, Elisaf MS. 2008. Orlistat-associated adverse effects and drug interactions: a critical review. *Drug Safety* **31**:53-65 DOI: 10.2165/00002018-200831010-00005.
- Garg A. 1996. Palynocontents of bee-collected pollen loads of autumn season in Bhimtal, India. *Taiwania* **41**:197-207 DOI: 10.6165/tai.1996.41.197.
- Ghoshal KP, Saoji AA. 2013. Phytochemical screening of the pollen of some selected plants with antidiabetic properties. *Australian Journal of Basic and Applied Sciences* **7**:105-109
- Jagdis A, Sussman G. 2012. Anaphylaxis from bee pollen supplement. *Canadian Medical Association Journal* **184**:1167-1169 DOI: 10.1503/cmaj.112181.
- Jamous RM, Abu-Zaitoun SY, Akkawi RJ, Ali-Shtayeh MS. 2018. Antiobesity and antioxidant potentials of selected palestinian medicinal plants. *Evidence-Based Complementary and Alternative Medicine* **2018**:1-21 DOI: 10.1155/2018/8426752.

- Khongkarat P, Ramadhan R, Phuwapraisirisan P, Chanchao C. 2020. Safflospemidines from the bee pollen of *Helianthus annuus* L. exhibit a higher *in vitro* antityrosinase activity than kojic acid. *Heliyon* **6**:e03638 DOI: 10.1016/j.heliyon.2020.e03638.
- Khongkarat P, Ramadhan R, Phuwapraisirisan P, Chanchao C. 2021. Screening and bioguided fractionation of *Mimosa pigra* L. bee pollen with antioxidant and anti-tyrosinase activities. *Journal of Apicultural Science* **65**:71-83 DOI:10.2478/jas-2021-0001.
- Kostic AZ, Milincic DD, Nedic N, Gasic UM, Trifunovic BS, Vojt D, Tesic ZL, Pesic MB. 2021. Phytochemical profile and antioxidant properties of bee-collected artichoke (*Cynara scolymus*) pollen. *Antioxidants* **10**:1091 DOI: 10.3390/antiox10071091.
- Li F, Guo S, Zhang S, Peng S, Cao W, Ho CT, Bai N. 2019. Bioactive constituents of *F. esculentum* bee pollen and quantitative analysis of samples collected from seven areas by HPLC. *Molecules* **24**:1-15 DOI: 10.3390/molecules24152705.
- Lima LCL, Silva FHM, Santos FDARD. 2008. Palinologia de espécies de Mimosa L. (Leguminosae-Mimosoideae) do semi-árido brasileiro. *Acta Botanica Brasilica* **22**:794-805 DOI: 10.1590/S0102-33062008000300016.
- Lopes AJO, Vasconcelos CC, Garcia JBS, Doria Pinheiro MS, Pereira FAN, Camelo DS, de Moraes SV, Freitas JRB, da Rocha CQ, de Sousa Ribeiro MN, do Socorro de Sousa Cartágenes M. 2020. Anti-inflammatory and antioxidant activity of pollen extract collected by *Scaptotrigona affinis postica*: in silico, *in vitro*, and in vivo studies. *Antioxidants* **9**:103 DOI: 10.3390/antiox9020103.
- Lopes AJO, Vasconcelos CC, Pereira FAN, Silva RHM, Queiroz PFDS, Fernandes CV, Garcia JBS, Ramos RM, Rocha CQD, Lima STJRM, Cartágenes MDSS, Ribeiro MNS. 2019. Anti-inflammatory and antinociceptive activity of pollen extract collected by stingless bee *Melipona fasciculata*. *International Journal of Molecular Sciences* **20**:4512 DOI: 10.3390/ijms20184512.
- Maqsood M, Ahmed D, Atique I, Malik W. 2017. Lipase inhibitory activity of *Lagenaria siceraria* fruit as a strategy to treat obesity. *Asian Pacific Journal of Tropical Medicine* **10**:305-310 DOI: 10.1016/j.apjtm.2017.03.010.

- Munoz E, Velasquez P, Rodriguez K, Montenegro G, Giordano A. 2020. Influence of *Brassica campestris* and *Galega officinalis* on antioxidant activity of bee pollen. *Revista Brasileira de Farmacognosia* **30**:444-449 DOI: 10.1007/s43450-020-00065-x.
- Orhan IE, Khan MTH, Erdem SA, Kartal M, Sener B. 2011. Selective cholinesterase inhibitors from *Buxus sempervirens* L. and their molecular docking studies. *Current Computer-Aided Drug Design* **7**:276-286 DOI: 10.2174/157340911798260296.
- Papoutsis K, Zhang J, Bowyer MC, Brunton N, Gibney ER, Lyng J. 2021. Fruit, vegetables and mushrooms for the preparation of extracts with  $\alpha$ -amylase and  $\alpha$ -glucosidase inhibition properties: a review. *Food Chemistry* **338**:128119 DOI: 10.1016/j.foodchem.2020.128119.
- Peukpiboon T, Benbow ME, Suwannapong G. 2017. Detection of *Nosema* spp. spore contamination in commercial *Apis mellifera* bee pollens of Thailand. *Journal of Apicultural Research* **56**:376-386 DOI: 10.1080/00218839.2017.1327936.
- Rattanawanee A, Chanchao C. 2011. Bee Diversity in Thailand and the Applications of Bee Products, In: *Changing Diversity in Changing Environment*, O Grillo, G Venora, (Ed.), 133-162, InTech, Vienna, Austria.
- Rebiai A, Lanez T. 2012. Chemical composition and antioxidant activity of *Apis mellifera* bee pollen from northwest Algeria. *Journal of Fundamental and Applied Sciences* **4**:155-163 DOI: 10.4314/jfas.v4i2.5.
- Richardson RT, Lin CH, Sponsler DB, Quijia JO, Goodell K, Johnson RM. 2015. Application of ITS2 metabarcoding to determine the provenance of pollen collected by honey bees in an agroecosystem. *Applications in Plant Sciences* **3**:1-6 DOI: 10.3732/ apps.1400066.
- Rzepecka-Stojko A, Stojko J, Kurek-Gorecka A, Gorecki M, Kabała-Dzik A, Kubina R, Mozdierz A, Buszman E. 2015. Polyphenols from bee pollen: structure, absorption, metabolism and biological activity. *Molecules* **20**:21732-21749. DOI: 10.3390/molecules201219800.
- Sangsuk R, Baslev H, Jampeetong A. 2021. Pollen morphology in various life-form of aquatic macrophytes. *Chiang Mai University Journal of Natural Sciences* **20**:1-11 DOI: 10.12982/CMUJNS.2021.050.

- Sellami M, Louati H, Kamoun J, Kchaou A, Damak M, Gargouri Y. 2017. Inhibition of pancreatic lipase and amylase by extracts of different spices and plants. *International Journal of Food Sciences and Nutrition* **68**:313-320 DOI: 10.1080/09637486.2016.1237479.
- Shahali Y. 2015. Allergy after ingestion of bee-gathered pollen: influence of botanical origins. *Annals of Allergy, Asthma and Immunology* **114**:250-251 DOI: 10.1016/j.anai.2014.11.009.
- Shamsiya TK, Manjunatha JR, Manonmani HK. 2016. Lipase inhibitors from *Nigella sativa* and *Punica granatum* as an effective approach towards controlling obesity. *International Journal of Health and Life Sciences* **2**:1-9 DOI: 10.20319/ijhls.2016.22.0119.
- Vieths S, Scheurer S, Ballmer-Weber B. 2002. Current understanding of cross-reactivity of food allergens and pollen. *Annals of the New York Academy of Sciences* **964**:47-68 <https://doi.org/10.1111/j.1749-6632.2002.tb04132.x>.
- Winkler FK, d'Arcy A, Hunziker W. 1990. Structure of human pancreatic lipase. *Nature* **343**:771-774 DOI: 10.1038/343771a0.
- Yang K, Wu D, Ye X, Liu D, Chen J, Sun P. 2013. Characterization of chemical composition of bee pollen in China. *Journal of Agricultural and Food Chemistry* **61**:708-718 DOI: 10.1021/jf304056b.
- Zafar M, Ahmad M, Khan MA. 2007. Palynology of family Asteraceae from flora of Rawalpindi-Pakistan. *International Journal of Agriculture and Biology* **9**:156-161
- Zhang D, Chen Q, Liu Q, Liu F, Cui L, Shao W, Tian D. 2019. Histological and cytological characterization of anther and appendage development in Asian lotus (*Nelumbo nucifera* Gaertn.). *International Journal of Molecular Sciences* **20**:1-15 DOI: 10.3390/ijms20051015.
- Zou Y, Hu J, Huang W, Zhu L, Shao M, Dordoe C, Ahn YJ, Wang D, Zhao Y, Xiong Y, Wang X. 2020. The botanical origin and antioxidant, anti-BACE1 and antiproliferative properties of bee pollen from different regions of South Korea. *BMC Complementary Medicine and Therapies* **20**:236 DOI: 10.1186/s12906-020-03023-1.

## Supplements

**Supplement 1:** Raw data for  $\alpha$ -amylase inhibition activity (%) of DCMXBP and PPLI activity (%) of DCM partitioned extracts, DCMMBP2, and DCMMBP2-1.

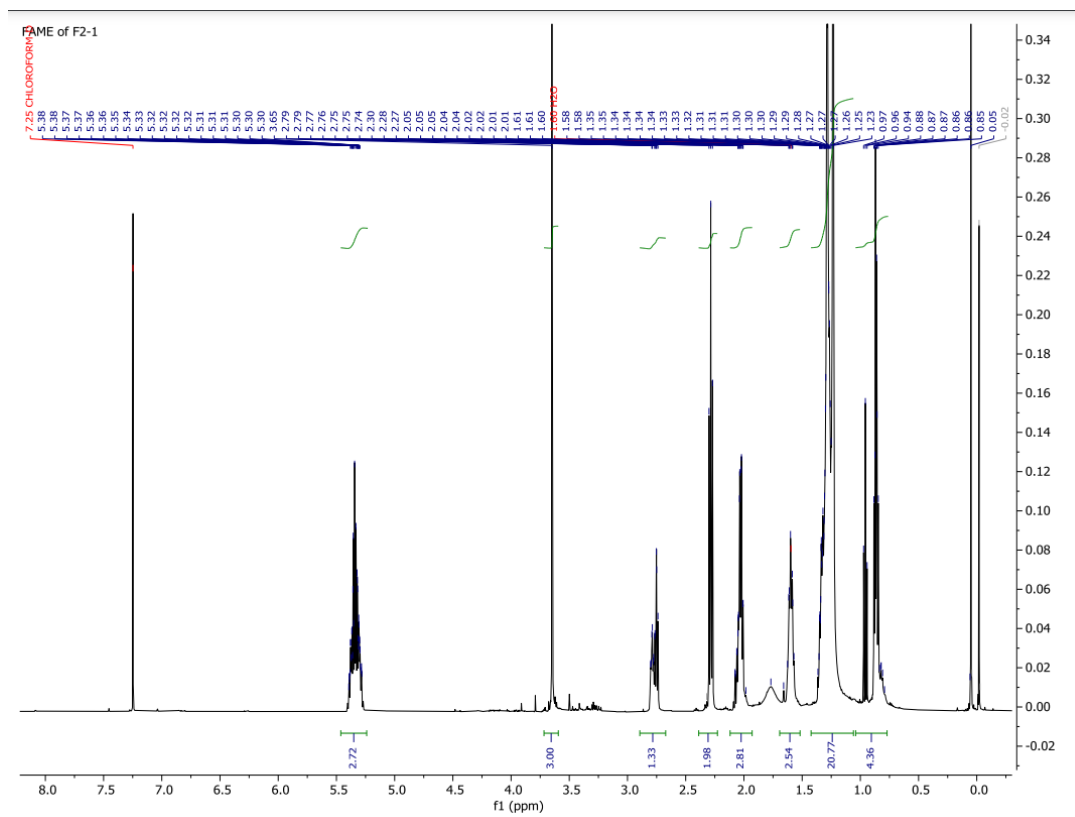
Inhibitory activity	Sample	Concentration ( $\mu\text{g/mL}$ )	Replication no.		
			R1	R2	R3
$\alpha$ -amylase	DCMXBP	125	31.08	28.79	30.33
		250	33.78	34.85	35.25
		500	33.78	39.39	34.43
		1,000	37.84	40.15	39.34
		2,000	53.38	51.52	54.10
		<b>IC<sub>50</sub></b>	<b>1,818.96</b>	<b>1,824.76</b>	<b>1,733.73</b>
Lipase	DCMCBP	200	32.33	31.60	30.58
		400	48.68	50.99	48.74
		600	58.83	56.37	57.37
		800	61.65	59.25	61.15
		1,000	65.04	61.22	65.11
		<b>IC<sub>50</sub></b>	<b>443.84</b>	<b>461.55</b>	<b>470.06</b>
	DCMMBP	200	22.36	20.20	22.77
		400	44.71	40.40	43.56
		600	57.68	55.80	55.25
		800	68.86	63.60	62.38
		1,000	71.86	70.60	68.91
		<b>IC<sub>50</sub></b>	<b>472.63</b>	<b>519.09</b>	<b>510.68</b>
	DCMNBP	200	28.01	32.14	33.27
		400	37.97	40.93	39.57
		600	41.92	44.17	42.81
		800	46.99	45.06	46.76
		1,000	55.26	53.32	53.78
		<b>IC<sub>50</sub></b>	<b>850</b>	<b>897.67</b>	<b>880.62</b>
	DCMXBP	200	26.03	25.18	26.66
		400	34.65	34.35	35.09
		600	42.01	42.63	42.37
		800	47.04	44.42	45.02
		1,000	50.45	54.86	52.96
		<b>IC<sub>50</sub></b>	<b>994.69</b>	<b>919.27</b>	<b>967.53</b>
DCMABP	200	21.76	21.00	22.57	
	400	39.52	34.80	37.82	
	600	47.90	43.80	46.93	
	800	52.50	55.20	53.47	
	1,000	65.47	63.80	62.57	
	<b>IC<sub>50</sub></b>	<b>624.83</b>	<b>662.86</b>	<b>650.57</b>	
DCMMBP2	12.5	1.87	1.33	2.13	
	25	11.21	11.82	14.49	
	50	18.96	15.14	14.10	

	100	47.80	50.07	48.27
	200	76.10	72.78	71.81
	<b>IC<sub>50</sub></b>	<b>125.23</b>	<b>129.05</b>	<b>131.17</b>
DCMMBP2-1	12.5	8.19	12.89	12.25
	25	21.14	28.76	28.52
	50	47.43	52.73	51.01
	100	68.38	71.40	70.13
	200	86.86	85.12	83.56
	<b>IC<sub>50</sub></b>	<b>56.49</b>	<b>49.66</b>	<b>51.73</b>

**Supplement 2:** Raw data for  $\alpha$ -amylase inhibition activity (%) of acarbose, AChEI activity (%) of physostigmine, and PPLI activity (%) of orlistat.

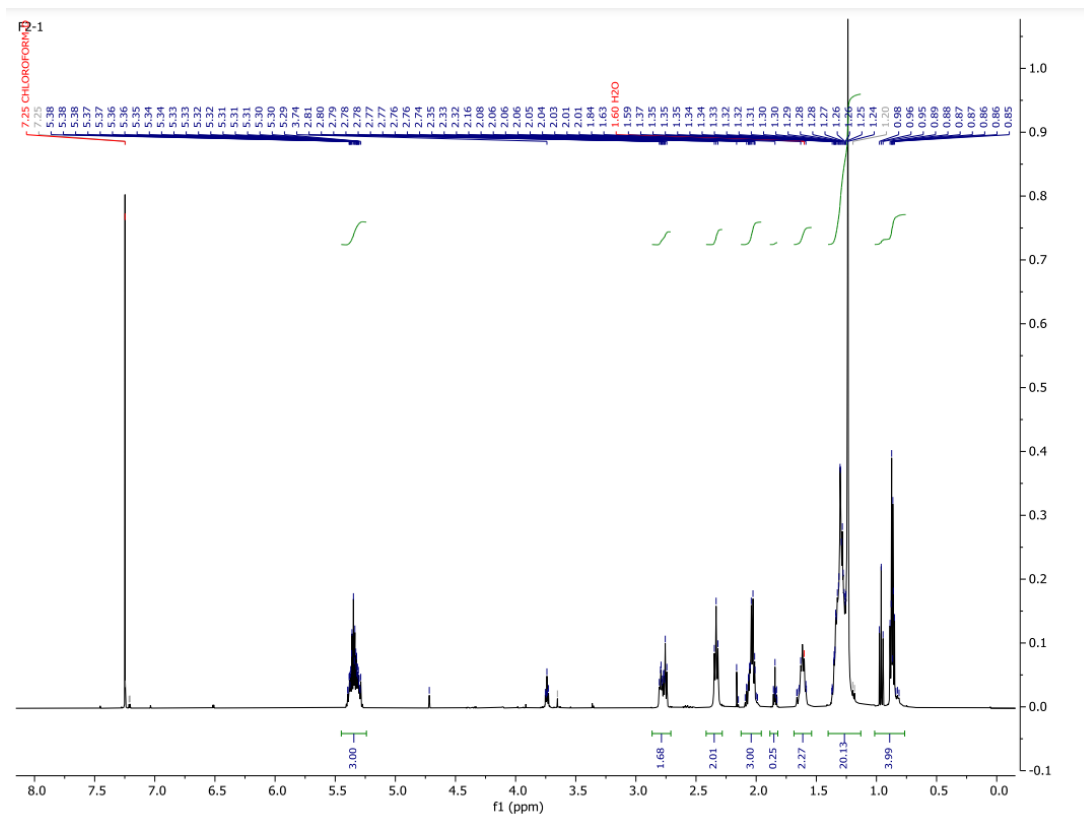
Inhibitory activity	Positive control	Concentration ( $\mu\text{g/mL}$ )	Replicate no.		
			R1	R2	R3
$\alpha$ -amylase	acarbose	2.5	1.02	2.08	5.43
		5	12.24	15.63	17.39
		10	20.41	25.00	27.17
		20	39.80	44.79	45.65
		40	59.18	61.46	57.61
		<b>IC<sub>50</sub></b>	<b>25.78</b>	<b>27.49</b>	<b>30.98</b>
		AChE	Physostigmine	0.015625	8.54
0.03125	26.92			23.00	23.67
0.0625	41.82			42.56	37.81
0.125	61.51			61.71	62.63
0.25	82.34			81.68	83.84
0.5	91.90			92.84	92.64
<b>IC<sub>50</sub></b>	<b>0.081</b>			<b>0.084</b>	<b>0.082</b>
Lipase	Orlistat	0.0025	10.95	8.58	11.96
		0.005	15.36	15.84	17.22
		0.01	26.80	23.10	24.08
		0.02	57.52	56.77	58.21
		0.04	86.27	86.96	88.52
		<b>IC<sub>50</sub></b>	<b>0.021</b>	<b>0.020</b>	<b>0.021</b>

**Supplement 3:**  $^1\text{H-NMR}$  peak data at chemical shift( $\delta$ ) 0.0-8.0 ppm in length of fraction DCMMBP2-1 methyl ester derivative in chloroform-d

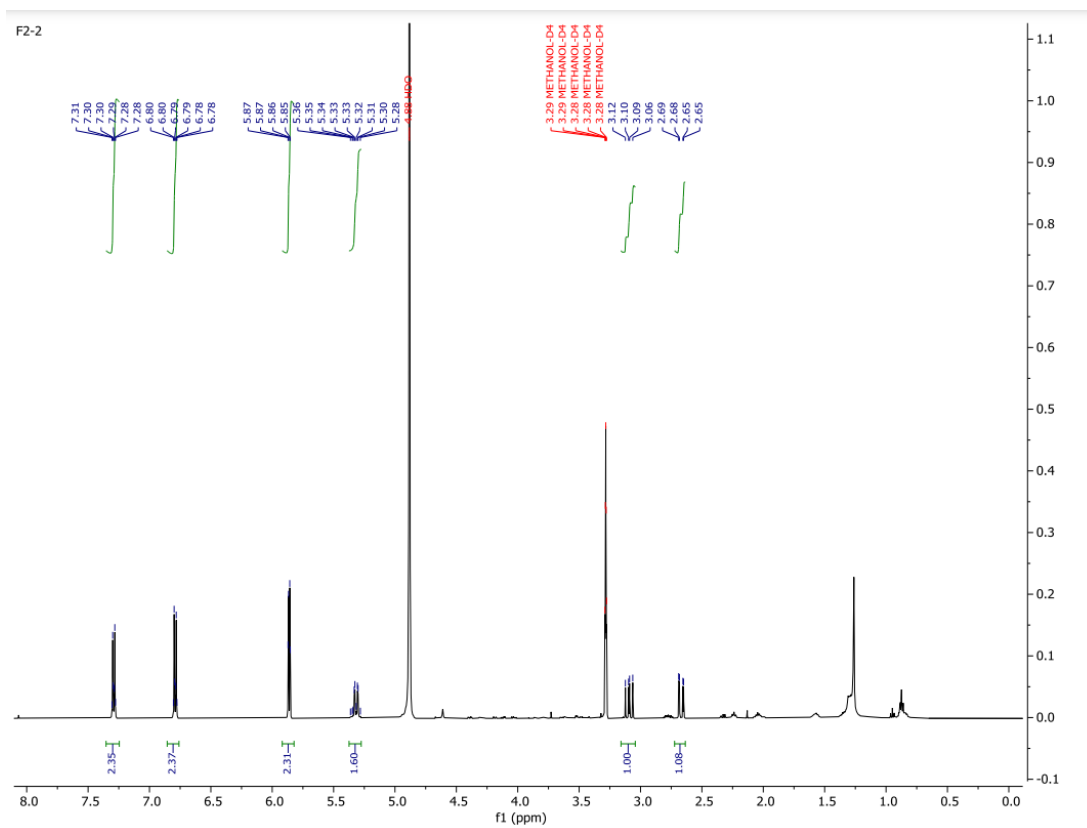


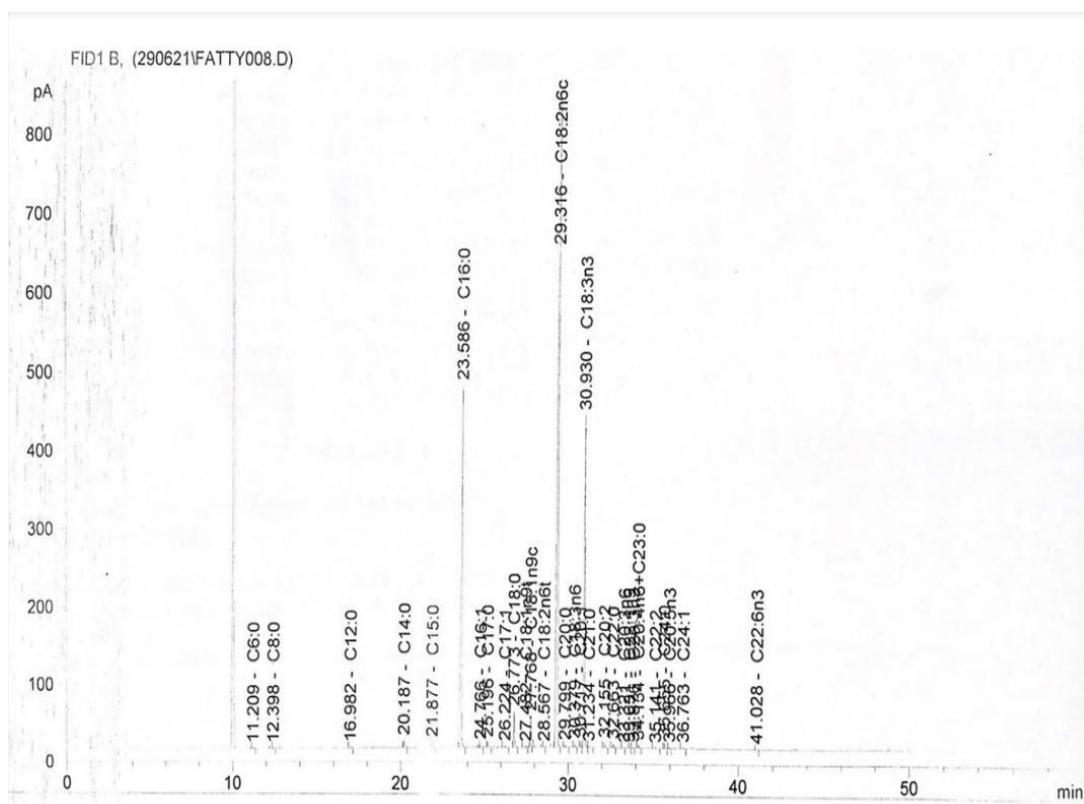


**Supplement 4:**  $^1\text{H-NMR}$  peak data at chemical shift( $\delta$ ) 0.0-8.0 ppm in length of fraction DCMMBP2-1 in chloroform-d



**Supplement 5:**  $^1\text{H-NMR}$  peak data at chemical shift( $\delta$ ) 0.0-8.0 ppm in length of DCMMP2-2(Naringenin) in methanol-d4



**Supplement 6: GC-FID chromatogram of DCMMBP2-1 methyl ester derivative**

## CHAPTER III

### **Phytochemical content, especially spermidine derivatives, presenting antioxidant and antilipoxygenase activities in Thai bee pollens**

#### **3.1 Authors**

##### 3.1.1 First author

- **Phanthiwa Khongkarat**

Affiliation: Program in Biotechnology, Faculty of Science, Chulalongkorn University, 254 Phayathai Road, Bangkok 10330, Thailand,

[parephanthiwa@gmail.com](mailto:parephanthiwa@gmail.com), +66824976525

##### 3.1.2 Corresponding author

- **Professor Chanpen Chanchao, Ph.D (Advisor)**

Affiliation: Department of Biology, Faculty of Science, Chulalongkorn University, 254 Phayathai Road, Bangkok 10330, Thailand,

[chanpen.c@chula.ac.th](mailto:chanpen.c@chula.ac.th), +66859130412

#### **3.2 Article status**

The article was published on 25<sup>th</sup> May 2022 in Peer J, volume 10 on pages of 13506-13526

### 3.3 Abstract

**Background:** Bee pollen (BP) is full of useful nutrients and phytochemicals. Its chemical components and bioactivities depend mainly on the type of floral pollen.

**Methods:** Monofloral BP from *Camellia sinensis* L., *Mimosa diplotricha*, *Helianthus annuus* L., *Nelumbo nucifera*, *Xyris complanata*, and *Ageratum conyzoides* were harvested. Crude extraction and partition were performed to yield solvent-partitioned extracts of each BP. Total phenolic content (TPC) was assayed by the Folin-Ciocalteu method, while the flavonoid content (FC) was measured by the aluminium chloride colorimetric method. Antioxidant capacity was measured by the (i) 1,1-diphenyl-2-picrylhydrazyl (DPPH) radical scavenging activity, (ii) 2,2'-azino-bis (3-ethylbenzthiazoline-6-sulphonic acid) (ABTS) scavenging activity and its Trolox equivalent antioxidant capacity (TEAC), and (iii) ferric reducing antioxidant power (FRAP). All samples were tested for lipoxygenase inhibitory (LOXI) activity. The most active sample was enriched by silica gel 60 column chromatography (SiG60-CC) and high performance liquid chromatography (HPLC), observing the chemical pattern of each fraction using thin layer chromatography. Chemical structure of the most active compound was analyzed by proton nuclear magnetic resonance and mass spectrometry.

**Results:** Dichloromethane (DCM)-partitioned BP extracts of *H. annuus* L. and *M. diplotricha* (DCMMBP) showed a very high TPC, while DCMMBP had the highest FC. In addition, DCMMBP had the strongest DPPH and ABTS radical scavenging activities (as a TEAC value), as well as FRAP value. Also, DCMMBP (60 µg/mL) gave the highest LOXI activity ( $78.60 \pm 2.81$  %). Hence, DCMMBP was chosen for further enrichment by SiG60-CC and HPLC. Following this, the most active fraction showed higher antioxidant and LOXI activities with an EC<sub>50</sub> for DPPH and ABTS of  $54.66 \pm 3.45$  µg/mL and  $24.56 \pm 2.99$  µg/mL (with a TEAC value of  $2,529.69 \pm 142.16$  µmole TE/g), respectively, and a FRAP value of  $3,466.17 \pm 81.30$  µmole Fe<sup>2+</sup>/g and an IC<sub>50</sub> for LOXI activity of  $12.11 \pm 0.36$  µg/mL. Triferuloyl spermidines were revealed to be the likely main active components.

**Conclusions:** TPC, FC, and spermidine derivatives played an important role in the antioxidant and antilipoxygenase activities in *M. diplotricha* bee pollen.

Keywords: bee pollen, bioactivity, flavonoid content, phytochemical, total phenolic content

### 3.4 Introduction

People nowadays have a longer expected life span due to advances in medicine and technology. In addition, people pay more attention to their health. Hence, a lot of nutrient supplements have been introduced, which are mostly from natural products. Bee pollen (BP) is one of the natural bee products that is widely used for nutritional and medical applications. It is produced by foraging bees by mixing the floral pollens with some nectar or honey, enzymes, wax, and bee secretion (Chantarudee et al., 2012). Bee pollens are a good protein source because they contain a high level of well-balanced proteins (those with all the essential amino acids necessary for the human body). Furthermore, BPs contain other required nutrients, including unsaturated fatty acids, vitamins, minerals, and trace elements. As a result, it is commonly used as a natural dietary supplement (Sommano et al., 2020).

Additionally, BP contains a variety of beneficial chemicals, particularly phenolic and flavonoid components, such as quercetin, kaempferol, caffeic acid, and naringenin (Saric et al., 2009). As a result, many bioactivities of BP have been discovered, such as antimicrobial and anti-inflammatory activities (Saral et al., 2022). The phenolic compounds from rape BP showed *in vitro* antioxidant and tyrosinase inhibition (TYRI) properties and could inhibit melanogenesis. These activities were attributed to rutin, the major flavonoid in the extract (Sun et al., 2017). Also, the phenol and flavonoid compounds in BP from Nigeria had an  $\alpha$ -amylase inhibitory activity, indicating the potential therapeutic potential of BP in the management of diabetes (Daudu, 2019). In addition, a monoamine oxidase (MAO) inhibitory activity was reported for chestnut BP (Yildez et al., 2014), and so its potential use in the treatment of depressive disorders, Parkinson's disease, and Alzheimer's disease. The relationship between MAO inhibition and the total phenolic content (TPC) as well as the antioxidant capacity of BP was subsequently reported (Yildez et al., 2014). Hence, the TPC and flavonoid contents (FC) from BP, which mainly depended on the floral origin, have the potential to be used as a natural antioxidant agent and enzyme inhibitor.

The antioxidant and lipoxygenase inhibition (LOXI) properties were found to be associated with anti-inflammatory, anti-cancer, and anti-aging effects (Eshwarappa et al., 2016). The antioxidant properties can protect cells from the oxidative damage of free radical molecules, which are unstable molecules with one or more unpaired electrons (Lobo et al., 2010). The antioxidant can react with other molecules, including the intracellular proteins, lipids, and DNA. After such damage, the cells are in an oxidative stress that can induce the development of many chronic diseases, such as cancer, autoimmune disorders, aging, cataracts, rheumatoid arthritis, and cardiovascular and neurodegenerative diseases (Pham-Huy et al., 2010).

Therefore, to help prevent oxidative damage to cells, antioxidant agents that can donate electrons or hydrogen atoms are important in order to reduce the free radical level (Shahidi and Zhong, 2015). The lipoxygenases (LOXs) are an important family of enzymes in inflammatory and immune responses. They catalyze the conversion of polyunsaturated fatty acids and arachidonic acid to inflammatory eicosanoids, including hydroperoxy-eicosatetraenoic acid and leukotrienes (Mashima and Okuyama, 2015). The overexpression of LOX promotes the development of several inflammation-related diseases, such as arthritis, asthma, cancer, and allergic diseases (Wang et al., 2021). This can be prevented via the inhibition of the LOX pathway and the targeting of LOX with LOXIs is a promising therapeutic target for treating a wide spectrum of human diseases (Eshwarappa et al., 2016).

The chemical composition of BP mainly depends on its floral and geological/geographical origins. In Thailand, some dominant floral origins are different from those in other countries (Chamchumroon et al., 2017), while the bioactivities of some BPs have not been reported before. This led to our interest in the bioactivities of different types of Thai monofloral BPs. Six such samples were collected and then sequentially extracted and partitioned with three organic solvents of different polarities. The enrichment of the active compounds, using bioactivity and chemical profile screening of the fractions, was performed. The structure of the isolated active compounds was analyzed by proton nuclear magnetic resonance spectroscopy ( $^1\text{H-NMR}$ ) and the molecular weight (MW) was measured by MALDI-TOF mass spectrometry (MS). The benefit of this work is the discovery of potential new antioxidant and LOXI compounds and the promotion of BP as a nutraceutical food to

be developed for use in the pharmaceutical industry. This may encourage the growth of Thai apiaries, resulting in an improved income for bee farmers.

### 3.5 Materials & Methods

#### 3.5.1 Sample collection

Six monofloral *Apis mellifera* BP samples were collected from five provinces in Thailand (Table 3.1) and stored at room temperature (25 °C) until used. The BP was identified by palynological analysis and sequence analysis of the ITS-2 region of the rRNA genes, as previously reported (Khongkarat et al., 2022). Both analyses were consistent and confirmed that the six *A. mellifera* BP samples were from *Camellia sinensis* L. (BP1), *Mimosa diplotricha* (BP2) (Chiangmai province), *Helianthus annuus* L. (BP3) (Lopburi province), *Nelumbo nucifera* (BP4) (Nakhon Sawan province), *Xyris complanata* (BP5) (Udon Thani), and *Ageratum conyzoides* (BP6) (Lamphun).

**Table 3.1** Detail of sample collection.

Type of BP	Sample code	Collecting time	Collecting site (province)	Geographical location	
				Longitude	Latitude
<i>Camellia sinensis</i> L. BP	BP1	February, 2018	Chiangmai	99°03'45.3"E	18°46'37.3"N
<i>Mimosa diplotricha</i> BP	BP2	February, 2018	Chiangmai	99°03'45.3"E	18°46'37.3"N
<i>Helianthus annuus</i> L. BP	BP3	February, 2018	Lopburi	101°01'07.5"E	14°51'31.7"N
<i>Nelumbo nucifera</i> BP	BP4	February, 2018	Nakhon Sawan	100°15'01.4"E	15°41'02.4"N
<i>Xyris complanata</i> BP	BP5	February, 2018	Udon Thani	102°45'28.8"E	17°21'12.7"N
<i>Ageratum conyzoides</i> BP	BP6	February, 2018	Lamphun	98°53'42.6"E	18°04'49.2"N

#### 3.5.2 Crude extraction and partition

All collected samples were extracted as previously described (Umthong et al., 2011). In brief, each BP sample (140 g) was extracted with 800 mL of methanol (MeOH) by shaking at 100 rpm, 15 °C, for 18 h. After that, the supernatant was collected and the residue was extracted two more times each with 800 mL of MeOH. The three supernatants were pooled and dried under reduced pressure to obtain the respective MeOH crude extract (MCE). Each MCE was further partitioned by hexane,



dichloromethane (DCM), and MeOH as follows. At first, the MCE was dissolved in MeOH (250 mL) and then mixed with an equal volume of hexane in a separating funnel and left to phase separate. The upper hexane phase was collected and the lower MeOH phase was further partitioned two more times in the same manner, with the three hexane extracts being pooled and dried under reduced pressure to yield the respective hexane-partitioned BP extract (HX); designated as HXCBP, HXMBP, HXHBP, HXNBP, HXXBP, and HXABP for BP1–6, respectively. Next, the residual MeOH phase was added to an equal volume of water and subsequently partitioned three times with DCM in the same manner as above (except the DCM phase was the lower layer), with the pooled DCM extracts being evaporated as above to provide the DCM-partitioned extracts; designated as DCMCBP, DCMMBP, DCMHBP, DCMNBP, DCMXBP, and DCMABP for BP1–6, respectively. Finally, the residual MeOH phases were evaporated as above to obtain the MeOH-partitioned extracts; designated as MTCBP, DCMMBP, MTHBP, MTNBP, MTXBP, and MTABP for BP1–6, respectively. All partitioned extracts were kept at -20 °C in the dark until used.

### 3.5.3 Determination of the TPC

The TPC of each partitioned extract was evaluated as previously reported (Märghitaş et al., 2009) based on the Folin-Ciocalteu method. The method was adapted to be performed in a 96 well plate. Firstly, 125 µL of 0.2 N Folin-Ciocalteu reagent was added to 25 µL of the diluted partitioned extract or gallic acid solution in dimethyl sulfoxide (DMSO) and mixed for 5 min. Then, 100 µL of 7.5% (w/v) sodium carbonate solution was added per well and incubated at room temperature for 2 h. The absorbance at a wavelength of 700 nm was measured using a microplate reader against DMSO as a blank. All reactions were performed in triplicate. The results were expressed as mg of gallic acid equivalents (GAE)/g of partitioned extract using a standard graph for gallic acid in the range of 0.02 to 0.1 mg/mL.

### 3.5.4 Determination of the FC

The FC of each partitioned extract was measured as previously described (Märghitaş et al., 2009) based on the aluminium chloride (AlCl<sub>3</sub>) colorimetric method but with adaptation for use in a 96 well microplate reader. Briefly, 25 µL of the

diluted partitioned extract solution dissolved in DMSO was mixed with 100  $\mu\text{L}$  of distilled water. Then, 7.5  $\mu\text{L}$  of 5% (w/v) sodium nitrite solution was added and incubated at room temperature for 5 min, followed by the addition of 7.5  $\mu\text{L}$  of 10% (w/v)  $\text{AlCl}_3$ . After 6 min of incubation at room temperature, 50  $\mu\text{L}$  of 1 M sodium hydroxide was added and the absorbance at wavelength of 510 nm was measured. Each assay was performed in triplicate. The FC was expressed as mg of quercetin equivalents (QE)/g of partitioned extract using a standard graph for quercetin (0.1 to 1 mg/mL).

### 3.5.5 Determination of the antioxidant capacity

#### *The DPPH free radical scavenging activity assay*

The potential of the partitioned extracts was determined as previously described (Khongkarat et al., 2020). Five different concentrations of each sample were prepared in DMSO. For each concentration, 20  $\mu\text{L}$  of the sample was mixed with 80  $\mu\text{L}$  of 0.15 mM DPPH in MeOH and incubated at room temperature for 30 min. The absorbance was measured at a wavelength of 517 nm ( $A_{517}$ ) using a microplate reader. Ascorbic acid (vitamin C) was used as the standard reference. Each assay was performed in triplicate. The free radical scavenging activity was calculated from Eq. (1):

$$\% \text{ DPPH radical scavenging activity} = [(A - B)/(A)] \times 100 \quad (1),$$

where A is the  $A_{517}$  of the negative control and B is the  $A_{517}$  of the treatment.

The % inhibition (Y axis) was plotted against the extract concentrations (X axis) and the effective concentration at 50% ( $\text{EC}_{50}$ ) was obtained from the graph.

#### *Determination of the Trolox equivalent antioxidant capacity (TEAC)*

The TEAC assay followed the described method (Suriyatem et al., 2017). The stock  $\text{ABTS}^{*+}$  solution was prepared by reacting 7 mM ABTS solution with 2.45 mM potassium persulphate solution in distilled water at a 1:1 (v/v) ratio in the dark at room temperature for 16 h before use. The working  $\text{ABTS}^{*+}$  solution was prepared by diluting the stock  $\text{ABTS}^{*+}$  solution (1 mL) with ethanol (35 mL) to get an absorbance at 734 nm ( $A_{734}$ ) of  $0.700 \pm 0.025$ . After that, 0.3 mL of each partitioned extract at different concentrations dissolved in DMSO was mixed with 2.7 mL of the prepared

ABTS<sup>•+</sup> solution, left for 6 min in the dark and then the A<sub>734</sub> was read. The percentage of inhibition was calculated according to Eq. (2),

$$\% \text{ ABTS radical scavenging activity} = [(A - B)/(A)] \times 100 \quad (2),$$

where A is the A<sub>734</sub> of the negative control and B is the A<sub>734</sub> of the treatment.

The % inhibition (Y axis) was plotted against the respective extract concentration (X axis) and the EC<sub>50</sub> value was obtained from the graph. The results were then compared with the Trolox standard curve (0–0.2 mM) and the results are expressed as μmole Trolox equivalents (TE)/g partitioned extract.

#### *Determination of the ferric reducing antioxidant power (FRAP)*

The FRAP assay was performed as previously described (Sun et al., 2017). The FRAP reagent was freshly prepared by mixing 100 mL of 300 mM acetate buffer (pH 3.6), 10 mL of 10 mM 2,4,6-tris(2pyridyl)-s-triazine solution in 40 mM hydrochloric acid, and 10 mL of 20 mM ferric chloride solution. Later, 100 μL of the sample at a desired concentration was added to 3 mL of the FRAP reagent and incubated at 37 °C in a water bath for 6 min. The absorbance was measured at a wavelength of 593 nm. Aqueous solutions of ferrous sulfate (0–2,000 μM) were used to establish the standard graph and the reducing capacity was expressed as μmole of Fe<sup>2+</sup>/g extract. Each assay was performed in triplicate.

#### 3.5.6 *In vitro* TYRI activity

The *in vitro* TYRI activity was determined as described (Khongkarat et al., 2020). The reaction mixture contained 120 μL of 2.5 mM L-DOPA in 80 mM phosphate buffer (pH 6.8), 30 μL of 80 mM phosphate buffer (pH 6.8), and 10 μL of partitioned extract or kojic acid (positive control) at different concentrations in DMSO. After mixing, the reaction was pre-incubated at 25 °C for 10 min. Then, 40 μL of 165 units (U)/mL mushroom TYR in phosphate buffer was added and incubated at 25 °C for 5 min. The absorbance at 475 nm (A<sub>475</sub>) was measured using a microplate reader. The TYRI activity was calculated as the IC<sub>50</sub> value. Each assay was performed in triplicate and the percentage TYRI was calculated from Eq. (3);

$$\text{Percentage of tyrosinase inhibition} = [ \{ (A-B) - (C-D) \} / (A-B) ] \times 100 \quad (3),$$

where: A is the  $A_{475}$  after incubation without extract, B is the  $A_{475}$  after incubation without an extract and tyrosinase, C is the  $A_{475}$  after incubation with an extract and tyrosinase, and D is the  $A_{475}$  after incubation with an extract, but without tyrosinase.

The % TYRI (Y axis) was plotted against the respective extract concentration (X axis) and the  $IC_{50}$  value was obtained from the graph.

### 3.5.7 *In vitro* LOXI activity

The LOXI activity of each partitioned extract was determined as described (Sethiya and Mishra, 2014) with some modifications. Firstly, 220  $\mu$ L of 0.2 M borate buffer pH 9.0, 30  $\mu$ L of the extract in DMSO, and 250  $\mu$ L of 20,000 U/mL LOX from soybean in 0.2 M borate buffer pH 9.0 were mixed and incubated at 25 °C for 5 min. After that, 1,000  $\mu$ L of 0.6 mM linoleic acid solution was added and the absorbance at 234 nm ( $A_{234}$ ) was measured. Nordihydroguaiaretic acid (NDGA) was used as the reference standard. Each assay was performed in triplicate. The percentage of LOXI was calculated from Eq. (4);

$$\text{Percentage of LOXI} = [(A-B) - (C-D)] / (A-B) \times 100 \quad (4),$$

where A is the  $A_{234}$  after incubation without an extract, B is the  $A_{234}$  after incubation without an extract and LOX, C is the  $A_{234}$  after incubation with an extract and LOX, and D is the  $A_{234}$  after incubation with an extract but without LOX.

The % LOXI (Y axis) was plotted against the respective extract concentration (X axis) and the  $IC_{50}$  value was obtained from the graph.

### 3.5.8 Enrichment of active fractions

Among the mentioned bioactivities, the most active extract for antioxidants and *in vitro* LOXI activity was further fractionated following the bioactivity as in previous studies (Teerasripreecha et al., 2011).

*Fractionation by silica gel 60 column chromatography (SiG60-CC; 500-mL size)*

The most active extract for antioxidant and *in vitro* LOXI activities was selected for fractionation by SiG60-CC. Briefly, the 500-mL column was packed with fine SiG60 (Merck, for CC). The partitioned extract (5.64 g) was dissolved in 20 mL

of MeOH and combined with 20 g of rough SiG60 (Merck, for CC). After drying, it was poured over the surface of the packed SiG60 column and then eluted with 6.5 L of DCM, 8.5 L of 7% (v/v) MeOH in DCM, and 3.5 L of MeOH, respectively. Eluted fractions (250 mL each) were collected, and the solvent was removed by evaporation under reduced pressure at a maximum temperature of 40–45 °C. The pattern of chemical compounds in each fraction was profiled by thin layer chromatography (TLC; see below). Fractions with the same TLC pattern were pooled together and tested for antioxidant and *in vitro* LOXI activities.

#### *Chemical profiling by TLC*

A sample was spotted onto the starting line of a 5 x 5 cm<sup>2</sup> TLC plate (silica immobile phase) using a capillary tube and then dried at room temperature. It was then resolved in one direction using 7% (v/v) MeOH: DCM as the mobile phase. The resolved compounds on the TLC plate were visualized under UV light at 254 nm or by dipping in 3% (v/v) anisaldehyde in MeOH and heating over a hot plate.

#### *Enrichment by HPLC*

To separate (enrich) the compounds of a similar polarity in the mixture (extract) the HPLC method reported by Lv et al. (2015) was further developed and modified. The optimal operating condition was found using a SB-PHENYL column (5 µm, 9.4 × 250 mm), loading 10 × 20 µL aliquots of the respective sample (100 mg/mL in MeOH) with a column temperature of 25 °C, and eluting in an isocratic mobile phase (2 mL/min) of milli Q H<sub>2</sub>O and MeOH ranging from 0:100 to 60:40 (v/v) H<sub>2</sub>O: MeOH. The eluted fractions were detected by UV-visible spectroscopy at 254 nm (A<sub>254</sub>). The retention time of the extract was determined.

#### 3.5.9 Chemical structure analysis by <sup>1</sup>H-NMR and MS

Among the selected fractions from the SiG60-CC (500 mL size) and HPLC fractions, the most active fraction for both activities was evaporated and analyzed as reported (Do et al., 2021). Briefly, the evaporated sample was dissolved in an appropriate deuterated solvent (methanol-d<sub>4</sub>, Merck) at a ratio of 5–20 mg of compound to 600 µL of the solvent. Next, it was transferred to an NMR tube and

shaken until totally dissolved. The  $^1\text{H-NMR}$  spectrum was recorded using a Jeol JNM-ECZ 500MHz operated at 500 MHz for  $^1\text{H-NMR}$  nuclei with tetramethylsilane as the internal standard. The chemical shift in  $\delta$  (ppm) was assigned with reference to the signal from the residual protons in the deuterated solvents, while the chemical shift and J coupling value were determined using the MestReNova version 12.0.3 software. The MW of the active fractions was analyzed using a microTOF focus II MS with electrospray ionization in the positive mode and  $\alpha$ -cyano-4-hydroxycinnamic acid as the matrix.

#### 3.5.10 Data analysis

All experiments were done in triplicate. Numerical data are reported as the mean  $\pm$  one standard deviation (SD), determined in the Microsoft Excel 2019 software (Khongkarat et al., 2022). One-way ANOVA and T-test were used to test for significant differences. Tukey's and Dunnett T3 test ( $p < 0.05$ ) was applied for pairwise multiple comparisons (Durovic et al., 2022). All statistical analyses were performed using the IBM SPSS statistics version 22 for windows software.

The overall procedure of BP screening and enrichment of the antioxidant and enzyme inhibitory activities from the most active extract is summarized schematically in Figure 3.1.

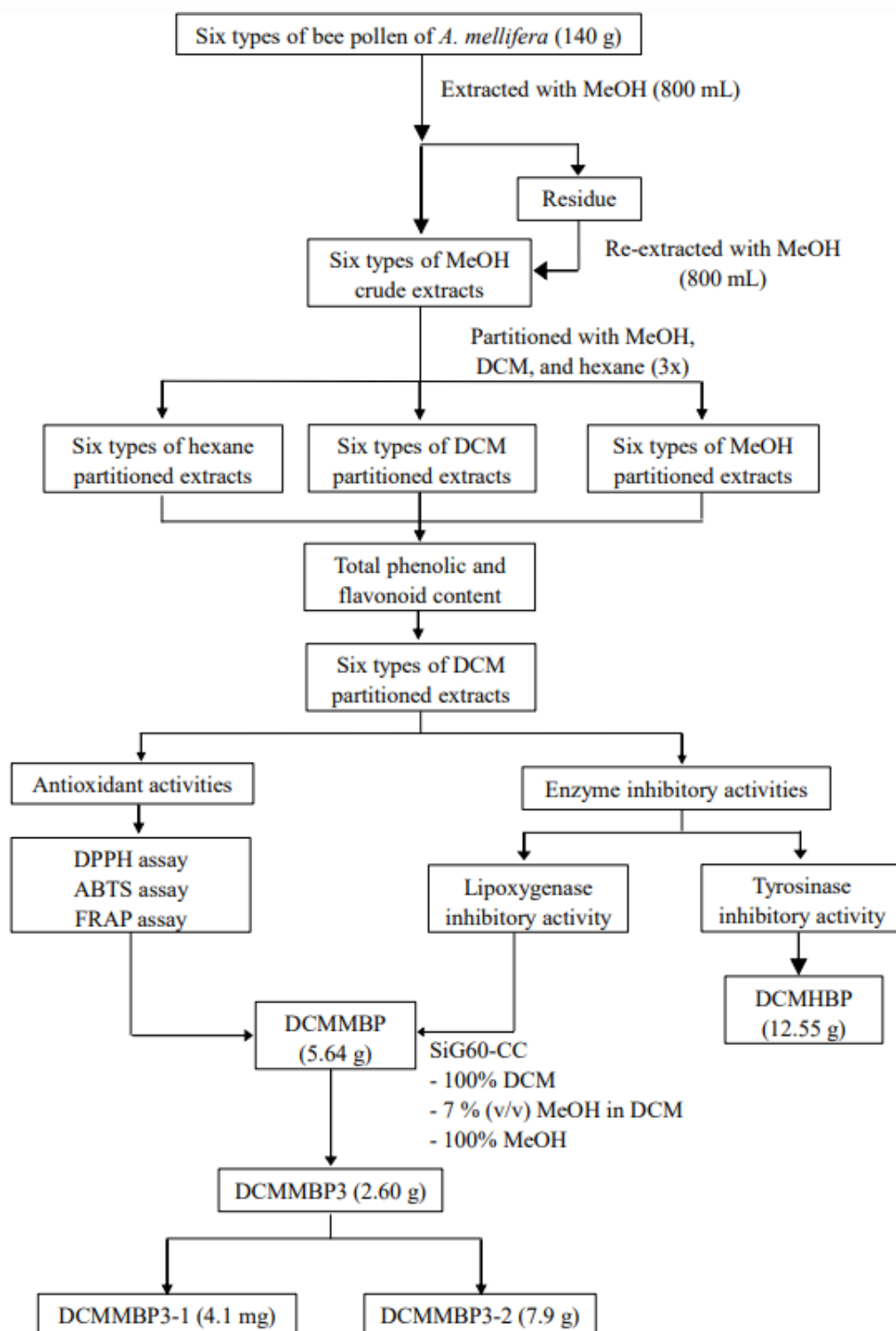


**Figure 3.1** Summary of the extraction, screening, and enrichment procedures for the selected BP.

### 3.6 Results

#### 3.6.1 The partitioned extracts of BPs

After partitioning the MCEs of the six different types of BPs with organic solvents from the lowest to the highest in polarity (hexane, DCM, and MeOH), a total of 18 partitioned extracts were obtained. These partitioned extracts were then evaporated and weighed, and the character of each extract was observed, with the results summarized in Supplement 1. The MeOH-partitioned extracts had the highest yield (above 40%). Only the DCM-partitioned extracts exhibited a sticky solid form, whereas the MeOH- and hexane-partitioned extracts exhibited an oil form. The TPC and FC of the MeOH-, DCM- and hexane-partitioned extracts of all six types of BP were then determined.

#### 3.6.2 Determination of the TPC and FC

The TPC and FC were determined from the calibration curves of gallic acid ( $y = 8.5519x - 0.0133$ ;  $R^2 = 0.9991$ ) and quercetin ( $y = 0.6342x + 0.0083$ ;  $R^2 = 0.9982$ ), respectively, with the TPC and FC of each extract shown in Table 3.2. The effect of the partition solvent on the TPC and FC was significantly evident, with the highest TPC and FC being found in the DCM-partitioned extracts of all six BP samples, followed by the MeOH-partitioned extracts, while the hexane-partitioned extracts had the lowest TPC and no FC. The TPC of these BP extracts varied between  $7.20 \pm 0.25$  and  $53.26 \pm 0.85$  mg GAE/g, being highest in DCMHBP ( $53.26 \pm 0.85$  mg GAE/g). The FC varied between  $3.09 \pm 0.59$  and  $104.13 \pm 3.80$  mg QE/g, being highest in DCMMBP ( $104.13 \pm 3.80$  mg QE/g). The FC of the hexane-partitioned extracts could not be determined due to the absorption being too low (below the range of the quercetin standard curve). Since the DCM-partitioned extract of each type of BP had the significantly highest TPC and FC, they were used in the subsequent screening for antioxidant and enzyme inhibitory activities.



**Table 3.2** The TPC and FC of the partitioned BP extracts.

Partitioned extract	CBP	HBP	MBP	NBP	XBP	ABP
<i>TPC (mg GAE/g):</i>						
MT	29.45 ± 0.94 <sup>b</sup>	20.19 ± 0.75 <sup>b</sup>	24.04 ± 0.37 <sup>b</sup>	11.84 ± 0.23 <sup>a</sup>	18.16 ± 0.16 <sup>b</sup>	26.55 ± 0.37 <sup>b</sup>
DCM	42.44 ± 0.25 <sup>c</sup>	53.26 ± 0.85 <sup>c</sup>	47.82 ± 0.39 <sup>c</sup>	16.83 ± 0.04 <sup>b</sup>	47.91 ± 0.36 <sup>c</sup>	39.33 ± 0.66 <sup>c</sup>
HX	10.45 ± 0.24 <sup>a</sup>	9.69 ± 0.47 <sup>a</sup>	7.20 ± 0.25 <sup>a</sup>	12.48 ± 0.41 <sup>a</sup>	10.03 ± 0.57 <sup>a</sup>	11.90 ± 0.18 <sup>a</sup>
<i>FC (mg QE/g):</i>						
MT	8.86 ± 0.44 <sup>a</sup>	3.09 ± 0.59 <sup>a</sup>	6.39 ± 0.27 <sup>a</sup>	–	4.27 ± 0.16 <sup>a</sup>	16.95 ± 0.44 <sup>a</sup>
DCM	31.07 ± 2.94 <sup>b</sup>	56.13 ± 2.52 <sup>b</sup>	104.13 ± 3.80 <sup>b</sup>	6.74 ± 0.45	58.44 ± 1.36 <sup>b</sup>	24.64 ± 0.44 <sup>b</sup>
HX	–	–	–	–	–	–

**Notes:**

Data are shown as the mean ± 1SD derived from three replicates. Means within a column with a different superscript letter are significantly different [ $p < 0.05$ ; one-way ANOVA and Post Hoc (Tukey) test (TPC) or Independent-Samples *T*-Test (FC)].

### 3.6.3 Antioxidant activity of the partitioned extracts

The results for the three different antioxidant assays of the DCM-partitioned extracts from the six types of BP are shown in the Table 3.3 along with that for ascorbic acid as the standard reference for the DPPH and ABTS assays. The  $EC_{50}$  values ranged from  $176.85 \pm 8.31$  to  $2,305.98 \pm 59.53$   $\mu\text{g/mL}$ . Only the DCMMBP extract showed a significantly strong DPPH radical scavenging ability ( $EC_{50}$  of  $176.85 \pm 8.31$   $\mu\text{g/mL}$ ), although this was still almost 2.6-fold less effective than ascorbic acid ( $EC_{50}$  of  $68.00 \pm 1.13$   $\mu\text{g/mL}$ ), while the DCMNBP extract had the weakest DPPH scavenging capacity.

For the ABTS assay, the  $EC_{50}$  values (Table 3.3) ranged from  $195.59 \pm 11.44$  to  $875.04 \pm 49.84$   $\mu\text{g/mL}$ . Again, only DCMMBP showed a significantly strong ABTS radical scavenging ability ( $EC_{50}$  of  $195.59 \pm 11.44$   $\mu\text{g/mL}$ ), although this was still over four-fold less effective than ascorbic acid ( $EC_{50}$  of  $44.54 \pm 0.19$   $\mu\text{g/mL}$ ), while DCMNBP demonstrated the weakest ABTS scavenging capacity.

Furthermore, the ABTS assay was also evaluated in terms of the TEAC, determined from the Trolox calibration curve ( $y = -3.0279x + 0.5931$ ;  $R^2 = 0.9978$ ).

The TEAC values of the BP extracts ranged from  $35.71 \pm 2.98$  to  $296.95 \pm 16.87$   $\mu\text{mole TE/g}$  (Table 3.3), where DCMMBP had the significantly highest TEAC value and DCMNBP the lowest.

The reducing power, in terms of the FRAP value, of the DCM-partitioned extracts was calculated from the calibration curve of  $\text{FeSO}_4$  ( $y = 0.0004x - 0.0292$ ;  $R^2 = 0.9947$ ). The significantly highest antioxidant activity was found in DCMMBP ( $1,058.92 \pm 28.78$   $\mu\text{mole Fe}^{2+}/\text{g}$ ) (Table 3.3), while the lowest was found in DCMNBP ( $141.83 \pm 5.61$   $\mu\text{mole Fe}^{2+}/\text{g}$ ).

Overall, from the three antioxidant assays (DPPH, ABTS, and FRAP), DCMMBP showed the strongest antioxidant activity. However, its activity was lower than ascorbic acid (positive standard). To increase its activity, DCMMBP was further enriched (fractionated) by chromatographic methods.

**Table 3.3** Antioxidant activity of the partitioned extracts.

Sample	DPPH EC <sub>50</sub> ( $\mu\text{g/mL}$ )	ABTS EC <sub>50</sub> ( $\mu\text{g/mL}$ )	ABTS ( $\mu\text{mole TE/g}$ )	FRAP ( $\mu\text{mole Fe}^{2+}/\text{g}$ )
DCMCBP	$1,952.99 \pm 8.44^c$	$563.85 \pm 23.48^{cd}$	$163.92 \pm 10.24^{bc}$	$412.11 \pm 11.04^c$
DCMHBP	$2,291.18 \pm 36.99^d$	$681.1 \pm 28.83^{cd}$	$164.80 \pm 7.60^{bc}$	$395.17 \pm 13.00^{bc}$
DCMMBP	$176.85 \pm 8.31^b$	$195.59 \pm 11.44^b$	$296.95 \pm 16.87^d$	$1,058.92 \pm 28.78^e$
DCMNBP	$>4,000^e$	$>2,000^e$	$35.71 \pm 2.98^a$	$141.83 \pm 5.61^a$
DCMXBP	$1,970 \pm 3.34^c$	$494.04 \pm 25.41^c$	$176.58 \pm 10.91^c$	$469.61 \pm 15.86^d$
DCMABP	$2,305.98 \pm 59.53^d$	$875.04 \pm 49.84^d$	$136.22 \pm 13.60^b$	$351.97 \pm 15.67^b$
Ascorbic acid	$68.00 \pm 1.13^a$	$44.54 \pm 0.19^a$	–	–

**Notes:**

Data are shown as the mean  $\pm$  1 SD. Within a column, EC<sub>50</sub> means with a different superscript letter are significantly different ( $p < 0.05$ ; one-way ANOVA and Post Hoc (Dunnett T3) test). Likewise, for the mean ABTS and FRAP  $\mu\text{mole TE g}^{-1}$  and  $\mu\text{mole Fe}^{2+} \text{g}^{-1}$  values, means within a column with a different superscript letter are significantly different [ $p < 0.05$ ; one-way ANOVA and Post Hoc (Tukey) test].

### 3.6.4 Enzyme inhibitory activity

#### *In vitro TYRI activity*

Due to the large number of fractions to be screened, all the partitioned extracts were initially screened for TYRI activity at a single final extract concentration of 200  $\mu\text{g/mL}$ . The obtained  $A_{475}$  was converted to the TYRI activity (%) and the results are presented as the mean  $\pm$  SD in Table 3.4. At this extract concentration, DCMCBP, DCMHBP, DCMXBP, and DCMABP showed a more than 50% TYRI activity, and so they were further evaluated at different concentrations and their derived  $\text{IC}_{50}$  values are shown in Table 3.4. Of these extracts, DCMHBP had the significantly highest TYRI activity ( $\text{IC}_{50}$  42.63  $\pm$  1.65  $\mu\text{g/mL}$ ) but this was significantly (some 4.4-fold) less effective than kojic acid ( $\text{IC}_{50}$  of 9.61  $\pm$  0.47  $\mu\text{g/mL}$ ).

#### *In vitro LOXI activity*

The partitioned extracts were also initially screened for LOXI activity at a single final extract concentration of 60  $\mu\text{g/mL}$ , with the LOXI activity (%) presented as the mean  $\pm$  SD in Table 3.4. At this extract concentration, only DCMMBP provided a high *in vitro* LOXI activity (78.60  $\pm$  2.81%) and so was further evaluated at different concentrations, revealing an  $\text{IC}_{50}$  value of 32.55  $\pm$  1.31  $\mu\text{g/mL}$  (Table 3.4), some 1.4-fold less significantly effective than NDGA (22.41  $\pm$  2.35  $\mu\text{g/mL}$ ).

**Table 3.4** The TYRI and LOXI activities (%/ $\text{IC}_{50}$ ) of the partitioned extracts.

Sample	TYRI (% at 200 $\mu\text{g/mL}$ )/ $\text{IC}_{50}$	LOXI (% at 60 $\mu\text{g/mL}$ )/ $\text{IC}_{50}$
DCMCBP	58.88 $\pm$ 0.36/101.13 $\pm$ 3.18 <sup>c</sup>	25.80 $\pm$ 4.73/–
DCMHBP	60.41 $\pm$ 0.45/42.63 $\pm$ 1.65 <sup>b</sup>	28.58 $\pm$ 4.96/–
DCMMBP	10.05 $\pm$ 0.86/–	78.60 $\pm$ 2.81/32.55 $\pm$ 1.31 <sup>b</sup>
DCMNBP	0.00 $\pm$ 0.00/–	15.64 $\pm$ 3.28/–
DCMXBP	52.95 $\pm$ 0.09/179.97 $\pm$ 3.77 <sup>d</sup>	28.27 $\pm$ 1.82/–
DCMABP	51.76 $\pm$ 0.93/193.87 $\pm$ 5.06 <sup>c</sup>	24.47 $\pm$ 2.95/–
Kojic acid	–/9.61 $\pm$ 0.47 <sup>a</sup>	–
NDGA	–	–/22.41 $\pm$ 2.35 <sup>a</sup>

Notes:

The  $IC_{50}$  values are shown as the mean  $\pm$  1SD. Within a column, means with a different superscript letter are significantly different ( $p < 0.05$ ; one-way ANOVA and Post Hoc Tukey test for TYRI activity and Independent-Samples T-Test for LOXI).

### 3.6.5 Antioxidant and LOXI activities of compounds from DCMMBP

#### *Fractionation of DCMMBP by SiG60-CC*

Since the DCMMBP provided the best LOXI and antioxidant activities, the sample (5.64 g) was further enriched using SiG60-CC. A total of 74 fractions were collected, but after pooling fractions with a similar TLC plate profile, five different fractions (DCMMBP1–5) were obtained (Supplement 2). The TLC profile DCMMBP1 (lane 2, Rf of 0.90) revealed one major band under UV light and a few bands after staining with anisaldehyde, while DCMMBP2 (lane 3, Rf of 0.26, 0.38, and 0.59) showed two bands under UV light and one more major band after staining. For DCMMBP3 (lane 4, Rf of 0.21), it showed only one major band under UV light and so it might be a pure compound, while DCMMBP 4 (lane 5, Rf of 0.00 and 0.21) and DCMMBP 5 (lane 6, Rf of 0.00 and 0.21) each showed a major band at the base line and a minor band under UV light. When the TLC profiles of each fraction were compared to the original fraction (lane 1, Rf of 0.23), the compound in fraction 3 was found to be the main active compound. Their respective weights and characteristics are recorded in Supplement 1.

All five pooled fractions were separately screened for their antioxidant and LOXI activities. An antioxidant activity of more than 50% was found in DCMMBP3 ( $81.21 \pm 1.38\%$ ) and DCMMBP4 ( $69.52 \pm 1.52\%$ ) at a concentration of 500  $\mu\text{g/mL}$  based on the DPPH assay. The ABTS assay revealed more 50% activity for the DCMMBP2 ( $92.87 \pm 4.00\%$ ), DCMMBP3 ( $99.32 \pm 0.01\%$ ), DCMMBP4 ( $97.97 \pm 0.57\%$ ), and DCMMBP5 ( $72.12 \pm 1.49\%$ ). However, at a concentration of 20  $\mu\text{g/mL}$ , a LOXI activity of over 50% was only found in DCMMBP3 ( $73.35 \pm 0.85\%$ ). Therefore, these fractions were further investigated at various concentrations and their respective  $EC_{50}$  and  $IC_{50}$  values derived.

The data for the DPPH assay are shown in Table 3.5, where the  $EC_{50}$  value of DCMMBP3 and DCMMBP4 was  $54.66 \pm 3.45$  and  $184.84 \pm 5.47$   $\mu\text{g/mL}$ , respectively, and DCMMBP3 was significantly more effective than ascorbic acid

( $68.00 \pm 1.13 \mu\text{g/mL}$ ) and the parental DCMMBP extract ( $176.85 \pm 8.31 \mu\text{g/mL}$ ; Table 3.3).

For the ABTS assay, the obtained  $\text{IC}_{50}$  values are shown in Table 3.5. The  $\text{EC}_{50}$  value and  $\mu\text{mole TE/g}$  for the ABTS assay of DCMMBP3 was  $24.56 \pm 2.99 \mu\text{g/mL}$  and  $2,529.69 \pm 142.16 \mu\text{mole TE/g}$ , respectively, which was significantly stronger than that for ascorbic acid ( $44.54 \pm 0.19 \mu\text{g/mL}$ ) and the parental DCMMBP extract ( $195.59 \pm 11.44 \mu\text{g/mL}$  and  $296.95 \pm 16.87 \mu\text{mole TE/g}$ , respectively).

For the FRAP assay (Table 3.5), DCMMBP3 was  $3,466.17 \pm 81.30 \mu\text{mole Fe}^{2+}/\text{g}$ , which was over three-fold higher than that the parental DCMMBP extract ( $1,058.92 \pm 28.78 \mu\text{mole Fe}^{2+}/\text{g}$ ; Table 3.5).

For the LOXI activity, the  $\text{IC}_{50}$  values are reported in Table 3.5. The  $\text{IC}_{50}$  value for the LOXI activity of DCMMBP3 was  $12.11 \pm 0.36 \mu\text{g/mL}$ , which was significantly (1.85- and 2.69-fold) more effective than that of NDGA ( $\text{IC}_{50}$  of  $22.41 \pm 2.35 \mu\text{g/mL}$ ) and the parental DCMMBP extract ( $\text{IC}_{50}$  of  $32.55 \pm 1.31 \mu\text{g/mL}$ ; Table 3.4), respectively. Therefore, DCMMBP3 was further enriched by HPLC.

#### *Fractionation of DCMMBP3 by HPLC*

To optimize the separation, the HPLC was eluted with an isocratic gradient of 0:100 to 60:40 (v/v)  $\text{H}_2\text{O}$ : MeOH, which separated DCMMBP3 into five peaks, with the two main peaks eluting at a retention time of 15.352 and 20.182 min, respectively, (Figure 3.2). These two fractions (DCMMBP3-1 and DCMMBP3-2) were defined as compounds **1** and **2**, respectively. Their weight and characters are summarized in Supplement 1. Compounds **1** and **2** were tested for their antioxidant and LOXI activities, where compounds **1** and **2** showed similar antioxidant and LOXI activities (Table 3.5). The structure of compounds **1** and **2** was characterized by  $^1\text{H-NMR}$  and MS analyses, and found to share the same structure, consistent with their bioactivities.

**Table 3.5** Antioxidant and LOXI activities of the respective fractions after SiG60 and HPLC chromatography.

Sample	DPPH EC <sub>50</sub> (µg/mL)	ABTS EC <sub>50</sub> (µg/mL)	ABTS (µmol TE/g)	FRAP (µmol Fe <sup>2+</sup> /g)	LOX IC <sub>50</sub> (µg/mL)
<i>After SiG60-CC:</i>					
DCMMBP1	–	–	86.63 ± 6.84 <sup>a</sup>	304.50 ± 33.46 <sup>a</sup>	–
DCMMBP2	–	125.81 ± 12.97 <sup>d</sup>	878.09 ± 73.48 <sup>c</sup>	1,038.11 ± 34.60 <sup>c</sup>	–
DCMMBP3	54.66 ± 3.45 <sup>a</sup>	24.56 ± 2.99 <sup>a</sup>	2,529.69 ± 142.16 <sup>e</sup>	3,466.17 ± 81.30 <sup>e</sup>	12.11 ± 0.36 <sup>a</sup>
DCMMBP4	184.84 ± 5.47 <sup>c</sup>	66.1 ± 3.55 <sup>c</sup>	1,482.24 ± 63.00 <sup>d</sup>	1,363.11 ± 47.30 <sup>d</sup>	–
DCMMBP5	–	318.66 ± 8.66 <sup>e</sup>	456.82 ± 45.31 <sup>b</sup>	657.56 ± 23.52 <sup>b</sup>	–
Ascorbic acid	68.00 ± 1.13 <sup>b</sup>	44.54 ± 0.19 <sup>b</sup>	–	–	–
NDGA	–	–	–	–	22.41 ± 2.35 <sup>b</sup>
<i>After HPLC:</i>					
DCMMBP3-1	53.05 ± 2.60 <sup>a</sup>	25.38 ± 0.67 <sup>a</sup>	2,527.63 ± 7.99 <sup>a</sup>	3,477.33 ± 52.07 <sup>a</sup>	11.31 ± 0.46 <sup>a</sup>
DCMMBP3-2	57.7 ± 2.77 <sup>a</sup>	28.29 ± 1.05 <sup>b</sup>	2,339.16 ± 34.62 <sup>b</sup>	3,091.78 ± 44.48 <sup>b</sup>	11.57 ± 0.93 <sup>a</sup>
Ascorbic acid	68.00 ± 1.13 <sup>b</sup>	44.54 ± 0.19 <sup>c</sup>	–	–	–
NDGA	–	–	–	–	22.41 ± 2.35 <sup>b</sup>

**Notes:**

Data are shown as the mean ± 1SD. Means within a column with a different superscript letter are significantly different ( $p < 0.05$ ; one-way ANOVA plus for samples after SiG60-CC: Post Hoc (Tukey) test for DPPH and FRAP data, Dunnett T3 test for ABTS data, independent samples T-Test for IC<sub>50</sub> values; for post-HPLC data: Tukey test for DPPH and ABTS EC<sub>50</sub> data, independent samples T-Test for ABTS µmol TE/g and FRAP values; and Dunnet test for LOX IC<sub>50</sub> values).

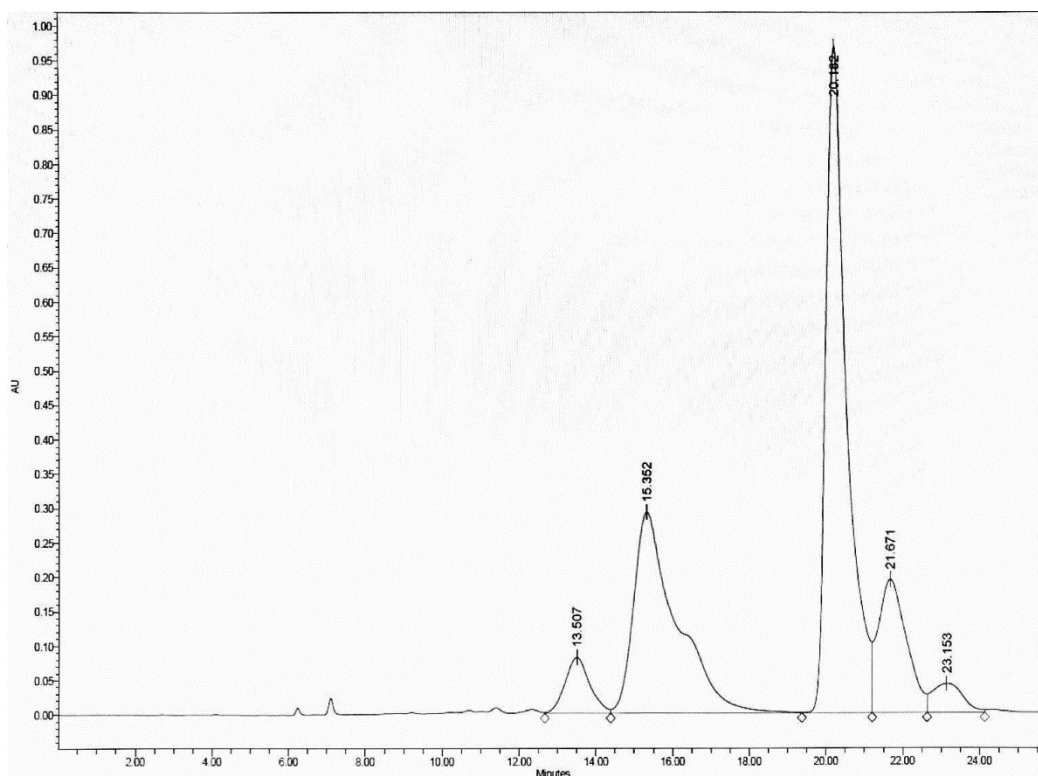


**Figure 3.2** The HPLC chromatogram of DCMMBP3 showing the elution of DCMMBP3-1 and DCMMBP3-2 at a retention time of 15.352 and 20.182 min, respectively.

### 3.6.6 Structural identification of compounds 1 and 2

After fractionation of DCMMBP3 by HPLC, compounds **1** and **2** were obtained. The  $^1\text{H-NMR}$  spectra of compounds **1** (Supplement 3) and **2** (Supplement 4) revealed essentially similar signals to each other. Their MS spectra also showed identical pseudomolecular ions  $[\text{M}+\text{Na}]^+$  and  $[\text{M}+\text{H}]^+$  as well as mass fragment ion  $[\text{M}+\text{Na}-177]^+$  (Supplements 5-7) at 696, 674, and 522, respectively. The above mentioned spectroscopic data suggested that compounds **1** and **2** were isomeric compounds. Compound **1** exhibited chemical shifts of the methylene hydrocarbon ( $-\text{CH}_2-$ ) at 1.43 and 1.87 ppm and of a methylene hydrocarbon connected to a nitrogen atom at 3.18 ppm, thus indicating the presence of a spermidine moiety. A cluster of singlet methoxy peaks at around 3.75 ppm together with the chemical shifts between 6.73 and 7.48 ppm suggested the presence of a phenolic compound containing methoxy groups. The chemical shifts at 5.95 and 6.40 ppm with small coupling

constants of 12.9 Hz indicated *cis*-olefinic protons, while those of 6.40 and 7.40 ppm with large coupling constants of 15.8 Hz suggested *trans*-olefinic protons. These signals in the aromatic region suggested the presence of *cis*- and *trans*-feruloyl moieties (Figure 3.3, A). To determine the ratio of *cis*- and *trans*-feruloyl moieties in the whole structure, the signal integration of olefinic protons was analyzed. A ratio of 1:2 suggested that compound **1** was comprised one *cis*-feruloyl and two *trans*-feruloyls in the molecule. Therefore, three possible structures of compound **1** were established;  $N^1, N^5, N^{10}$ -tri-(*Z,E,E*)-,  $N^1, N^5, N^{10}$ -tri-(*E,Z,E*)-, and  $N^1, N^5, N^{10}$ -tri-(*E,E,Z*)-feruloyl spermidine, respectively, as shown in Figures 3.3, C–E. An attempt to determine exactly which structure matched to the spectroscopic data was unsuccessful due to the severely overlapped olefinic protons. In nature, the *cis*-isomer is less stable and gradually isomerizes into the *trans*-congener. Compound **2** was nearly identical to compound **1**, except for the lack of *cis*-olefinic protons (Figure 3.3, B). This data suggested that compound **2** is acyl spermidine containing all *trans*-feruloyl moieties. Therefore, the structure of **2** was established as  $N^1, N^5, N^{10}$ -tri-(*E,E,E*)-feruloyl spermidine, as shown in Figure 3.3, F.

*DCMMBP3 fraction (Mixture of compounds 1 and 2)*

$^1\text{H-NMR}$  (500 MHz, methanol- $d_4$ )  $\delta$  7.54 – 7.33 (m, 5H), 7.14 – 6.62 (m, 17H), 6.61 – 6.43 (m, 1H), 6.43 – 6.31 (m, 3H), 3.81 (qd,  $J = 7.5, 3.5$  Hz, 20H), 3.76 – 3.70 (m, 3H), 3.60 – 3.48 (m, 4H), 3.48 – 3.39 (m, 2H), 3.32 (d,  $J = 5.8$  Hz, 12H), 3.26 – 3.13 (m, 1H), 1.95 – 1.78 (m, 3H), 1.74 – 1.51 (m, 7H), 1.50 – 1.36 (m, 1H), and 1.31 – 1.23 (m, 1H).



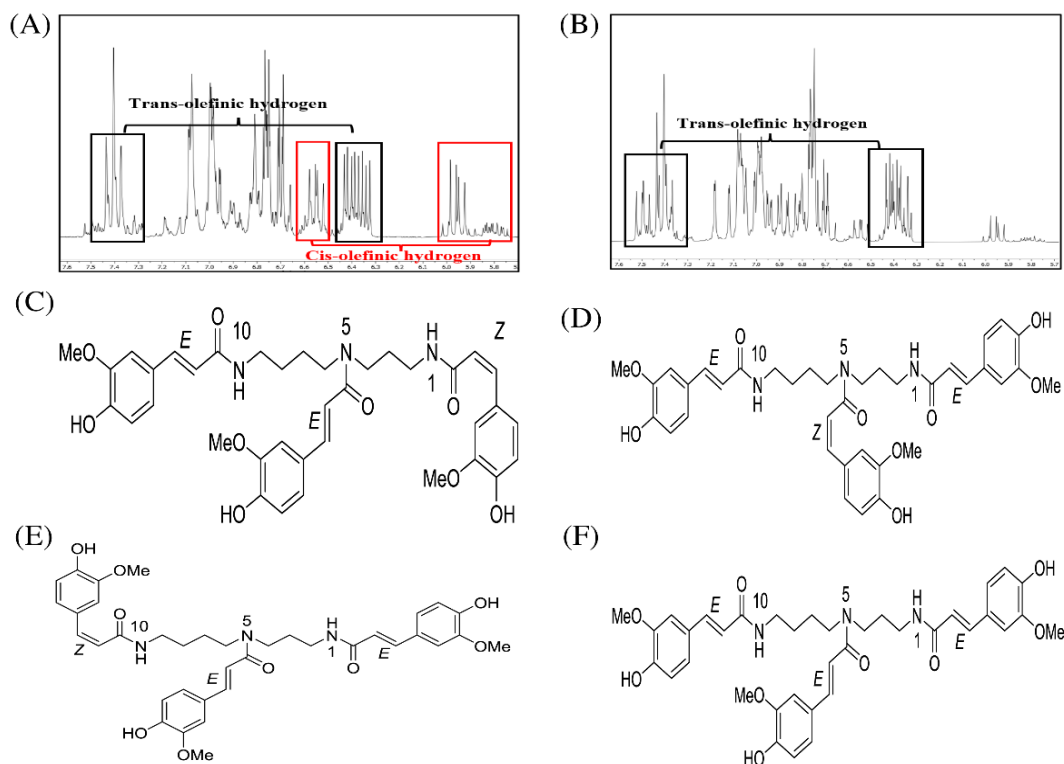


**Figure 3.3**  $^1\text{H-NMR}$  (500 MHz,  $\text{MeOD-D}_4$ ) in the range of 7.6–5.7 ppm of (A) compound 1 and (B) compound 2. The chemical structures of (C–F) spermidine derivatives.  $^1\text{H-NMR}$  (500 MHz,  $\text{MeOD-D}_4$ ) in the range of 7.6–5.7 ppm of (A) compound 1 and (B) compound 2. The chemical structures of (C)  $N^1, N^5, N^{10}$ -tri-(*Z,E,E*)-feruloyl spermidine, (D)  $N^1, N^5, N^{10}$ -tri-(*E,Z,E*)-feruloyl spermidine, (E)  $N^1, N^5, N^{10}$ -tri-(*E,E,Z*)-feruloyl spermidine, and (F)  $N^1, N^5, N^{10}$ -tri-(*E,E,E*)-feruloyl spermidine.

### 3.7 Discussion

Different types of BP can provide different amounts and types of secondary metabolites, depending on their floral origin, which can result in a wide range of bioactivities between different BPs (Rzepecka-Stojko et al., 2015). In our work, six monofloral *A. mellifera* BPs were evaluated because many types of monofloral BP are harvested in Thailand due to the large amount of diverse monocrops that are cultivated. Moreover, the floral origin of monofloral BP is easier to identify, which makes it easier to control the quality and pharmaceutical properties of the BP compared to that of multifloral BP (Campos et al., 2010). Since bee products are edible, the food safety aspect should be considered, including the risks associated with

pesticides, toxic metals, mycotoxins, allergens, and pollen grains of inedible plants (Vegh et al., 2021). There is a risk bias in certain plant groups (*Helianthus*, *Rosaceae*, *Raxinus*, and *Sophora*) that can contain high concentrations of toxic metals (Kostic et al., 2015). In addition, BPs from pine, canola, kiwi, willow, corn poppy, rose, lotus, and camellia contain allergens that can induce anaphylaxis in some people (Yang et al., 2019).

The most practical method to determine the principal botanical origin(s) of BP is palynological analysis using microscopic examination (Kieliszek et al., 2018), but molecular analysis can also be used for minor components. Partitioning of BP with different polar organic solvents can separate the compounds based upon their polarity. This process makes further enrichment easier by screening for only the active extracts to undergo further fractionation. Of the different solvent extracts, the DCM-partitioned extracts of the six BPs in this study all showed the highest TPC and FC. Among these six DCM-partitioned BP extracts, DCMMBP and DCMHBP had the highest amount of both TPC and TFC. This result was consistent with Chantarudee et al. (2012) who reported that the DCM-partitioned extracts of corn (*Zea mays*) BP had the highest antioxidant activity compared to that of the MeOH- and hexane-partition extracts. Moreover, Bittencourt et al. (2015) reported that DCM partitioning of Brazilian BP enriched its antioxidant activity. As in previous reports, the active component for the antioxidant, TYRI, and LOXI activities in natural products were found to be phenolic and flavonoid compounds (Rebiai and Lanez, 2012; Sroka et al, 2017; Kim et al., 2015). Therefore, the DCM-partitioned extracts of the BPs that provided the highest TPC and TFC were selected to study for their antioxidant, TYRI, and LOXI activities.

In this work, the *in vitro* LOXI and TYRI activities were assayed using soybean LOX and mushroom TYR since both of these enzymes show structural and functional similarities with human enzymes. Therefore, they are commonly used as a model for human enzyme inhibition (Moita et al., 2014; Chang, 2009). The highest TYRI activity was found in DCMHBP followed by in DCMMBP, while the strongest LOXI activity was found in DCMMBP. Both activities were also correlated with the very high TPC and FC found in DCMHBP and DCMMBP. It was previously reported that phenol or flavonoid compounds can chelate the copper and iron ions in the active

sites of TYR and LOX enzymes, respectively, and so it is highly possible that an antioxidant compound, especially a phenolic compound, can also inhibit 5-LOX (Obaid et al., 2021; Ratnasari et al., 2017).

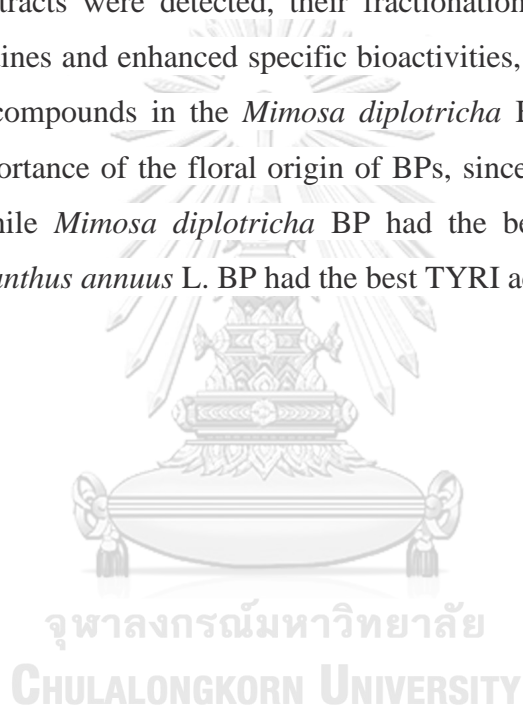
By comparison to the polyamine derivatives separated from *Microdesmis keayana* roots (Zamble et al., 2006), the two main active components in our work are likely to be  $N^1, N^5, N^{10}$ -triferuloyl spermidine or Keayanidine C. This finding agrees with the report on the phenolic profile in monofloral BP in Brazil, which also found  $N^1, N^5, N^{10}$ -triferuloyl spermidine in *Mimosa scabrella* BP (De-Melo et al., 2018). However, in our work, the  $^1\text{H-NMR}$  of compound **1** showed *cis*-olefinic hydrogen and *trans*-olefinic hydrogen at a 1:2 ratio, while compound **2** showed *trans*-olefinic hydrogens. Therefore, compounds **1** and **2** are  $N^1, N^5, N^{10}$ -tri(*E,E,E*)feruloyl spermidine and  $N^1, N^5, N^{10}$ -tri(*Z,Z,Z*)feruloyl spermidine, respectively, which are different in their configuration. The HPLC chromatographic profile agreed with previous works that reported on the separation of this compound by HPLC from *Hippesastrum x hortorum* pollen (Youhnovski et al., 2001) and *Sambucus nigra* L. (Kite et al., 2013). According to their findings, the HPLC chromatogram of this compound revealed four peaks corresponding to the four isomers: *ZZZ*, *EZZ*, *ZZE*, and *EEE*. These support that the peaks in our chromatogram are  $N^1, N^5, N^{10}$ -triferuloyl spermidine in different conformations. In fact, the *E*- and *Z*-feruloyl moiety can be interconverted on exposure to UV light, in which the *Z*-isomer is dominant. Although compound **1** contained a small proportion of *Z*-feruloyl moiety, the antioxidation and LOXI activity were comparable to those of compound **2**, whose structure had no *Z*-feruloyl residues. These observations preliminarily suggest that the geometry of C=C unsaturation contributed to a low or no effect on the biological activity. Thus, the feruloyl spermidines could potentially be applied as a mixture of isomers without the need for further time-consuming separation processes, such as HPLC, to obtain an individual pure isomer. In addition to feruloyl spermidines, other related spermidines acylated by a series of phenolics have been reported. A variety of coumaroyl spermidines isolated from rape BP (Zhang et al., 2020) were also demonstrated to have potent antioxidant activities in the DPPH, ABTS, and FRAP assays.

From the data mentioned above, these results showed that the BP samples harvested in Thailand, especially *M. diplotricha* BP, had potential bioactivities. The

findings additionally indicated the relationship between the phytochemicals and functional/pharmacological application. Also, the obtained data supported the traditional or alternative use of *M. diplotricha* BP in the indigenous medicine of Thailand.

### 3.8 Conclusions

*Mimosa diplotricha* BP had the highest antioxidant and LOXI activities, which were correlated to the highest TPC and FC. Although both bioactivities of the DCM-partitioned BP extracts were detected, their fractionation led to an enrichment of triferuloyl spermidines and enhanced specific bioactivities, suggesting these might be the major active compounds in the *Mimosa diplotricha* BP. In addition, this work supported the importance of the floral origin of BPs, since it affected the bioactivity directly. Here, while *Mimosa diplotricha* BP had the best antioxidant and LOXI bioactivities, *Helianthus annuus* L. BP had the best TYRI activity.



## References

- Bittencourt ML, Ribeiro PR, Franco RL, Hilhorst HW, de Castro RD, Fernandez LG. Metabolite profiling, antioxidant and antibacterial activities of Brazilian propolis: Use of correlation and multivariate analyses to identify potential bioactive compounds. *Food Res Int.* 2015; doi:10.1016/j.foodres.2015.07.008.
- Campos MGR, Frigerio C, Lopes J, Bogdanov S. What is the future of Bee-Pollen? *JAAS.* 2010; doi:10.3896/IBRA.4.02.4.01.
- Chamchumroon V, Suphuntee N, Tetsana N, Poopath M, Tanikkool S. Threatened plants in Thailand. 2017; Omega Printing Co., Ltd.; Bangkok.
- Chang TS. An updated review of tyrosinase inhibitors. *Int J Mol Sci.* 2009; doi:10.3390/ijms10062440.
- Chantarudee A, Phuwapraisirisan P, Kimura K, Okuyama M, Mori H, Kimura A, Chanchao C. Chemical constituents and free radical scavenging activity of corn pollen collected from *Apis mellifera* hives compared to floral corn pollen at Nan, Thailand. *BMC Complement Altern Med.* 2012; doi:10.1186/1472-6882-12-45.
- Daudu OM. Bee pollen extracts as potential antioxidants and inhibitors of  $\alpha$ -amylase and  $\alpha$ -glucosidase enzymes *in vitro* assessment. *J Apic Sci.* 2019; doi:10.2478/jas-2019-0020.
- De-Melo AAM, Estevinho LM, Moreira MM, Delerue-Matos C, Freitas ADSD, Barth OM, Almeida-Muradian LBD. Phenolic profile by HPLC-MS, biological potential, and nutritional value of a promising food: monofloral bee pollen. *J Food Biochem.* 2018; doi:10.1111/jfbc.12536.
- Do TML, Duong T-H, Nguyen V-K, Phuwapraisirisan P, Doungwichitkul T, Niamnont N, Jarupinthusophon S, Sichaem J. Schomburgkixanthone, a novel bixanthone from the twigs of *Garciniaschomburgkiana*. *Nat Prod Res.* 2021; doi:10.1080/14786419.2020.1716351.
- Durovic S, Sorgic S, Popov S, Pezo L, Maskovic P, Blagojevic S, Zekovic Z. Recovery of biologically active compounds from stinging nettle leaves part I: Supercritical carbon dioxide extraction. *Food Chem.* 2022; <https://doi.org/10.1016/j.foodchem.2021.131724>.

- Eshwarappa RS, Ramachandra YL, Subaramaihha SR, Subbaiah SG, Austin RS, Dhananjaya BL. Anti-lipoxygenase activity of leaf gall extracts of *Terminalia chebula* (Gaertn.) Retz.(Combretaceae). *Pharmacognosy Res.* 2016; doi:10.4103/0974-8490.171103.
- Khongkarat P, Ramadhan R, Phuwapraisirisan P, Chanchao C. Safflospermidines from the bee pollen of *Helianthus annuus* L. exhibit a higher *in vitro* antityrosinase activity than kojic acid. *Heliyon.* 2020; doi:10.1016/j.heliyon.2020.e03638.
- Khongkarat P, Traiyasut P, Phuwapraisirisan P, Chanchao C. First report of fatty acids in *Mimosa diplotricha* bee pollen with *in vitro* lipase inhibitory activity. *PeerJ.* 2022; <http://doi.org/10.7717/peerj.12722>.
- Kieliszek M, Piwowarek K, Kot AM, Blazejak S, Chlebowska-Smigiel A, Wolska I. Pollen and bee bread as new health-oriented products: a review. *Trends Food Sci Technol.* 2018; <https://doi.org/10.1016/j.tifs.2017.10.021>.
- Kim SB, Jo YH, Liu Q, Ahn JH, Hong IP, Han SM, Hwang BY, Lee MK. Optimization of extraction condition of bee pollen using response surface methodology: correlation between anti-melanogenesis, antioxidant activity, and phenolic content. *Molecules.* 2015; doi:10.3390/molecules201119656.
- Kite GC, Larsson S., Veitch NC, Porter EA, Ding N, Simmonds MSJ. Acyl spermidines in inflorescence extracts of elder (*Sambucus nigra* L., Adoxaceae) and elderflower drinks. *J Agric Food Chem.* 2013; doi:10.1021/jf304602q.
- Kostic AZ, Pesic MB, Mosaic MD, Dojcinovic BP, Natic MM, Trifkovic JD. Mineral content of bee pollen from Serbia. *Arh Hig Rada Toksikol.* 2015; <https://doi.org/10.1515/aiht-2015-66-2630>.
- Lobo V, Patil A, Phatak A, Chandra N. Free radicals, antioxidants, and functional foods: impact on human health. *Pharmacogn Rev.* 2010; doi:10.4103/0973-7847.70902.
- Lv H, Wang X, He Y, Wang H, Suo Y. Identification and quantification of flavonoid aglycones in rape bee pollen from Qinghai-Tibetan Plateau by HPLC-DADAPCI/MS. *J Food Compos Anal.* 2015; doi:10.1016/j.jfca.2014.10.011.
- Marghitas LA, Stanciu OG, Dezmirean DS, Bobis O, Popescu O, Bogdanov S, Campos MG. *In vitro* antioxidant capacity of honeybee-collected pollen of

- selected floral origin harvested from Romania. *Food Chem.* 2009;  
doi:10.1016/j.foodchem.2009.01.014.
- Mashima R, Okuyama T. The role of lipoxygenases in pathophysiology; new insights and future perspectives. *Redox Biol.* 2015; doi:10.1016/j.redox.2015.08.006.
- Moita E, Sousa C, Andrade PB, Fernandes F, Pinho BR, Silva LR, Valentao P. Effects of *Echium plantagineum* L. bee pollen on basophil degranulation: relationship with metabolic profile. *Molecules.* 2014;  
doi:10.3390/molecules190710635.
- Obaid RJ, Mughal EU, Naeem N, Sadiq A, Alsantali RI, Jassas RS, Moussa Z, Ahmed SA. Natural and synthetic flavonoid derivatives as new potential tyrosinase inhibitors: a systematic review. *RSC Adv.* 2021;  
doi:10.1039/d1ra03196a.
- Pham-Huy LA, He H, Pham-Huy C. Free radicals, antioxidants in disease, and health. *Int J Biomed Sci.* 2010;4:89.
- Ratnasari N, Walters M, Tsopmo A. Antioxidant and lipoxygenase activities of polyphenol extracts from oat brans treated with polysaccharide degrading enzymes. *Heliyon.* 2017; doi:10.1016/j.heliyon.2017.e00351.
- Rebiai A, Lanez T. Chemical composition and antioxidant activity of *Apis mellifera* bee pollen from northwest Algeria. *J Fundam Appl Sci.* 2012;  
doi:10.4314/jfas.v4i2.5.
- Rzepecka-Stojko A, Stojko J, Kurek-Gorecka A, Gorecki M, Kabala-Dzik A, Kubina R, Mozdziejz A, Buszman E. Polyphenols from bee pollen: structure, absorption, metabolism and biological activity. *Molecules.* 2015;  
doi:10.3390/molecules201219800.
- Saral O, Sahin H, Saral S, Alkanat M, Akyildiz K, Topcu A, Yilmaz A. Bee pollen increases hippocampal brain-derived neurotrophic factor and suppresses neuroinflammation in adult rats with chronic immobilization stress. *Neurosci Lett.* 2022; <https://doi.org/10.1016/j.neulet.2021.136342>.
- Saric A, Balog T, Sobocanec S, Kusic B, Sverko V, Rusak G, Likic S, Bubalo D, Pinto B, Reali D, Marotti T. Antioxidant effects of flavonoid from Croatian *Cystus incanus* L. rich bee pollen. *Food Chem Toxicol.* 2009;  
doi:10.1016/j.fct.2008.12.007.

- Sethiya NK, Mishra SH. Investigation of mangiferin, as a promising natural polyphenol xanthone on multiple targets of Alzheimer's disease. *J Biol Act Prod Nat*. 2014; doi:10.1080/22311866.2014.921121.
- Shahidi F, Zhong Y. Measurement of antioxidant activity. *J Funct Foods*. 2015; doi:10.1016/j.jff.2015.01.047.
- Sommano SR, Bhat FM, Wongkeaw M, Sriwichai T, Sunanta P, Chuttong B, Burgett M. Amino acid profiling and chemometric relations of black dwarf honey and bee pollen. *Front Nutr*. 2020; doi:10.3389/fnut.2020.558579.
- Sroka Z, Sowa A, Drys A. Inhibition of lipoxygenase and peroxidase reaction by some flavonols and flavones: The structure-activity relationship. *Nat Prod Commun*. 2017; doi:10.1177/1934578X1701201111.
- Sun L, Guo Y, Zhang Y, Zhuang Y. Antioxidant and anti-tyrosinase activities of phenolic extracts from rape bee pollen and inhibitory melanogenesis by cAMP/MITF/TYR pathway in B16 mouse melanoma cells. *Front Pharmacol*. 2017; doi:10.3389/fphar.2017.00104.
- Suriyatem R, Auras RA, Intipunya P, Rachtanapun P. Predictive mathematical modeling for EC<sub>50</sub> calculation of antioxidant activity and antibacterial ability of Thai bee products. *J App Pharm Sci*. 2017; doi:10.7324/JAPS.2017.70917.
- Teerasripreecha D, Phuwapraisirisan P, Puthong S, Kimura K, Okuyama M, Mori H, Kimura A, Chanchao C. *In vitro* antiproliferative/cytotoxic activity on cancer cell lines of a cardanol and a cardol enriched from Thai *Apis mellifera* propolis. *BMC Complement Altern Med*. 2012; doi:10.1186/1472-6882-11-37.
- Umthong S, Phuwapraisirisan P, Puthong S, Chanchao C. *In vitro* antiproliferative activity of partially purified *Trigona laeviceps* propolis from Thailand on human cancer cell lines. *BMC Complement Altern Med*. 2011; doi:10.1186/1472-6882-11-37.
- Vegh R, Csoka M, Soros C, Sipos L. Food safety hazards of bee pollen – a review. *Trends Food Sci Technol*. 2021; <https://doi.org/10.1016/j.tifs.2021.06.016>.



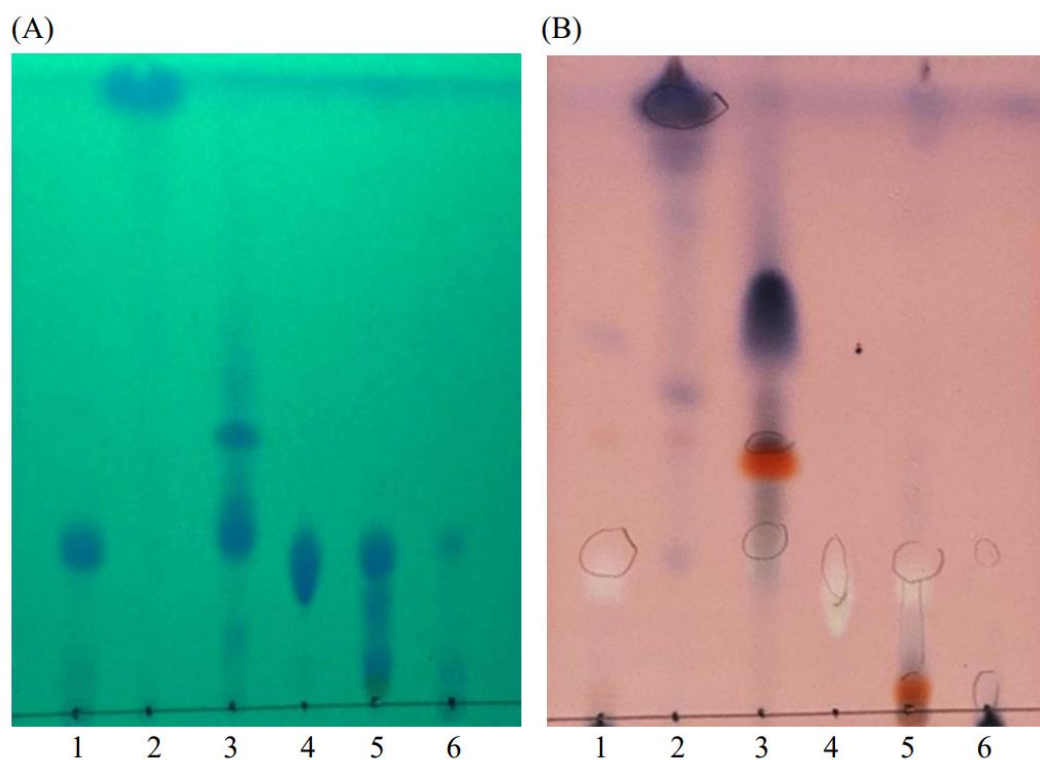
- Wang B, Wu L, Chen J, Dong L, Chen C, Wen Z, Hu J, Fleming I, Wang DW. Metabolism pathways of arachidonic acids: mechanisms and potential therapeutic targets. *Signal Transduct Target Ther.* 2021; doi:10.1038/s41392-020-00443-w.
- Yang Y, Wang H, Liu M, Huang W, Wang Y, Wu Y. A multiplex real-time PCR method applied to detect eight pollen species in food for the prevention of allergies. *Eur Food Res Technol.* 2019; <https://doi.org/10.1007/s00217-019-03327-8>.
- Yildiz OK, Karahalil FA, Can Z, Sahin H, Kolayli SE. Total monoamine oxidase (MAO) inhibition by chestnut honey, pollen, and propolis. *J Enzyme Inhib Med Chem.* 2014; doi:10.3109/14756366.2013.843171.
- Youhnovski N, Werner C, Hesse M. "N,N',N"-Triferuloylspermidine, a new UV absorbing polyamine derivative from pollen of *Hippeastrum × hortorum*. *Z Naturforsch C.* 2001; <https://doi.org/10.1515/znc-2001-7-809>.
- Zamble A, Sahpaz S, Hennebelle T, Carato P, Bailleul F. N<sup>1</sup>, N<sup>5</sup>, N<sup>-10</sup>Tris (-4 hydroxycinnamoyl) spermidines from *Microdesmis keayana* roots. *Chem Biodivers.* 2006; doi:/10.1002/cbdv.200690107.
- Zhang H, Liu R, Lu Q. Separation and characterization of phenolamines and flavonoids from rape bee pollen, and comparison of their antioxidant activities and protective effects against oxidative stress. *Molecules.* 2020; doi:10.3390/molecules25061264.

## Supplements

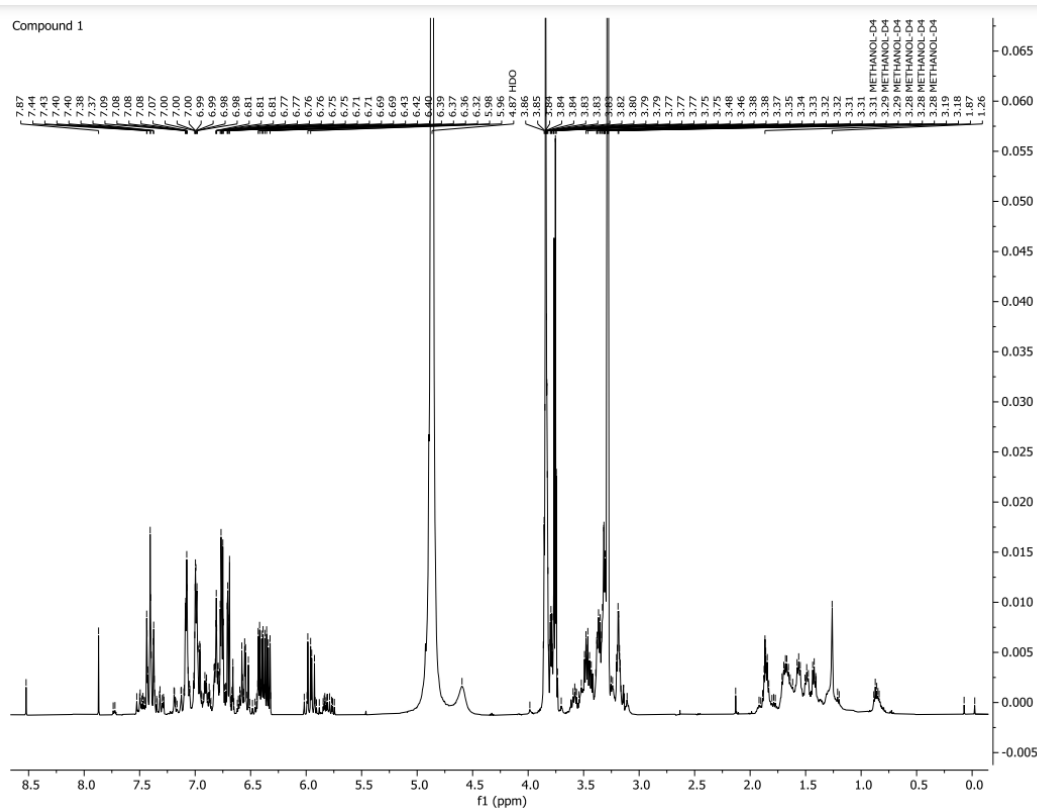
**Supplement 1:** The weight, yield, and the character of the different bee pollen (BP) extracts.

Sample	Weight (g)	Yield (%)	Character
<i>Partitioned extracts:</i>			
MTCBP	64.93	46.38	Pale brown oil
DCMCBP	7.41	5.29	Sticky dark brown solid
HXCBP	7.73	5.52	Dark brown oil
MTHBP	79.97	57.12	Dark brown oil
DCMHBP	12.55	8.96	Sticky dark brown solid
HXHBP	8.98	6.41	Dark brown oil
MTMBP	57.9	41.36	Dark brown oil
DCMMBP	9.89	7.06	Sticky dark brown solid
HXMBP	7.43	5.31	Dark brown oil
MTNBP	79.49	56.8	Pale brown oil
DCMNBP	4.68	3.34	Sticky brown solid
HXNBP	5.31	3.79	Pale brown oil
MTXBP	96.81	69.15	Dark brown oil
DCMXBP	8.04	56.8	Sticky dark brown solid
HXXBP	11.7	8.36	Dark brown oil
MTABP	79.28	56.63	Dark brown oil
DCMABP	5.75	4.11	Sticky dark brown solid
HXABP	8.47	6.05	Dark brown oil
<i>After SiG60-CC:</i>			
DCMMBP1	210	3.72	Sticky brown solid
DCMMBP2	300	5.32	Sticky brown solid
DCMMBP3	2,060	36.52	Sticky pale yellow solid
DCMMBP4	410	7.27	Sticky brown solid
DCMMBP5	2,380	42.2	Sticky dark brown solid
<i>After HPLC:</i>			
DCMMBP3-1	4.1	20.5	White solid
DCMMBP3-2	7.9	39.5	Pale yellow solid

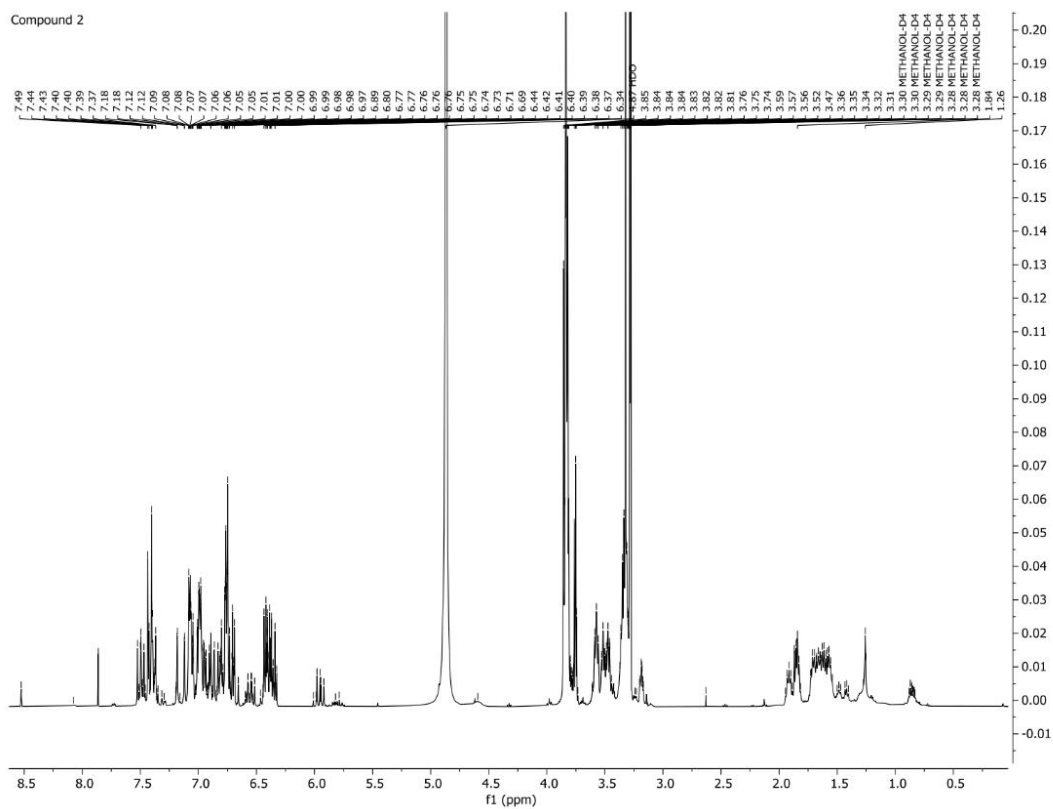
**Supplement 2:** Representative thin layer chromatography (TLC) images showing the compound profile of the original dichloromethane-partitioned BP extracts of *M. diplotricha* or DCMMBP (lane 1), and its subfractions DCMMBP1 (lane 2), DCMMBP2 (lane 3), DCMMBP3 (lane 4), DCMMBP4 (lane 5), and DCMMBP5 (lane 6) under (A) UV light and (B) after dipping in 3% (v/v) anisaldehyde in MeOH. The mobile phase was 7% MeOH-DCM.



**Supplement 3:**  $^1\text{H-NMR}$  peak data at chemical shift( $\delta$ ) 0.0-8.5 ppm in length of DCMMBP3-1 fraction or compound 1 in deuterated methanol (MeOD-D4).



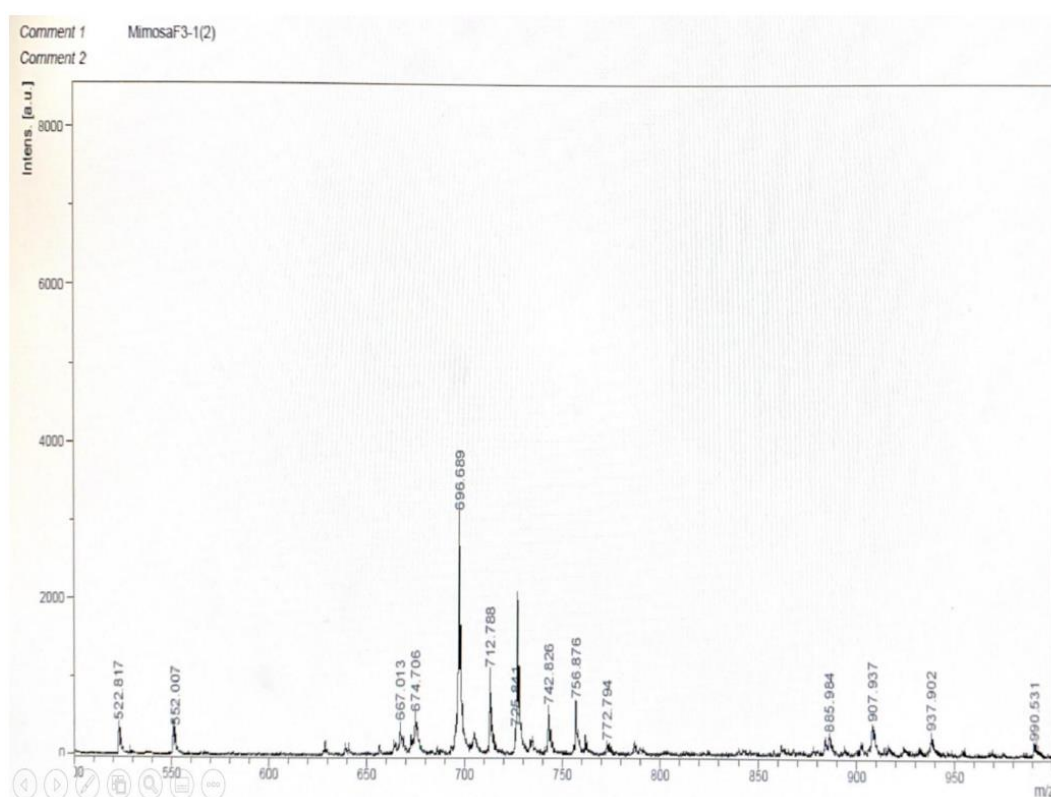
**Supplement 4:**  $^1\text{H-NMR}$  peak data at chemical shift( $\delta$ ) 0.0-8.5 ppm in length of DCMMBP3-2 fraction or compound 2 in MeOD-D4.



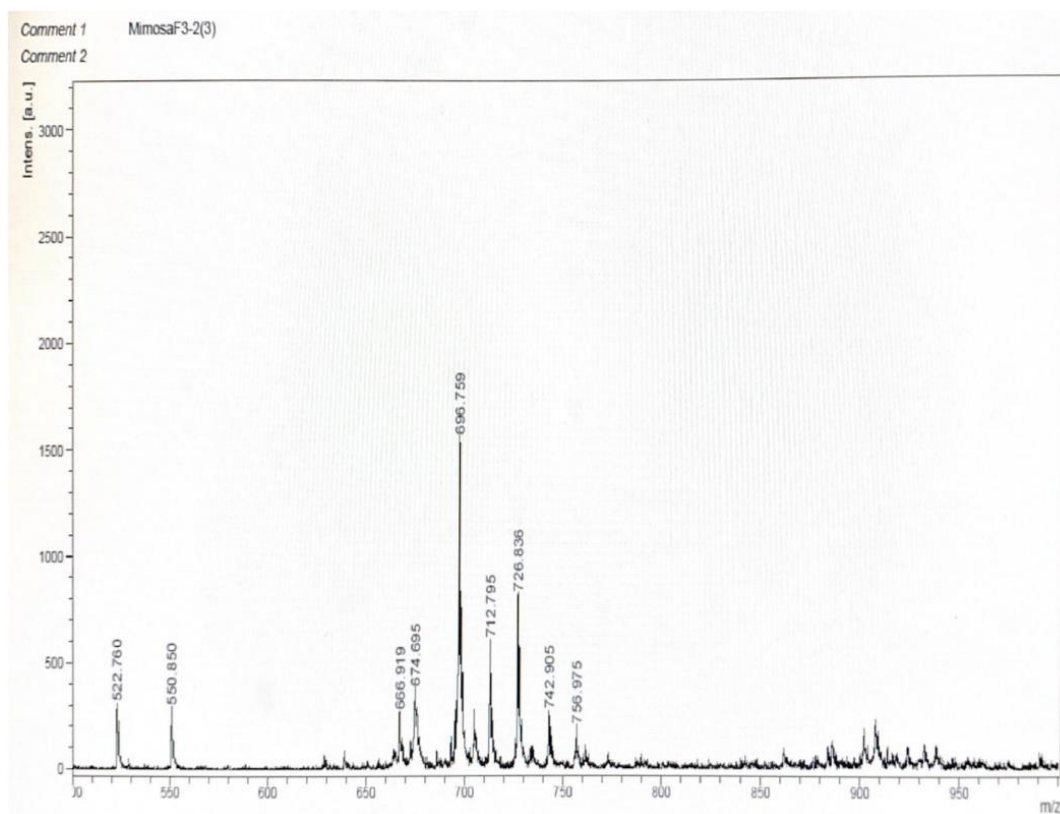
**Supplement 5:** Mass fragment of compound 1 and compound 2 in positive mode.

Mass fragment	Compound 1	Compound 2
$[M+Na]^+$	696.689	696.759
$[M+H]^+$	674.706	674.695
$[M+Na-177]^+$	522.817	522.76

**Supplement 6:** Mass spectrum of DCMMBP3-1 fraction or compound 1 at m/z 500-1000.



**Supplement 7:** Mass spectrum of DCMMBP3-2 fraction or compound 2 at m/z 500-1000.



## CHAPTER IV

### **Inhibitory effect of safflospermidines from the bee pollen of *Helianthus annuus* L. on melanogenesis of B16F10 melanoma cells**

#### **4.1 Abstract**

Tyrosinase is an essential enzyme in mammalian melanin synthesis. Extrinsic and intrinsic variables, including hormone changes, inflammation, aging, and subsequent ultraviolet light exposure, affect melanin formation. However, abnormal melanin production causes various pigmentation disorders, such as melasma, senile lentigines, freckling, and a general dulling of the skin's tone leading to a desire for skin whitening treatments to treat various skin diseases. Many of these products have limited efficiency, harmful side effects, and severe responses, especially with prolonged usage. Therefore, a safe and efficacious skin whitening agent is still required. Bee pollen contains many phytochemical compositions that are very nutritional. In addition, bee pollen is dominant in a variety of bioactivities. In our previous report, sunflower (*Helianthus annuus* L.) bee pollen is the source of safflospermidine A and B isomers with interesting *in vitro* anti-mushroom tyrosinase activity. However, their anti-melanogenesis activity at the cellular level has not been reported. Therefore, the potential effect of safflospermidine A and B as a mixture on melanogenesis were investigated at the cellular level. B16F10 mouse melanoma cells were tested for cytotoxicity, and melanin content was measured in  $\alpha$ -MSH-treated B16F10 cells, compared to kojic acid as the positive control. Results showed that at concentrations in the range of 3.91-1,000  $\mu$ g/mL, the compound was not cytotoxic to B16F10 cells. In contrast, kojic acid showed severe cytotoxicity. Safflospermidine A and B decreased intracellular and extracellular melanin content by 31.63 and 40.98%, respectively, at the concentration of 1000  $\mu$ g/mL (1.65 mM). In contrast, kojic acid at a concentration of 250  $\mu$ g/mL (1.76 mM) reduced intracellular and extracellular melanin content by 38.17 and 68.47%, respectively. These results revealed that safflospermidine A and B mixture is a safe and effective melanin inhibitor and can be applied as pharmaceutical agents and cosmetics to protect cells from abnormal melanogenesis.



Keyword: B16F10 mouse melanoma cells, cytotoxicity, kojic acid, melanin content.

## 4.2 Introduction

Melanin is a dark pigment generated in melanosomes of melanocyte. The overproduction and accumulation of melanin content in skin can lead to pigmentation disorders such as age spots, freckles, and melasma (Hernandez-Barrera et al., 2008). Furthermore, it can cause serious harm, leading to aging and skin cancer (Briganti et al., 2003; Blume-Peytavi et al., 2016). The response of melanocytes to ultraviolet (UV) radiation directly causes melanin overproduction. UV stimulates the secretion of  $\alpha$ -melanocyte-stimulating hormone ( $\alpha$ -MSH) from keratinocytes, which then induces melanogenesis in melanocytes. Then,  $\alpha$ -MSH binds to the melanocortin 1 receptor (MC1R) in melanocytes and promotes the transcription and production of enzymes in melanogenesis pathway including tyrosinase (TYR), tyrosinase-related protein-1 (TRP-1), and -2 (TRP-2) (Chatatikun et al., 2019).

Tyrosinase is a key enzyme in melanin synthesis. It catalyzes the hydroxylation of L-tyrosine and the oxidation of 3,4-dihydroxy-L-phenylalanine (L-DOPA). Furthermore, TRP-1 and TRP-2 are engaged in L-tyrosine oxidation, while TYR is the rate-limiting enzyme in melanogenesis (Bourhim et al., 2018). Thus, tyrosinase inhibitors have been used to limit melanin production in skin (Kim & Uyama, 2005).

However, a more effective and safer tyrosinase inhibitor is still in focus because some recent tyrosinase inhibitors have been associated with cell cytotoxic effects or other side effects such as irritation, skin peeling, redness, or skin sting. Despite being an effective *in vitro* and *in vivo* tyrosinase inhibitor, hydroquinone is cytotoxic to melanocytes and makes skin hypopigmentation or vitiligo (O' Donoghue, 2006; Manini et al., 2009).

Natural products have potential to be the source of tyrosinase inhibitors, such as caffeine from camellia pollen (Yuanfan et al., 2019), ellagic acid from nuts, soft fruits, and other plant tissues (Pitchakarn et al., 2013), and phloretin from apples (Chen et al., 2019a; Wang et al., 2018). Bee pollen is one of natural products that has been found to use in nutritional and medical applications (Schuh et al., 2019) according to its several bioactivities, such as the neurotoxic protection and treatment

(Ben Bacha et al., 2019), anti-inflammatory and antinociceptive activity (Lopes et al., 2019), and antibacterial and pro-regenerative effects. These activities were predominantly dependent on botanical and geographical origin (Arruda et al., 2013). In addition, the reported activity following fractionation is depended on the extraction procedures, extraction solvents, extraction numbers, and extraction times (Li et al., 2019), as well as the assay conditions.

In previous study, bee pollen from monofloral sunflower (*Helianthus annuus* L.) in Thailand was found to be the natural source of tyrosinase inhibitor in *in vitro* study, and the active compound is safflospermidine A and B. This compound showed higher anti-tyrosinase activity than kojic acid (Khongkarat et al., 2020). Moreover, safflospermidine A is also found in *Quercus mongolica* bee pollen in Korea with good tyrosinase inhibitory activity (Kim et al., 2018). This compound is classified as polyamine compound composed of three coumaroyl parts conjugated with spermidine backbone. However, anti-melanogenesis activity of the compound at the cellular level has not been reported. In order to develop this compound as skin whitening agent in cosmetic products, the study of anti-melanogenesis at the cellular level is required.

In this work, safflospermidine from sunflower (*Helianthus annuus* L.) bee pollen was treated to B16F10 mouse melanoma cells and examined effects of compound by comparing with kojic acid, positive control. After treatment, B16F10 cells were examined for cell viability and cytotoxicity using the 3-(4,5-dimethylthiazol-2-yl)-2,5-diphenyltetrazolium bromide (MTT) assay. Later, extracellular melanin content was measured in culture media using UV-visible absorption spectroscopy. Furthermore, intracellular melanin content was measured in lysed melanoma cells.

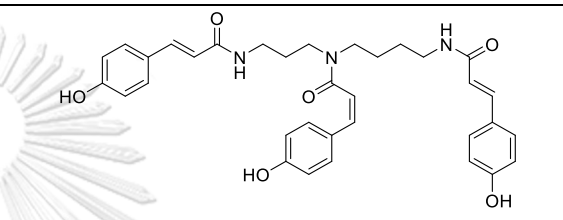
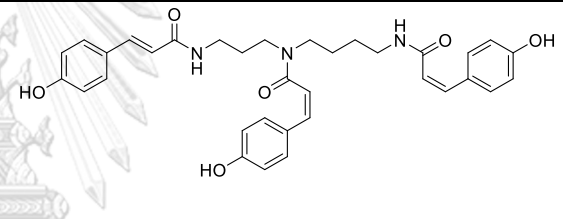
## 4.3 Materials and methods

### 4.3.1 Compound preparation

The sample for this experiment was a combination of  $N^1, N^{10}-(E)-N^5-(Z)$ -tri-*p*-coumaroyl spermidine or safflospermidine A and  $N^1-(E)-N^5, N^{10}-(Z)$ -tri-*p*-coumaroyl spermidine or safflospermidine B. The structures and descriptions of both compounds are shown in Table 4.1. According to our previous research, they were isolated from a dichloromethane partitioned extract of sunflower (*Helianthus annuus* L.) bee pollen

with a strong inhibitory activity on *in vitro* tyrosinase enzymes (Khongkarat et al., 2020). To prepare various concentrations of safflospermidine A and B, the test sample was dissolved in a stock solution with dimethyl sulfoxide (DMSO) and then diluted with cell culture media to the non-cytotoxic concentrations (DMSO < 1%).

**Table 4.1** Chemical structures and descriptions of pure compounds.

Compound	Molecular weight	Chemical structure
$N^1, N^{10}$ -( <i>E</i> )- $N^5$ -( <i>Z</i> )-tri- <i>p</i> -coumaroyl spermidine or safflospermidine A	606.2522	
$N^1$ -( <i>E</i> )- $N^5, N^{10}$ -( <i>Z</i> )-tri- <i>p</i> -coumaroyl spermidine or safflospermidine B	606.2576	

#### 4.3.2 Cell culture

The B16F10 mouse melanoma cells (ATCC No. CRL-6475) were used as a model. These B16F10 cells were obtained from the Institute of Biotechnology and Genetic Engineering, Chulalongkorn University. The B16F10 cells were grown in 7 mL Dulbecco's Modified Eagle's Medium (DMEM) supplemented with 10% (v/v) fetal calf serum (FCS) and 1% (w/v) penicillin/streptomycin in a 25 cm<sup>2</sup> cell culture flask in 5% (v/v) CO<sub>2</sub> in a humidified environment at 37 °C. When the confluency reached 80%, the B16F10 cells were subcultured to detach from a culture flask using 0.05% trypsin-EDTA. The B16F10 cells were counted using a hemocytometer. The B16F10 cells were seeded into a culture plate for further experiments.

#### 4.3.3 Cell viability assay

The viability of the B16F10 cells was determined using the 3-(4,5-dimethylthiazol-2-yl)-2,5-diphenyltetrazolium bromide (MTT) assay. In a well of 96-well plates containing 200  $\mu\text{L}$  of the medium, B16F10 cells were seeded at  $1 \times 10^4$  cells/well and allowed to adhere overnight. The B16F10 cells were then treated with different concentrations of safflospermidine A and B, kojic acid (positive control) (3.91-1000  $\mu\text{g}/\text{mL}$ ), and DMSO solvent only (control) in the presence and absence of  $\alpha$ -MSH. B16F10 cells were exposed to the treatment for 72 h. When the incubation period ended, 10  $\mu\text{L}$  of 5 mg/mL MTT in normal saline solution was added to each well. The culture plates were incubated at 37  $^{\circ}\text{C}$  for 4 h to allow formazan formation. Then, the culture medium was removed, 150  $\mu\text{L}$  of DMSO was added to dissolve the formazan crystals, and the absorbance at 540 nm was recorded using a microplate reader. The cell viability (%) was calculated using an equation as follows:

$$\text{Percentage of cell viability} = (A \times 100)/B$$

Where: A indicated the absorbance of treated B16F10 cells.

B indicated the absorbance of untreated B16F10 cells.

Triplication of experiments was done. The sample concentration that resulted in more than 80% of cell viability would be selected for the next experiments.

#### 4.3.4 Melanin content assay

The cellular melanin content of the cultured B16F10 cells was measured by following the previous report with slight modifications (Jiménez-Pérez et al., 2018). In six-well culture plates, B16F10 melanoma cells were seeded at a density of  $5 \times 10^4$  cells/well and then incubated for 24 h at 37  $^{\circ}\text{C}$  in a humidified atmosphere containing 5%  $\text{CO}_2$  in air. The B16F10 cells were then treated with various concentrations of safflospermidine A and B (62.5, 125, 250, 500, and 1,000  $\mu\text{g}/\text{mL}$ ) or kojic acid (250  $\mu\text{g}/\text{mL}$ ) in the presence of 100 nM of  $\alpha$ -MSH for 72 h while B16F10 cells in the negative control group were not treated with  $\alpha$ -MSH or sample. The medium was removed after the treatment, and the B16F10 cells were washed with PBS. The cell pellets were solubilized in 500  $\mu\text{L}$  of 1N NaOH containing 10% DMSO at 80  $^{\circ}\text{C}$  for 1 h to extract melanin. The absorbance at 492 nm was measured using a microplate reader. For measuring extracellular melanin content, 200  $\mu\text{L}$  of the cell culture media

was transferred to a well of 96-well plate, and the absorbance at 492 nm was measured. A standard curve of synthetic melanin concentrations in the range of 0 - 300  $\mu\text{g/mL}$  was created to convert the absorbance value to the amount of melanin. The results were expressed as a percentage of  $\alpha$ -MSH treated controls. In addition, the morphology of B16F10 cells in the treatment groups was observed under light microscope at 200X magnification.

#### 4.3.5 Data analysis

Numerical data are presented as the mean  $\pm$  standard deviation (S.D.), derived from three independent repeats in each experiment. One-way ANOVA was used to test for significant differences. Tukey's and Dunnett T3 test ( $p < 0.05$ ) was applied for the pairwise multiple comparisons. All statistical analyses were performed using the IBM SPSS statistics version 22 for windows software.

## 4.4 Results

### 4.4.1 Effect of safflospermidine A and B on cell viability

To investigate whether safflospermidine A and B have cytotoxic effect, B16F10 mouse melanoma cells were treated with various concentrations of safflospermidine A and B or kojic acid (3.91, 7.81, 15.63, 31.25, 62.5, 125, 250, 500, and 1,000  $\mu\text{g/mL}$ ) in the presence and absence of  $\alpha$ -MSH for 72 h. Results are expressed as percentages of viability relative to the control. In the absence of  $\alpha$ -MSH as shown in Figure 4.1, the results indicated that safflospermidine A and B at concentrations in the range of 3.91-1,000  $\mu\text{g/mL}$  showed no cytotoxic effect on B16F10 cell viability due to the percentage of cell viability of more than 80%, comparing with the control group. However, at concentration of 1,000  $\mu\text{g/mL}$  of kojic acid, cytotoxicity was observed. There was a significant reduction, approximately 53.25% decrease in cell viability. In the presence of  $\alpha$ -MSH, as shown in Figure 4.2, the results indicated that safflospermidine A and B at concentrations in the range of 3.91-1,000  $\mu\text{g/mL}$  showed no cytotoxic effect on B16F10 cell viability, comparing with the control group. However, cytotoxicity was observed at concentrations of 500 and 1,000  $\mu\text{g/mL}$  of kojic acid. In addition, there was a significant reduction in cell viability, approximately 24.37 and 62.46 %, respectively. Therefore, in this study, the

concentration of safflospermidine A and B in the range of 62.5-1,000  $\mu\text{g}/\text{mL}$  and kojic acid at a dose of 250  $\mu\text{g}/\text{mL}$  were selected because they provided the cell viability more than 80% in both conditions and had been used in previous report (Chatatikun et al., 2019) as a positive control, to determine their effect on melanogenesis in B16F10 cells.

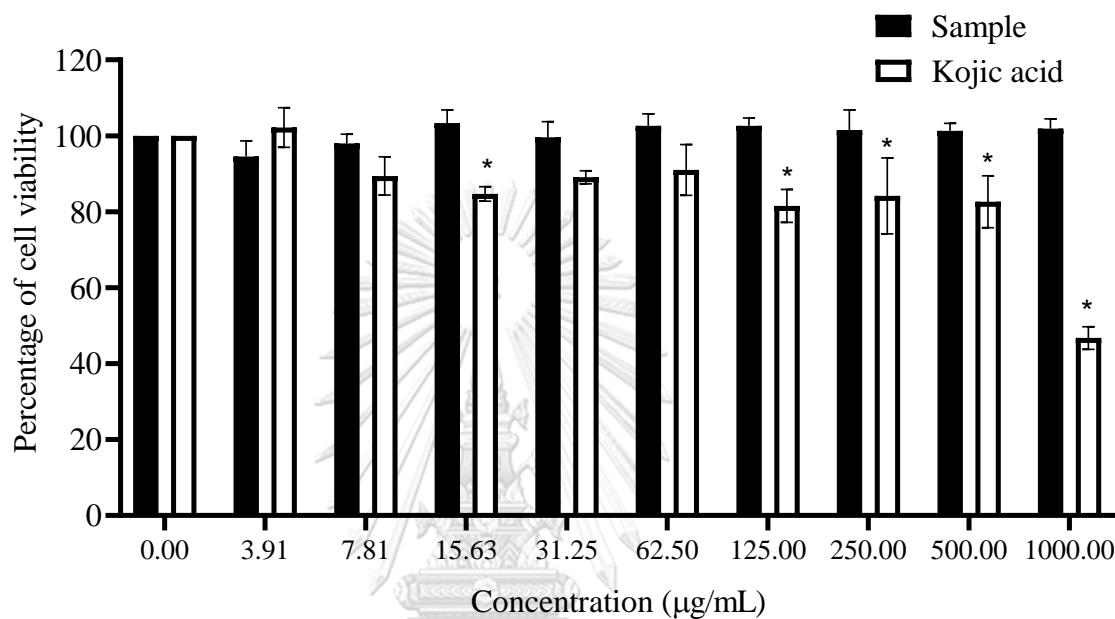


**Figure 4.1** Effect of safflospermidine A and B and kojic acid on cell viability of B16F10 melanoma cells in the absence of  $\alpha$ -MSH using MTT assay. The percentage value of treated B16F10 cells was reported by being relative to that of the control group. The values were the mean  $\pm$  S.D. from three independent experiments. \* indicates a value significantly different from the control group [ $p < 0.05$ ; one-way ANOVA and Post Hoc (Tukey) test].

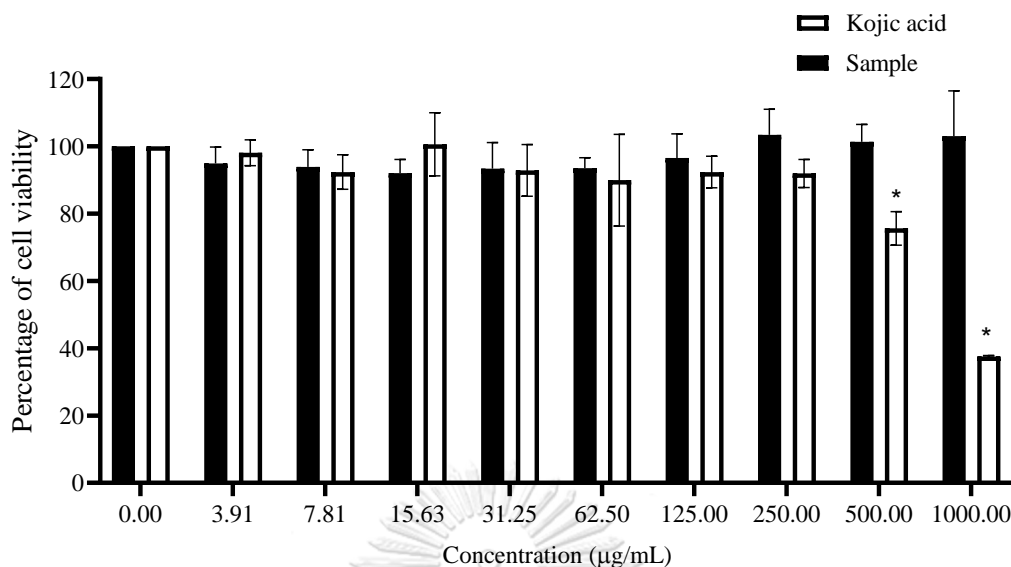
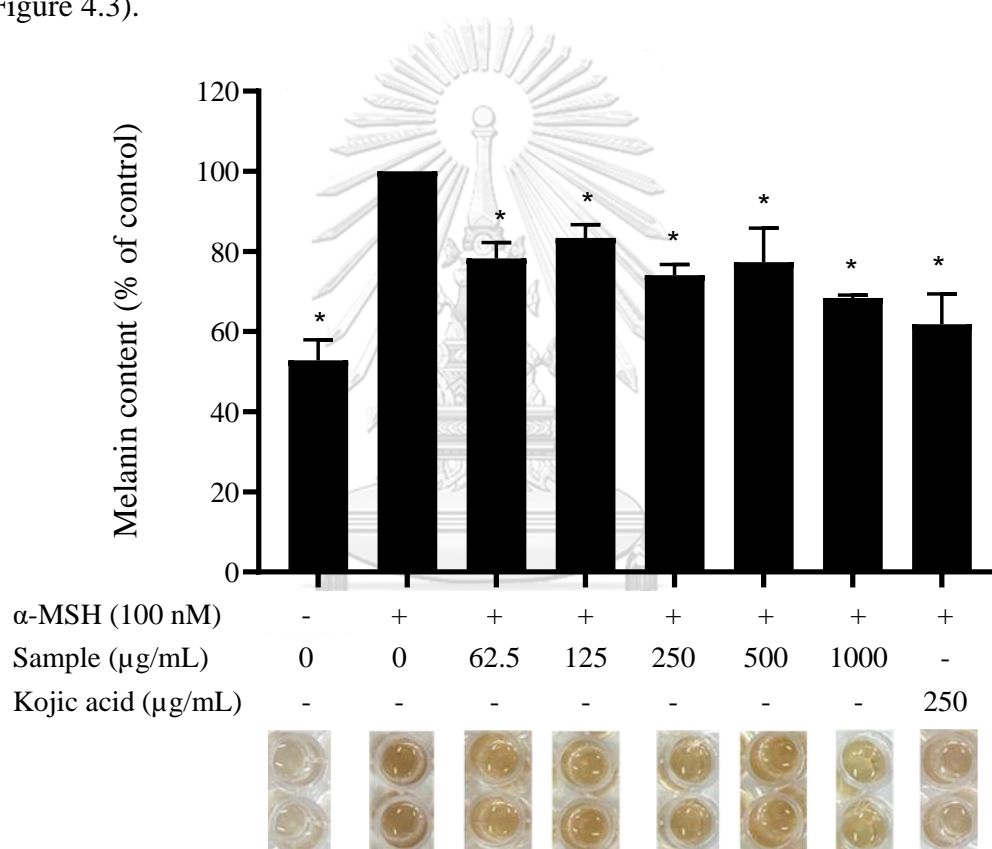


**Figure 4.2** Effect of safflospermidine A and B and kojic acid on cell viability of B16F10 melanoma cells in the presence of  $\alpha$ -MSH using MTT assay. The percentage value of treated B16F10 cells was reported by being relative to that of the control group. The values were the mean  $\pm$  S.D. from three independent experiments. \* indicates a value significantly different from the control group [ $p < 0.05$ ; one-way ANOVA and Post Hoc (Tukey) test].

#### 4.4.2 Effect of safflospermidine A and B on cellular melanin content

The inhibitory effect of safflospermidine A and B on melanin production was investigated by both intracellular and extracellular melanin content assays. The B16F10 cells were treated with various concentrations of safflospermidine A and B for 72 h in the presence of 100 nM  $\alpha$ -MSH. Kojic acid was a positive control for inhibiting melanin content in the B16F10 cells. In comparison, B16F10 cells in the negative control group were not treated with  $\alpha$ -MSH or safflospermidine A and B. The melanin content of all experiments was calculated from a standard curve of synthetic melanin ( $y = 0.004x + 0.0398$ ;  $R^2 = 1$ ) and compared against  $\alpha$ -MSH treated B16F10 cells. For intracellular melanin content assay, after lysing B16F10 cells and dissolving melanin, the brown solution was derived and measured for melanin content. The results showed that B16F10 cells treated with  $\alpha$ -MSH had higher melanin content than the negative control group (without  $\alpha$ -MSH) about 2-fold. Therefore,  $\alpha$ -MSH affected B16F10 cells by stimulating the melanin production.

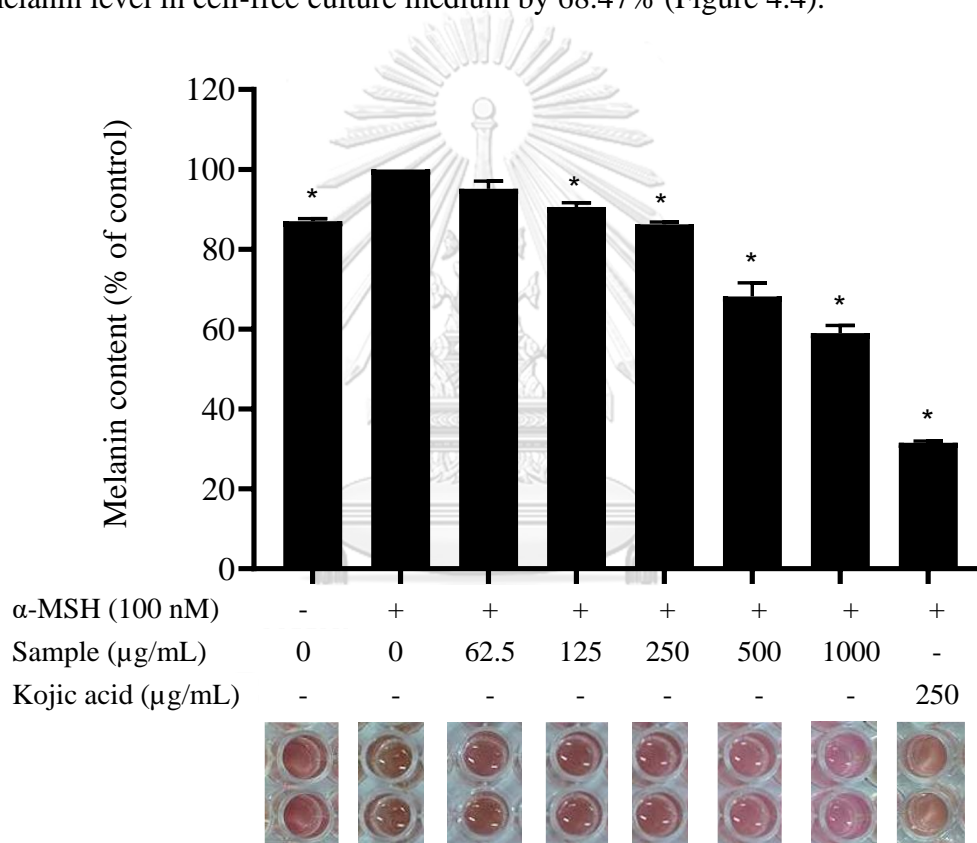
However, in the treated group (with both  $\alpha$ -MSH and safflospemidine A and B), the higher concentrations of safflospemidine A and B, the fader in brown color of the solution would be noticed. It indicated the decrease in melanin production. The results were coincided with the reduction in melanin content if B16F10 cells were cultured with increasing concentrations (62.5, 125, 250, 500, and 1,000  $\mu$ g/mL) of safflospemidine A and B. It showed the significant inhibition of melanin production, decreasing by 21.78, 16.61, 25.94, 22.70, and 31.63%, respectively. In contrast, kojic acid (250  $\mu$ g/mL) significantly reduced the melanin level in B16F10 cells by 38.17% (Figure 4.3).



**Figure 4.3** Effect of a sample (safflospemidine A and B) on intracellular melanin content in B16F10 melanoma cells. Baseline melanin content in control wells exposed to only  $\alpha$ -MSH was set at 100%. Data were expressed as a percentage of control. Each column represents the mean  $\pm$  SD from three independent experiments. \* indicates a value significantly different from control group [ $p < 0.05$ ; one-way ANOVA and Post Hoc (Tukey) test]. The bottom panel represents the color intensity of dissolving melanin after cell lysis.

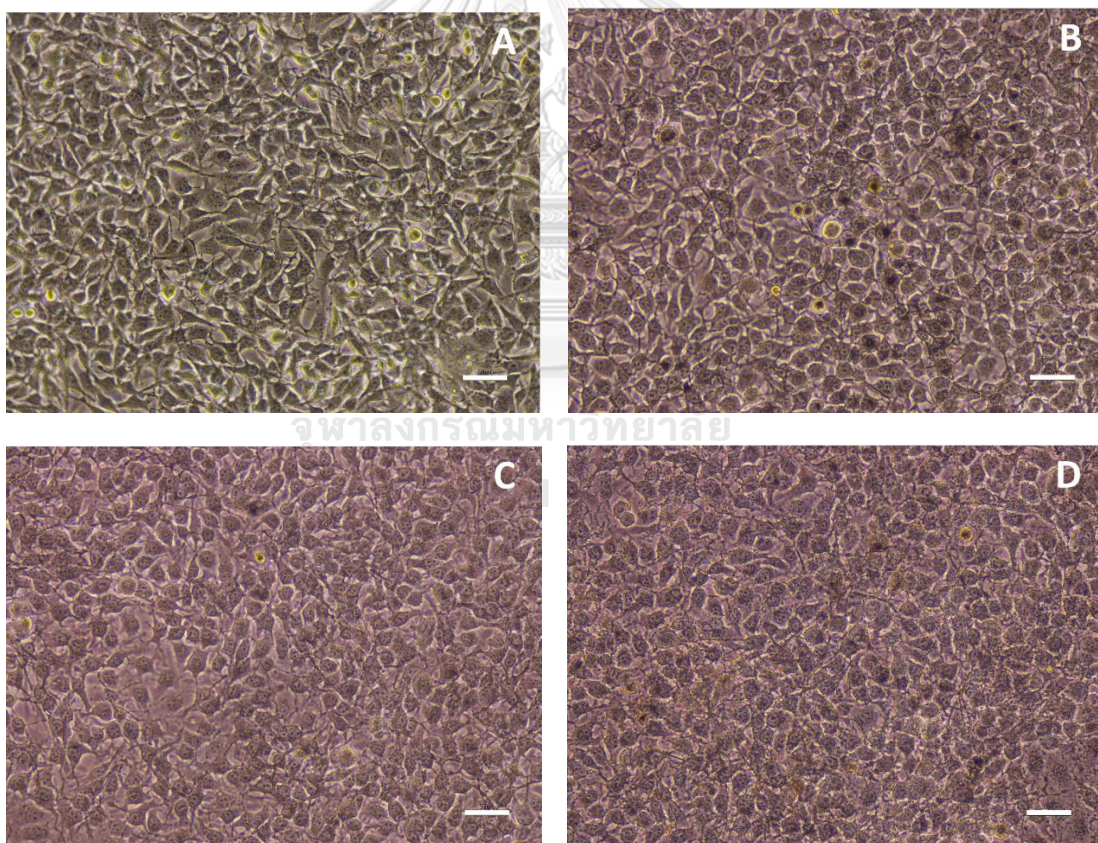


The extracellular melanin (melanin in culture media) was also determined. The results showed a similar trend to intracellular melanin content by the color of the culture media of the sample-treated group was lighter than that of the control group. It was noticed when the sample concentration increased, the melanin releasing was decreased. When B16F10 cells were exposed to safflospermidine A and B at 125, 250, 500, and 1,000  $\mu\text{g/mL}$ , the melanin production was decreased by 9.39, 13.76, 31.82, and 40.98%, respectively. However, 62.5  $\mu\text{g/mL}$  of safflospermidine A and B did not reduce secreted melanin. Kojic acid (250  $\mu\text{g/mL}$ ) significantly reduced the melanin level in cell-free culture medium by 68.47% (Figure 4.4).



**Figure 4.4** Effect of a sample(safflospermidine A and B) on extracellular melanin content in B16F10 melanoma cells. Baseline melanin content in control wells exposed to only  $\alpha$ -MSH was set at 100%. Data were expressed as a percentage of control. Each column represents the mean  $\pm$  SD from three independent experiments. \* indicates value significantly different from control group [ $p < 0.05$ ; one-way ANOVA and Post Hoc (Dunnett T3) test]. The bottom panel represents the color intensity of melanin production in media.

Furthermore, the morphology of B16F10 cells was observed under light microscope at 200X magnification. The results showed that the B16F10 cells in the control group were mixed between spindle-shaped and epidermal-like cells, in close contact with neighbouring cells, and adhered to the surface of a well plate (Figure 4.5, B). B16F10 cells treated with safflospermidine A and B at 62.5 and 125  $\mu\text{g}/\text{mL}$  (Figures 4.5, C and D), kojic acid at 250  $\mu\text{g}/\text{mL}$  (Figure 4.5, H), and the negative control group (without  $\alpha\text{-MSH}$ ) (Figure 4.5, A) were not morphologically changed. In contrast, the morphology of B16F10 cells treated with safflospermidine A and B at 250, 500, and 1,000  $\mu\text{g}/\text{mL}$  cannot be observed because the compound could not be dissolved well in the DMEM media, causing the compound to precipitate (Figures 4.5, E-G).



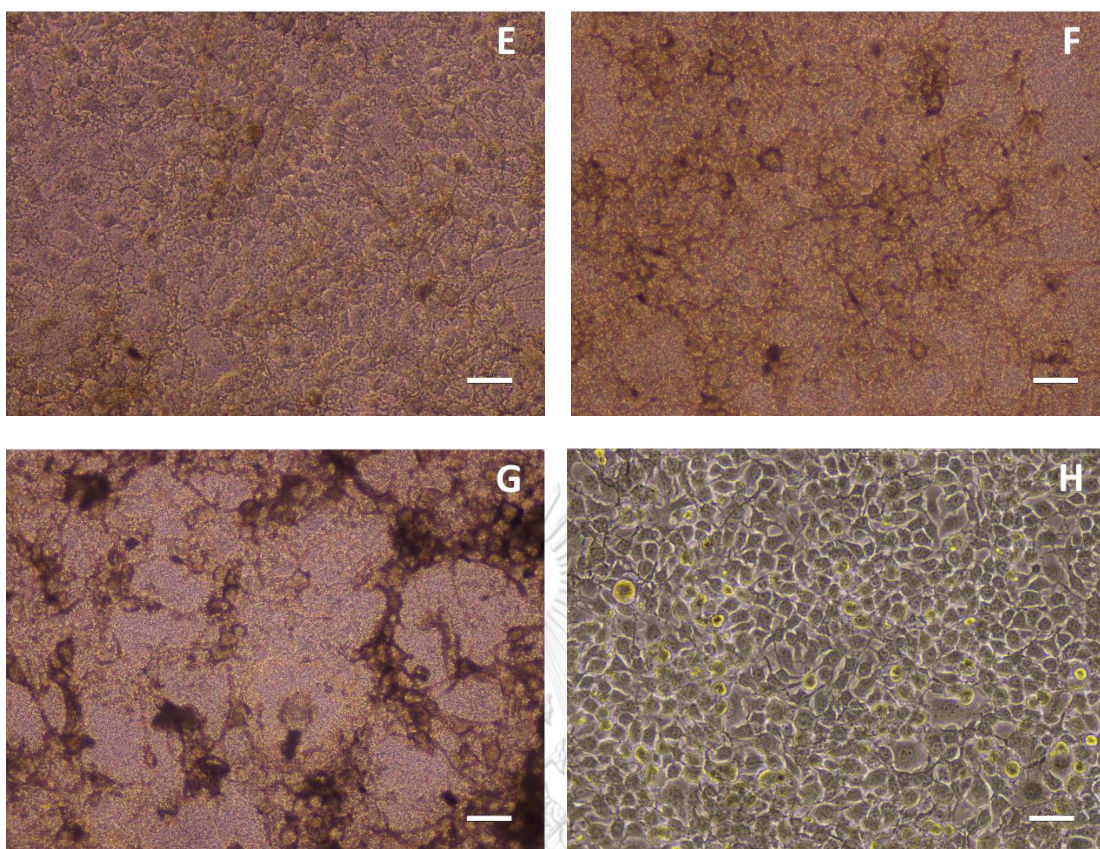


**Figure 4.5** Morphology of B16F10 cells after exposed to safflospermidine A and B for 72 h under light microscope (200X); (A) negative control, (B) control, (C) B16F10 cells with 62.5  $\mu\text{g}/\text{mL}$  of compound, (D) B16F10 cells with 125  $\mu\text{g}/\text{mL}$  of compound, (E) B16F10 cells with 250  $\mu\text{g}/\text{mL}$  of compound, (F) B16F10 cells with 500  $\mu\text{g}/\text{mL}$  of compound, (G) B16F10 cells with 1,000  $\mu\text{g}/\text{mL}$  of sample, and (H) B16F10 cells with 250  $\mu\text{g}/\text{mL}$  of kojic acid. Each picture is a representative of three independent experiments. Scale bar = 50  $\mu\text{m}$

#### 4.5 Discussion

Melanin, dark pigment, is produced by melanocytes to protect the skin from UV light and reactive oxygen species (ROS). Nevertheless, the excessive production of melanin is caused by long-time exposure to UV light resulting in various skin disorders such as melasma and freckles. In the melanogenesis pathway, tyrosinase is the key and rate-limiting enzyme responsible for melanin production. Therefore, inhibition of tyrosinase activity results in the reduction of melanin overproduction of skin cells. For this reason, researchers are still searching for safe and effective tyrosinase inhibitors from natural sources.

In this study, safflospermidine fraction, which consists of safflospermidine A and B from sunflower bee pollen, was studied for anti-melanogenesis at the cellular level using B16F10 mouse melanoma cells as a model. This cell line showed more suitable for melanogenesis study than human melanoma by producing higher melanin content (Lin et al., 2015). The MTT assay was used in the cytotoxicity study by detection of formazan, a product derived from the catalysis of mitochondrial dehydrogenase in live cells. Safflospermidine A and B showed non-cytotoxicity to B16F10 cells although it was used in a high concentration of 1,000  $\mu\text{g/mL}$  (0.1% w/v). At this concentration, kojic acid showed very high cytotoxicity to cells by reducing cell viability more than 60% although the Cosmeceutical Ingredient Review (CIR) approved kojic acid as safe at a concentration of 1% in cosmeceutical products (Phasha et al., 2022). In the melanogenesis study, 100 nM of  $\alpha\text{-MSH}$  was used to stimulate melanogenesis and mimic the situation of cells exposed to UV light. The concentration of  $\alpha\text{-MSH}$  at 100 nM is the most appropriate because it can reduce the factors that interfere with the study of anti-melanogenesis, such as cell proliferation and division (Chung et al., 2019). The anti-melanogenesis effect of safflospermidine A and B mixture was studied in terms of intra- and extra-melanin content. This compound reduced melanin production by 31.63% at 1,000  $\mu\text{g/mL}$  or 1.65 mM concentration, while kojic acid showed 38.17% at 250  $\mu\text{g/mL}$  or 1.76 mM. This result can conclude that the activity of this compound is comparable with kojic acid in the case of extracellular melanin content. This compound reduced extracellular melanin content by 40.98% at the concentration of 1,000  $\mu\text{g/mL}$  or 1.65 mM, while kojic acid showed more effective in reducing melanin release by 68.47% at the concentration of

250  $\mu\text{g/mL}$  or 1.76 mM. Although safflospermidine showed lower anti-melanogenesis activity than kojic acid, it is safer for skin cells. Under a light microscope, it was found that, at the high concentration of 1,000  $\mu\text{g/mL}$ , the compound precipitates and floats on the media because its molecular structure composes of long-chain hydrocarbon and three aromatic groups, which limits solubility in high concentration. That results in lower activity. However, An et al. (2008) found that *p*-coumaric acid, which is a part of safflospermidine in this study, showed more effective in anti-melanogenesis than arbutin used as positive control. In addition, *p*-coumaric acid was reported as a multi-antimelanogenic inhibitor by absorbing the UV light, reducing ROS, inhibiting the tyrosinase expression signaling, and inhibiting tyrosinase (Boo, 2019). Therefore, improvement for the solubility or cell membrane permeability of safflospermidine should promote the effectiveness of this compound. The encapsulation process is one of the promising methods that can improve the absorption of anti-melanogenesis agents into cells. Ephrem et al. (2017) reported that encapsulation can enhance the stability and increase the concentration of the encapsulated compound at the targeted site by improving skin permeation, penetration, or distribution. However, a mechanism of safflospermidine on anti-melanogenesis activity can be revealed if the intracellular tyrosinase inhibitory activity and the expression of tyrosinase, TRP-1, and TRP-2 genes are reported.

#### 4.6 Conclusion

In conclusion, safflospermidine isomers can inhibit melanin production at the cellular level and also show non-cytotoxicity properties. Compared with kojic acid at a similar concentration, safflospermidine isomers showed distinguishable activity by reducing intracellular melanin content. Although kojic acid showed a higher reduction of extracellular melanin content, it showed higher cytotoxicity. The results supported that safflospermidine isomers are one of the anti-melanogenic agents derived from sunflower bee pollen in Thailand.

## References

- An SM, Lee SI, Choi SW, Moon SW, Boo YC. 2008. p-Coumaric acid, a constituent of *Sasa quepaertensis* Nakai, inhibits cellular melanogenesis stimulated by  $\alpha$ -melanocyte stimulating hormone. *British Journal of Dermatology* **159**: 292-299 DOI 10.1111/j.1365-2133.2008.08653.x.
- Ben Bacha A, Norah AO, Al-Osaimi M, Harrath AH, Mansour L, El-Ansary A. 2020. The therapeutic and protective effects of bee pollen against prenatal methylmercury induced neurotoxicity in rat pups. *Metabolic Brain Disease* **35**:215-224 DOI 10.1007/s11011-019-00496-z.
- Blume-Peytavi U, Kottner J, Sterry W, Hodin MW, Griffiths TW, Watson RE, Griffiths CE. 2016. Age-associated skin conditions and diseases: current perspectives and future options. *Gerontologist* **56**: 230-242 DOI 10.1093/geront/gnw003.
- Boo YC. 2019. p-Coumaric acid as an active ingredient in cosmetics: a review focusing on its antimelanogenic effects. *Antioxidants* **8**: 275-290 DOI 10.3390/antiox8080275.
- Bourhim T, Villareal MO, Gadhi C, Hafidi A, Isoda H. 2018. Depigmenting effect of argan press-cake extract through the down-regulation of Mitf and melanogenic enzymes expression in B16 murine melanoma cells. *Cytotechnology* **70**: 1389-1397 DOI 10.1007/s10616-018-0232-6.
- Briganti S, Camera E, Picardo M. 2003. Chemical and instrumental approaches to treat hyperpigmentation. *Pigment Cell Research* **16**: 101-110 DOI 10.1034/j.1600-0749.2003.00029.x.
- Chatatikun M, Yamauchi T, Yamasaki K, Aiba S, Chiabchalard A. 2019. Anti melanogenic effect of *Croton roxburghii* and *Croton sublyratus* leaves in  $\alpha$ -MSH stimulated B16F10 cells. *Journal of Traditional and Complementary Medicine* **9**: 66-72 DOI 10.1016/j.jtcme.2017.12.002.
- Chen YM, Li C, Zhang WJ, Shi Y, Wen ZJ, Chen QX, Wang Q. 2019. Kinetic and computational molecular docking simulation study of novel kojic acid derivatives as anti-tyrosinase and antioxidant agents. *Journal of Enzyme Inhibition and Medicinal Chemistry* **34**: 990-998 DOI 10.1080/14756366.2019.1609467.

- Chung S, Lim GJ, Lee JY. 2019. Quantitative analysis of melanin content in a three-dimensional melanoma cell culture. *Scientific Reports* **9**: 1-9 DOI 10.1038/s41598-018-37055-y.
- de Arruda VAS, Pereira AAS, de Freitas AS, Barth OM, de Almeida-Muradian LB. 2013. Dried bee pollen: B complex vitamins, physicochemical, and botanical composition. *Journal of Food Composition and Analysis* **29**: 100-105 DOI 10.4067/s0717-75182018000400232.
- Ephrem E, Elaissari H, Greige-Gerges H. 2017. Improvement of skin whitening agents efficiency through encapsulation: current state of knowledge. *International Journal of Pharmaceutics* **526**: 50-68 DOI 10.1016/j.ijpharm.2017.04.020.
- Hernández-Barrera R, Torres-Alvarez B, Castanedo-Cazares JP, Oros-Ovalle C, Moncada B. 2008. Solar elastosis and presence of mast cells as key features in the pathogenesis of melasma. *Clinical and Experimental Dermatology* **33**: 305-308 DOI 10.1111/j.1365-2230.2008.02724.x.
- Jiménez-Pérez ZE, Singh P, Kim YJ, Mathiyalagan R, Kim DH, Lee MH, Yang DC. 2018. Applications of *Panax ginseng* leaves-mediated gold nanoparticles in cosmetics relation to antioxidant, moisture retention, and whitening effect on B16BL6 cells. *Journal of Ginseng Research* **42**: 327-333 DOI 10.1016/j.jgr.2017.04.003.
- Khongkarat P, Ramadhan R, Phuwapraisirisan P, Chanchao C. 2020. Safflospermidines from the bee pollen of *Helianthus annuus* L. exhibit a higher *in vitro* antityrosinase activity than kojic acid. *Heliyon* **6**: e03638 DOI 10.1016/j.heliyon.2020.e03638.
- Kim SB, Liu Q, Ahn JH, Jo YH, Turk A, Hong IP, Lee MK. 2018. Polyamine derivatives from the bee pollen of *Quercus mongolica* with tyrosinase inhibitory activity. *Bioorganic Chemistry* **81**: 127-133 DOI 10.1016/j.bioorg.2018.08.014.
- Kim YJ, Uyama H. 2005. Tyrosinase inhibitors from natural and synthetic sources: structure, inhibition mechanism, and perspective for the future. *Cellular and Molecular Life Sciences* **62**: 1707-1723 DOI 10.1007/s00018-005-5054-y.

- Li F, Guo S, Zhang S, Peng S, Cao W, Ho CT, Bai N. 2019. Bioactive constituents of *F. esculentum* bee pollen and quantitative analysis of samples collected from seven areas by HPLC. *Molecules* **24**: 2705 DOI 10.3390/molecules24152705.
- Lin CC, Yang CH, Lin YJ, Chiu YW, Chen CY. 2015. Establishment of a melanogenesis regulation assay system using a fluorescent protein reporter combined with the promoters for the melanogenesis-related genes in human melanoma cells. *Enzyme and Microbial Technology* **68**: 1-9 DOI 10.1016/j.enzmictec.2014.09.008.
- Lopes AJO, Vasconcelos CC, Pereira FAN, Silva RHM, Queiroz PFDS, Fernandes CV, Ribeiro MNDS. 2019. Anti-inflammatory and antinociceptive activity of pollen extract collected by stingless bee *Melipona fasciculata*. *International Journal of Molecular Sciences* **20**: 4512 DOI 10.3390/ijms20184512.
- Manini P, Napolitano A, Westerhof W, Riley PA, d'Ischia M. 2009. A reactive ortho-quinone generated by tyrosinase-catalyzed oxidation of the skin depigmenting agent monobenzone: self-coupling and thiol-conjugation reactions and possible implications for melanocyte toxicity. *Chemical Research in Toxicology* **22**: 1398-1405 DOI 10.1021/tx900018q.
- O'Donoghue J. 2006. Hydroquinone and its analogues in dermatology—a risk-benefit viewpoint. *Journal of Cosmetic Dermatology* **5**: 196-203 DOI 10.1111/j.1473-2165.2006.00253.x.
- Phasha V, Senabe J, Ndzotoyi P, Okole B, Fouche G, Chaturgoon A. 2022. Review on the use of kojic acid—a skin-lightening ingredient. *Cosmetics* **9**: 64-74 DOI 10.3390/cosmetics9030064.
- Pitchakarn P, Chewonarin T, Ogawa K, Suzuki S, Asamoto M, Takahashi S, Limtrakul P. 2013. Ellagic acid inhibits migration and invasion by prostate cancer cell lines. *Asian Pacific Journal of Cancer Prevention* **14**: 2859-2863 DOI 10.7314/apjcp.2013.14.5.2859.
- Schuh CM, Aguayo S, Zavala G, Khoury M. 2019. Exosome-like vesicles in *Apis mellifera* bee pollen, honey, and royal jelly contribute to their antibacterial and pro-regenerative activity. *Journal of Experimental Biology* **222**: jeb208702 DOI 10.1242/jeb.208702.



- Wang H, Yang T, Wang T, Hao N, Shen Y, Wu Y, Wen F. 2018. Phloretin attenuates mucus hypersecretion and airway inflammation induced by cigarette smoke. *International Immunopharmacology* **55**: 112-119 DOI 10.1016/j.intimp.2017.12.009.
- Yang Y, Sun X, Ni H, Du X, Chen F, Jiang Z, Li Q. 2019. Identification and characterization of the tyrosinase inhibitory activity of caffeine from camellia pollen. *Journal of Agricultural and Food Chemistry* **67**: 12741-12751 DOI: 10.1021/acs.jafc.9b04929.



## CHAPTER V

### CONCLUSION

In overall, the obtained data showed that, among the three partition solvents, dichloromethane (DCM) was the best solvent for extraction of the total phenolic compounds and flavonoids according to the highest total phenolic and flavonoid content in the DCM partition extract of all bee pollen samples. The DCM partition extract of *H. annuus* L. bee pollen contained the highest content of total phenolic compounds while the DCM partition extract of *M. diplotricha* bee pollen contained both total phenolic and flavonoid contents at very high levels resulting in its highest antioxidant activity. For the enzyme inhibitory activity, it showed that *M. diplotricha* bee pollen exhibited the highest antilipoxygenase activity and also showed the comparable anti-lipase activity to *C. sinensis* bee pollen. After purification, triferuloyl spermidines were classified as a phenolic compound responsible for antilipoxygenase and antioxidant activities. The mixture of palmitic acid, linoleic, and linolenic acid was found to be the lipase inhibitor. In addition, the best anti-amylase activity was found in *X. complanata* bee pollen. However, the activity was relatively low, compared to the positive control. Furthermore, *H. annuus* L. bee pollen showed the best antityrosinase activity. After purification, safflospermidine A and B were found to be active compounds for antityrosinase activity. According to the outstanding IC<sub>50</sub> value of safflospermidine A and B isomers, the mixture of both compounds was further examined for antimelanogenesis at a cellular level. The results showed that safflospermidines significantly reduced intracellular and extracellular melanin levels in B16F10 melanoma cells with no cytotoxicity. All obtained data were suggested that consuming *M. diplotricha* bee pollen as supplementary food should help to repair the damage and prevent a disease caused by a free radical and inflammation in our bodies. Moreover, it should reduce lipid digestion and absorption by inhibiting lipase, which should be beneficial on consumers with obesity. In addition, safflospermidines should be developed as an additive in skin care products because of melasma and fickle-reducing effects. However, to ensure the safe consumption and use of bee pollen in terms of nutraceutical food and medicine for humans, testing should be carried out at the cellular level, laboratory animals (mice and zebrafish), and clinical trials. Therefore, bee pollen is considered as a natural product that has a potential source of

active ingredients. Moreover, promoting bee pollen as a nutritional supplement to be developed for use in the pharmaceutical and cosmetic industry may eventually increase Thai bee farmers' incomes.



## REFERENCES



จุฬาลงกรณ์มหาวิทยาลัย  
**CHULALONGKORN UNIVERSITY**



จุฬาลงกรณ์มหาวิทยาลัย  
**CHULALONGKORN UNIVERSITY**

## VITA

**NAME** Phanthiwa Khongkarat

**DATE OF BIRTH** 9 January 1994

**PLACE OF BIRTH** Nakhonpathom

**INSTITUTIONS ATTENDED** B.Sc Silpakorn University  
M.Sc Chulalongkorn University

**HOME ADDRESS** 4 M. 1 Sampran, Nakhonpathom ,73110

**PUBLICATION**

Phytochemical content, especially spermidine derivatives, presenting antioxidant and antilipoxygenase activities in Thai bee pollens  
Khongkarat, P., Phuwapraisirisan, P., Chanchao, C.  
PeerJ, 2022, 10, e13506

First report of fatty acids in *Mimosa diplotricha* bee pollen with in vitro lipase inhibitory activity  
Khongkarat, P., Traiyasut, P., Phuwapraisirisan, P., Chanchao, C.  
PeerJ, 2022, 9, e12722

Screening and Bioguided Fractionation of *Mimosa pigra* L. Bee Pollen with Antioxidant and Anti-Tyrosinase Activities  
Khongkarat, P., Ramadhan, R., Phuwapraisirisan, P., Chanchao, C.  
Journal of Apicultural Science, 2021, 65(1), pp. 71–83

Safflospemidines from the bee pollen of *Helianthus annuus* L. exhibit a higher in vitro antityrosinase activity than kojic acid  
Khongkarat, P., Ramadhan, R., Phuwapraisirisan, P., Chanchao, C.  
Heliyon, 2020, 6(3), e03638